Opa protein-based interactions of pathogenic *Neisseriae* with the human receptors CEACAM3 and CEA

Dissertation

zur Erlangung des akademischen Grades eines

Doktors der Naturwissenschaften

(Dr. rer. nat)

vorgelegt von

Griseldis Goob

an der

Universität Konstanz

Mathematisch-Naturwissenschaftliche Sektion

Fachbereich Biologie

Konstanz, 2022

Tag der mündlichen Prüfung: 20.12.2022

1. Referent: Prof. Dr. Christof R. Hauck

2. Referent: Prof. Dr. Thomas U. Mayer

Parts of this work are published in:

Goob G., Adrian J., Cossu C., Hauck C. R. “Phagocytosis mediated by the human granulocyte receptor CEACAM3 is limited by the receptor-type protein tyrosine phosphatase PTPRJ.” (2022) Journal of Biological Chemistry, 298(9), 102269. https://doi.org/10.1016/j.jbc.2022.102269

In addition, parts of this work are the content of a manuscript that will soon be submitted:

Goob G.*, Kress A.*, Roth A., Seiffert C., von Werthern K., Hauck C. R. “A CEACAM3 polymorphism prevalent in subsaharan Africa directs opsonin-independent recognition of *Neisseria meningitidis* by human phagocytes.” (***** both authors contributed equally). Manuscript in preparation.

Important findings by collaborators essential to understanding and interpreting the results have been included, and their work is explicitly mentioned in the corresponding figure legend and in the chapter declaration of contributions.

Table of content

Abstract

Carcinoembryonic antigen-related cell adhesion molecules (CEACAMs) are a group of glycoproteins that belong to the immunoglobulin superfamily and are expressed on various cell types of the body. Several of the total 12 human CEACAM members are known to serve as receptors for various human-specific pathogens. Bacterial adhesins that allow binding to these pathogen receptors are found, for example, on the surface of the gram-negative pathogens *Neisseria meningitidis*, *Moraxella catarrhalis*, and *Haemophilus influenzae*, which colonize the epithelial mucosa of the nasopharynx, and in *Neisseria gonorrhoeae*, that colonizes the mucosal surfaces of the genital tract. Interaction with epithelial CEACAMs facilitates pathogen colonization of their epithelial target tissue by modulating innate and adaptive defences. Therefore, interaction with the epithelial-expressed CEACAMs CEACAM1, CEA, and CEACAM6 appears to provide a selective advantage for these microorganisms. On the other hand, a granulocyte-restricted member of the CEACAM family, CEACAM3, is also functioning as a receptor for bacterial CEACAM-binding adhesins. In contrast to epithelial CEACAMs, engagement of CEACAM3 results in the opsonin-independent phagocytosis and efficient elimination of microbes.

Since binding to CEACAM3 is to the disadvantage of pathogens, several bacteria seem to have evolved CEACAM-binding adhesins, which retain binding to CEACAM1 and CEA, yet escape recognition by granulocyte CEACAM3. Indeed, we show that this selective binding to epithelial CEACAMs is a common feature of CEACAM-binding adhesins of the potentially lethal pathogen *N. meningitidis*. However, a polymorphic variant of CEACAM3, CEACAM3-RQAP, which is found in human populations inhabiting the sub-Saharan meningitis belt, is able to recognize *N. meningitidis*. As demonstrated by bacterial pull-down analyses, the CEACAM3-RQAP allele binds Opa-expressing meningococcal strains of serogroups A, B, C, W, and Y, which are not recognized by the common CEACAM3 allele. Moreover, CEACAM3-RQAP-expressing cells rapidly internalized bacteria expressing CEACAM3-RQAP-binding meningococcal Opa proteins. Our results thus highlight the ongoing evolutionary arms race between the human innate immune receptor CEACAM3 and a human-restricted bacterial pathogen in the meningitis belt of sub-Saharan Africa.

The ability of CEACAM3 to engulf and eliminate bacteria depends on the phosphorylation of two tyrosine residues of the immunoreceptor tyrosine-based activation motif (ITAM)-like sequence located in the cytoplasmic tail of the receptor. While numerous factors involved in the activation and propagation of CEACAM3 signaling have been described in recent years, it is unclear which enzyme(s) is responsible for the reversal of CEACAM3 phosphorylation. In our search for protein phosphatases that inhibit CEACAM3-induced signaling, we identified the receptor-type protein tyrosine phosphatase PTPRJ as a negative regulator of CEACAM3-mediated phagocytosis. Overexpression of the active PTPRJ phosphatase domain strongly reduced the CEACAM3-mediated bacterial uptake, whereas PTPRJ-deficient cells showed a gain-of-function phenotype. We further demonstrated that the recombinant phosphatase domain of PTPRJ is capable of directly dephosphorylating both tyrosine residues of the cytoplasmic ITAM-like motif of purified CEACAM3. This direct action of PTPRJ on CEACAM3 was confirmed in *in vitro* studies demonstrating dephosphorylation of synthetic CEACAM3-derived phospho-peptides by recombinant PTPRJ. Consistent with the prominent role of tyrosine phosphorylation of the ITAM-like sequence in the induction of lamellipodia formation, human phagocytes lacking PTPRJ exhibited excessive lamellipodia and enhanced opsonin-independent phagocytosis in response to CEACAM-binding bacteria. Our results indicate that PTPRJ is a negative regulator of CEACAM3-mediated phagocyte functions and represents a potential target to restrict CEACAM3-initiated inflammatory processes.

It is thought that CEACAM3 activity may be one reason why CEACAM-binding pathogens such as *N. gonorrhoeae* are mostly kept in check by the human body. Nevertheless, in rare cases, gonococci can spread beyond the original site of infection and cause disseminating gonococcal infections. In view of the rise of multidrug-resistant *N. gonorrhoeae* strains, it is becoming increasingly important to better model gonococcal infections in experimental animals as an essential first step to develop new treatment strategies. The use of mice expressing the Opa-binding human CEA receptor on the vaginal mucosa has already been instrumental to overcome a major weakness of mice as gonococcal infection model. Nevertheless, infections in mice are limited in duration and disease development due to the highly adapted nature of *N. gonorrhoeae* to humans. In this work, we describe several approaches to optimize the female CEA transgenic (CEAtg) mouse model. The focus of this work was to extend the previously used 24h-infection model, so that gonococcal infections in CEAtg mice can be

maintained for at least 48 hours. Consistent with reports from other investigators, our findings suggest that intraperitoneal administration of the antibiotics vancomycin HCl and streptomycin sulfate minimizes the commensal flora of the mouse vaginal tract, thereby improving gonococcal colonization. Furthermore, we observed that mouse passaging of *N. gonorrhoeae* appears to have a positive effect on gonococcal survival in the mouse vaginal tract. Further experiments will need to clarify, whether these modifications can reliably ensure gonococcal colonization of CEAtg mice over a period of at least 48 hours. If these modifications will lead to consistent colonization of the mouse vaginal tract for at least 48h, studying the course of gonococcal infection during this initial period and testing the efficacy of new drug therapies will be possible.

Zusammenfassung

Carcinoembryonic antigen-related cell adhesion molecules (CEACAMs) sind eine Gruppe von Glykoproteinen, die zur Superfamilie der Immunglobuline gehören und auf verschiedenen Zelltypen des Körpers vorkommen. Es ist bekannt, dass mehrere der insgesamt 12 menschlichen CEACAM-Mitglieder als Rezeptoren für verschiedene humanspezifische Krankheitserreger dienen. Bakterielle Adhäsine, die eine Bindung an diese Erregerrezeptoren ermöglichen, finden sich beispielsweise auf der Oberfläche der gramnegativen Erreger *Neisseria meningitidis*, *Moraxella catarrhalis* und *Haemophilus influenzae*, die die epitheliale Schleimhaut des Nasen-Rachen-Raums besiedeln, sowie bei *Neisseria gonorrhoeae*, der die Schleimhautoberflächen des Genitaltrakts besiedelt. Die Interaktion mit epithelialen CEACAMs erleichtert den Erregern durch Modulation der angeborenen und adaptiven Abwehr die Besiedlung ihres epithelialen Zielgewebes. Daher scheint die Interaktion mit den epithelialen CEACAMs CEACAM1, CEA und CEACAM6 einen Selektionsvorteil für diese Mikroorganismen zu bieten. Andererseits fungiert ein auf Granulozyten beschränktes Mitglied der CEACAM-Familie, CEACAM3, auch als Rezeptor für bakterielle CEACAM-bindende Adhäsine. Im Gegensatz zu den epithelialen CEACAMs führt die Bindung an CEACAM3 zur Opsonin-unabhängigen Phagozytose und effizienten Eliminierung der Mikroben.

Da die Bindung an CEACAM3 für Krankheitserreger von Nachteil ist, scheinen einige Bakterien CEACAM-bindende Adhäsine entwickelt zu haben, die die Bindung an CEACAM1 und CEA erhalten, der Erkennung durch Granulozyten-CEACAM3 aber entgehen. Tatsächlich zeigen wir, dass diese selektive Bindung an epitheliale CEACAMs ein gemeinsames Merkmal der CEACAM-bindenden Adhäsine des potenziell tödlichen Erregers *N. meningitidis* ist. Eine polymorphe Variante von CEACAM3, CEACAM3-RQAP, die in menschlichen Populationen im sub-saharischen Meningitisgürtel vorkommt, ist jedoch in der Lage, *N. meningitidis* zu erkennen. Wie wir durch bakterielle Pull-Down-Analysen nachweisen konnten, bindet das CEACAM3-RQAP-Allel Opa-exprimierende Meningokokkenstämme der Serogruppen A, B, C, W und Y, die vom gewöhnlichen CEACAM3-Allel nicht erkannt werden. Darüber hinaus internalisierten CEACAM3-RQAP-exprimierende Zellen schnell Bakterien, die CEACAM3-RQAP-bindende Meningokokken-Opa-Proteine exprimierten. Unsere Ergebnisse verdeutlichen somit das anhaltende evolutionäre Wettrüsten zwischen dem menschlichen

angeborenen Immunrezeptor CEACAM3 und einem auf den Menschen beschränkten bakteriellen Erreger im Meningitisgürtel von Subsahara-Afrika.

Die Fähigkeit von CEACAM3, Bakterien zu verschlingen und zu eliminieren, hängt von der Phosphorylierung zweier Tyrosinreste der Immunrezeptor Tyrosin-basierten Aktivierungsmotiv (ITAM)-ähnlichen Sequenz im zytoplasmatischen Abschnitt des Rezeptors ab. Während in den letzten Jahren zahlreiche Faktoren beschrieben wurden, die an der Aktivierung und Weiterleitung der CEACAM3-Signalübertragung beteiligt sind, ist unklar, welches Enzym bzw. welche Enzyme für die Umkehrung der CEACAM3-Phosphorylierung verantwortlich sind. Bei unserer Suche nach Proteinphosphatasen, die die CEACAM3-induzierte Signalübertragung hemmen, identifizierten wir die rezeptorartige Protein-Tyrosin-Phosphatase PTPRJ als negativen Regulator der CEACAM3-vermittelten Phagozytose. Die Überexpression der aktiven PTPRJ-Phosphatase-Domäne reduzierte die CEACAM3-vermittelte Bakterienaufnahme stark, während PTPRJ-defiziente Zellen einen Funktionsgewinn-Phänotyp zeigten. Wir konnten außerdem zeigen, dass die rekombinante Phosphatase-Domäne von PTPRJ in der Lage ist, beide Tyrosinreste des zytoplasmatischen ITAM-ähnlichen Motivs von gereinigtem CEACAM3 direkt zu dephosphorylieren. Diese direkte Wirkung von PTPRJ auf CEACAM3 wurde in *In-vitro*-Studien bestätigt, in denen die Dephosphorylierung von synthetischen CEACAM3-abgeleiteten Phospho-Peptiden durch rekombinantes PTPRJ nachgewiesen wurde. Im Einklang mit der herausragenden Rolle der Tyrosinphosphorylierung der ITAM-ähnlichen Sequenz bei der Induktion der Lamellipodienbildung zeigten menschliche Phagozyten, denen PTPRJ fehlt, als Reaktion auf CEACAM-bindende Bakterien übermäßige Lamellipodien und eine verstärkte Opsonin-unabhängige Phagozytose. Unsere Ergebnisse deuten darauf hin, dass PTPRJ ein negativer Regulator der CEACAM3-vermittelten Phagozytenfunktionen ist und ein potenzielles Ziel zur Einschränkung von CEACAM3-initiierten Entzündungsprozessen darstellt.

Es wird vermutet, dass die CEACAM3-Aktivität ein Grund dafür sein könnte, dass CEACAM-bindende Krankheitserreger wie *N. gonorrhoeae* vom menschlichen Körper meist in Schach gehalten werden. In seltenen Fällen können sich Gonokokken jedoch über den ursprünglichen Infektionsort hinaus ausbreiten und disseminierende Gonokokkeninfektionen verursachen. Angesichts der Zunahme multiresistenter *N. gonorrhoeae*-Stämme wird es immer wichtiger,

Gonokokken-Infektionen in Versuchstieren besser zu modellieren, da dies ein wichtiger erster Schritt zur Entwicklung neuer Behandlungsstrategien ist. Die Verwendung von Mäusen, die den Opa-bindenden humanen CEA-Rezeptor auf der Vaginalschleimhaut exprimieren, hat bereits dazu beigetragen, eine große Schwäche von Mäusen als Gonokokken-Infektionsmodell zu überwinden. Dennoch sind Infektionen aufgrund der starken Anpassung von *N. gonorrhoeae* an den Menschen bei Mäusen in ihrer Dauer und Krankheitsentwicklung begrenzt. In dieser Arbeit beschreiben wir mehrere Ansätze zur Optimierung des weiblichen CEA-transgenen (CEAtg) Mausmodells. Der Fokus dieser Arbeit war es, das zuvor verwendete 24-Stunden-Infektionsmodell zu erweitern, um Gonokokken-Infektionen in CEAtg-Mäusen für mindestens 48 Stunden aufrecht erhalten zu können. In Übereinstimmung mit Berichten anderer Forscher deuten unsere Ergebnisse darauf hin, dass die intraperitoneale Verabreichung der Antibiotika Vancomycin HCl und Streptomycinsulfat die kommensale Flora des Vaginaltrakts der Maus minimiert und dadurch die Gonokokkenbesiedlung verbessert. Darüber hinaus haben wir beobachtet, dass das Passagieren von *N. gonorrhoeae* in der Maus einen positiven Effekt auf das Überleben der Gonokokken im Vaginaltrakt von Mäusen zu haben scheint. Weitere Experimente müssen klären, ob diese Modifikationen eine zuverlässige Gonokokkenbesiedlung von CEAtg-Mäusen über einen Zeitraum von mindestens 48 Stunden sicherstellen können. Wenn diese Modifikationen zu einer konsistenten Besiedlung des Vaginaltrakts von Mäusen über einen Zeitraum von mindestens 48 Stunden führen, wird es möglich sein, den Verlauf der Gonokokkeninfektion während dieser Anfangszeit zu untersuchen und die Wirksamkeit neuer medikamentöser Therapien zu testen.

1. Introduction

1.1 The immune system

Through contact with other human beings and our environment, we encounter potentially pathogenic microorganisms every day. These can enter the body through intimate contact, they can be ingested via the oral route, or they can be inhaled so that they colonize the mucous membranes in the respiratory, intestinal or urogenital tracts of our body (Doron & Gorbach, 2008). An effective protection of our body against these pathogens are the anatomical and physiological barriers. For example, an intact cornified skin is a very efficient protection against invasion of pathogens (Baroni et al., 2012; Turvey & Broide, 2010). Secreted antimicrobial peptides and lipids such as the fatty acid sphingosine contribute to this protection by suppressing the growth of bacteria (Bibel et al., 1992; Chambers & Vukmanovic-Stejic, 2020; Wertz, 2018). Mucins, which make up the main component of the mucus layer on surfaces of the gastrointestinal tract, respiratory tract, or genital tract, trap specific pathogens via their carbohydrate side-chains and prevent the further penetration of the microorganisms to the underlying tissue (Belley et al., 1996, 1999). In the stomach, in turn, the acidic pH prevents the proliferation of harmful organisms, inhibiting the spread of foodborne pathogens to the gut (Tennant et al., 2008), and in the tear fluid, there are antimicrobial peptides and proteins such as lysozyme or lactoferrin restricting pathogen growth (Flanagan & Willcox, 2009; Flemming, 1922; McDermott, 2013; Oram & Reiter, 1968). If these barriers are not sufficient to keep pathogens from entering the organism, the most important protection against the invasion and pathogenic effects of these microorganisms is the immune system. It has the task of detecting pathogens and exhibits various features to counteract harmful microbial agents (Beutler, 2004; Parkin & Cohen, 2001). Jawed vertebrates (and thus also humans) have an immune system that is generally divided into two branches, the innate and the adaptive or acquired immune defense. However, both branches work closely together and support each other's activities against pathogenic invaders (**Figure 1**) (Cooper & Alder, 2006; McDaniel et al., 2021). Components of the innate immune system recognize conserved microbial structures and induce a rapid immune response to inhibit the proliferation of infectious pathogens and promote their elimination (Medzhitov & Janeway Jr., 2000). In contrast, the adaptive immune system intervenes in the defense processes with a

delay, but enables the pathogen-specific immune response through the recognition of specific antigens and thus forms an important complementary defense component of the immune system (Bonilla & Oettgen, 2010).

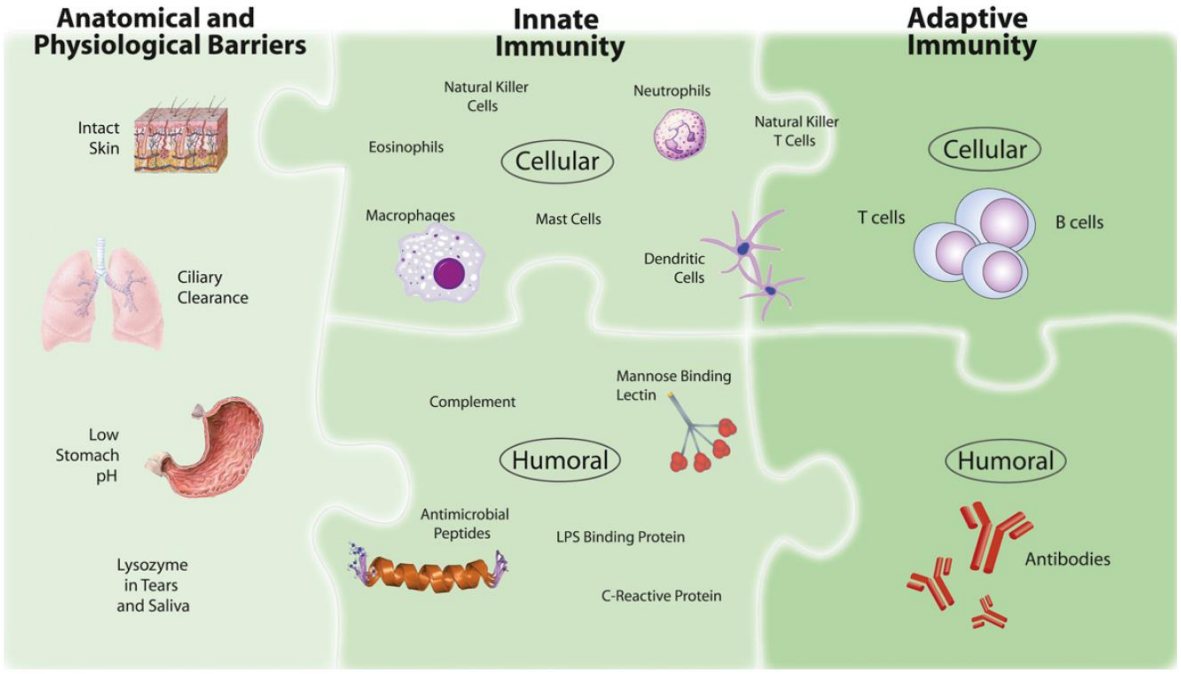

Figure 1: The mediators of immunity. In simple terms, the human defense system consists of three levels: anatomical and physiological barriers, innate immunity, and adaptive immunity. Important components of the anatomical or physiological barrier are, for example, the intact skin or the low pH in the stomach, which prevent pathogens from entering and proliferating. Factors of the innate immune system are immediately ready to defend the body against invaders. Innate immunity is mediated by various immune cells, including macrophages, dendritic cells, granulocytes (eosinophils and neutrophils), and natural killer cells. In addition, humoral factors also play a critical role in the innate immune response. Among the best-known humoral components are the proteins of the complement system. The adaptive immune response is mediated by B cells, antibodies, and T cells and enables an antigen-specific response. As the adaptive and innate immune systems work closely together, some elements are difficult to categorize. In particular, NK T cells, dendritic cells, and macrophages can be classified at the interface between innate and adaptive immunity (Turvey & Broide, 2010).

1.1.1 Cellular and humoral components of the innate immune system

Components of the innate immune system are immediately able to mount an immune response after the recognition of pathogens. This recognition is achieved by a set of germ-line encoded receptors that bind conserved microbial components, i.e. structures and patterns that are found in a broad spectrum of microorganisms (Medzhitov & Janeway Jr., 2000). Among these receptors, often referred to as pattern recognition receptors (PRRs) and

expressed by both, professional phagocytes (neutrophils, macrophages, and dendritic cells) and non-myeloid non-professional immune cells such as epithelial cells, the Toll-like receptors (TLRs), RIG-I-like receptors, nucleotide-binding oligomerization domain-like receptors (NLRs), and C-type lectin receptors (CLEC) are among the best-known receptor families (Medzhitov, 2007; Takeuchi & Akira, 2010). Depending on the receptor, they are expressed on the plasma membrane, the membrane of endolysosomes or in the cytoplasm of the cell, where they bind their receptor-specific ligand (Takeuchi & Akira, 2010). Although some of the pathogen structures recognized by innate immune receptors are also found in non-pathogenic microbes, they are often summarized as pathogen-associated molecular patterns (PAMPs) (Medzhitov & Janeway Jr., 2002). These include lipopolysaccharides (LPS) found in the outer membrane of gram-negative bacteria, bacterial or viral single strand RNAs, double strand RNAs of various viruses, the bacterial protein flagellin, or β-glucan found in the cell wall of fungi (Fitzgerald & Kagan, 2020; Kim et al., 2016; Rehwinkel & Gack, 2020; Shiokawa et al., 2017; Takeuchi & Akira, 2010).

In addition to the cell-mediated immune defense, various humoral factors play important roles in the recognition of pathogen-associated structures and the containment of the pathogens. These include the complement system, pentraxins, collectins, such as the mannose-binding protein (MBP), and antimicrobial peptides like defensins or cathelicidins (Beutler, 2004; Degn & Thiel, 2013; Ganz, 2003; Turvey & Broide, 2010). The complement system represents one of the best studied tools of the innate humoral defense. It consists of more than 30 proteins that are activated sequentially in a cascade by proteolytic cleavage and can perform several functions in the pathogen defense. One of these functions is the opsonization of pathogens, which enables complement receptors (CRs) of the immune system to recognize and phagocytose the invaders (Sarma & Ward, 2011). Moreover, the complement system is capable of lysing pathogens, an activity, that relies on the formation of the membrane attack complex (MAC), which consists of the complement factors C5b, C6, C7, C8 and several C9 proteins. The formation of these pore-forming complexes in the pathogen membrane increases the membrane permeability, eventually leading to the destruction of the pathogen (Sarma & Ward, 2011). In addition, the complement system also contributes to the defense against microbes and microbial particles by releasing the anaphylatoxins C3a and C5a, that result from the cleavage of the complement factors C3 and C5 and act as messengers to

attract phagocytes and other immune cells to the site of infection (Degn & Thiel, 2013; Merle et al., 2015). Anaphylatoxins also induce the generation of reactive oxygen species (ROS) in macrophages and neutrophilic granulocytes, leading to further pathogen damage (Elsner et al., 1994; Goldstein et al., 1975).

1.1.2 Neutrophilic granulocytes – the soldiers of immunity

All human cells are to some extent able to phagocytose larger particles (≥ 0.5 µm). However, while non-professional phagocytes can only ingest apoptotic bodies or pathogen debris, professional phagocytes are well equipped and capable of rapidly and efficiently internalizing and eliminating entire pathogens. This group of professional phagocytes includes macrophages, dendritic cells and neutrophilic granulocytes (Uribe-Querol & Rosales, 2020).

Neutrophilic granulocytes (polymorphonuclear neutrophils, neutrophils) are by far the most abundant immune cells in the human body and represent one of the most important arms of the cellular immune defense (Burn et al., 2021). They are also referred to as polymorphonuclear neutrophils (PMNs) because of the characteristic morphology of their nucleus, which is divided into three to five lobes. They originate in the bone marrow and have a lifespan of only hours to a few days after they leave the bone marrow niche as mature neutrophilic granulocytes (Lehman & Segal, 2020; Pillay et al., 2010). Mature neutrophils circulate in the bloodstream until they leave the circulation in response to inflammatory or infection signals to advance in droves to the damaged tissue or site of infection (de Oliveira et al., 2016). Activated neutrophils are capable of activating a variety of different defense mechanisms and components to defend the integrity and health of the body. For example, neutrophils possess various surface receptors that trigger phagocytosis of pathogens either after direct binding to defined microbial structures (opsonin-independent phagocytosis) or after recognition of opsonins that label microbes or microbial particles as targets for phagocytosis (opsonin-dependent phagocytosis) (Mayadas et al., 2014; Uribe-Querol & Rosales, 2020). For example, the receptor Dectin-I binds β-glucan in the cell wall of fungi in an opsonin-independent manner and promotes internalization of these microbes into human neutrophils (Flannagan et al., 2012; Kennedy et al., 2007). In contrast, Fcγ receptors and

complement receptors are among the best known opsonin-dependent phagocytosis-mediating receptors. Fcγ receptors (FcγRs) bind the Fc fragment of immunoglobulin G (IgG) antibodies attached to foreign particles (Anderson et al., 1990; Cox & Greenberg, 2001), and complement receptors rely on the labelling of pathogens by specific complement factors in order to recognize them and to contribute to their elimination by phagocytosis (Bianco et al., 1975; Dustin, 2016; Fällman et al., 1993).

In addition to phagocytosis, neutrophil microbicidal activities also include the formation of neutrophil extracellular traps (NETs) (Brinkmann et al., 2004), the production of reactive oxygen species (Mayadas et al., 2014) and the secretion of anti-microbial and pro-inflammatory proteins, which neutrophils store in various granules until they are released (**Figure 2**) (Othman et al., 2022). Neutrophils have a total of three types of granules which are formed at different stages of neutrophil development and differ in part by their protein content (Borregaard et al., 1995; Borregaard & Cowland, 1997). These granules fuse with the phagosome membrane during phagosome maturation or release their protein content into the extracellular space in a process known as degranulation, allowing neutrophils to exert their antimicrobial activity beyond their cellular boundaries (Othman et al., 2022).

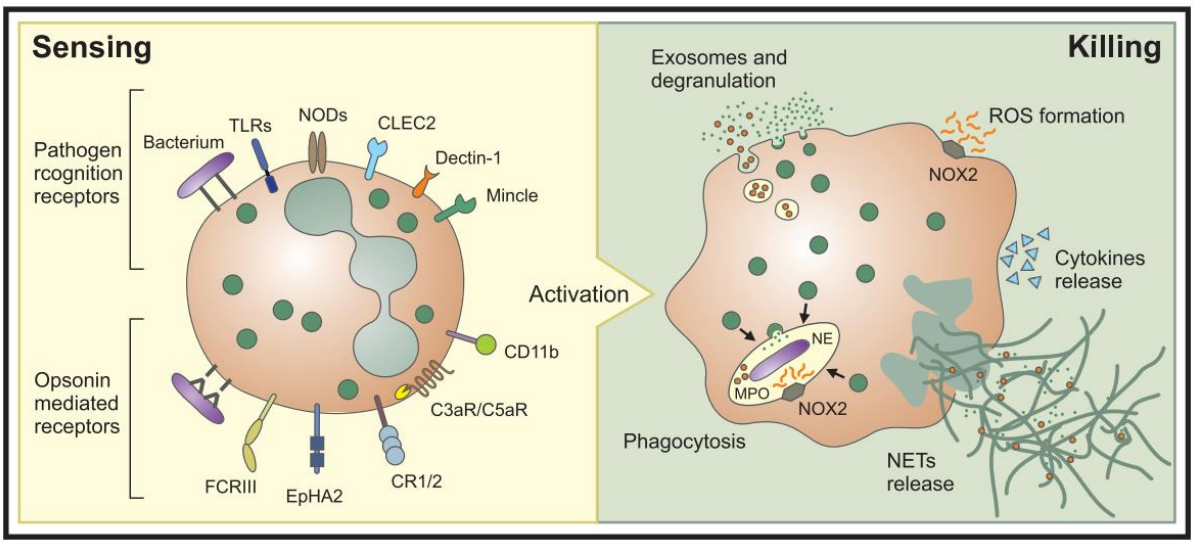

Figure 2: Neutrophil immune receptors and microbicidal activities. Neutrophil granulocytes possess a variety of pathogen recognition receptors (PRRs), such as TLRs or the receptor Dectin-1, which recognizes ß-glucans in the cell wall of yeasts. In addition to PRRs, neutrophils also express a number of receptors that recognize opsonized pathogens or opsonized microbial particles. These include, for example, the FC receptors or the complement receptors CR1 and CR2. Binding of these receptors to pathogenic structures or to pathogen-bound opsonins leads to activation of a range of neutrophil microbicidal activities. These control the phagocytosis of pathogens, the

formation of neutrophil extracellular traps (NETs), the formation of reactive oxygen species (ROS) or the degranulation of the various granules (Burn et al., 2021).

1.2 The CEACAM family

Members of the carcinoembryonic antigen (CEA) family belong to the immunoglobulin (Ig) superfamily and include two subgroups: the pregnancy-specific glycoproteins (PSG) and the CEA-related cell adhesion molecules (CEACAMs) (Thompson et al., 1991). In humans, ten protein-coding PSG genes exist, encoding the soluble proteins PSG1-9 and PSG11, which are produced during pregnancy by the placental syncytiotrophoblast in such large quantities that they are among the most abundant placental proteins in maternal blood during gestation (Lin et al., 1974; Moore & Dveksler, 2014). In contrast to the secreted PSG proteins, members of the CEACAM family, with the exception of CEACAM16, are all membrane-associated. This membrane binding occurs either via a glycosylphosphatidylinositol (GPI) anchor, as in the case of CEA (the product of the *CEACAM5* gene) and CEACAM6-8, or via a carboxy-terminal transmembrane domain that is part of the CEACAMs CEACAM1, CEACAM3, CEACAM4, and CEACAM18-21 (**Figure 3**) (Kuespert et al., 2006). In total, the human CEACAM family consists of twelve members that share besides the membrane anchoring additional features. For example, all CEACAMs are highly glycosylated proteins, and all have an amino-terminal immunoglobulin variable-like (IgV) domain. In addition, most CEACAM members possess between one and six immunoglobulin constant-like (IgC) domains, with CEACAM3, 4, and 19 being the exception as, besides the N-terminal IgV domain, they have no additional Ig domains (Kuespert et al., 2006). CEACAMs are mainly expressed on epithelial cells and/or granulocytes, with individual CEACAMs showing specific expression patterns (Hammarström, 1999). Among them, CEACAM1 has the broadest expression spectrum, encompassing surface expression on epithelial cells, endothelial cells, lymphocytes, and granulocytes (Kammerer et al., 1998; Prall et al., 1996). CEACAM3 and CEACAM4, on the other hand, are found exclusively on granulocytes, whereas CEA is expressed only on epithelial cells, particularly on the gastrointestinal epithelium (Hammarström, 1999; Kuespert et al., 2006; Kuroki et al., 1991; Thompson, 1995).

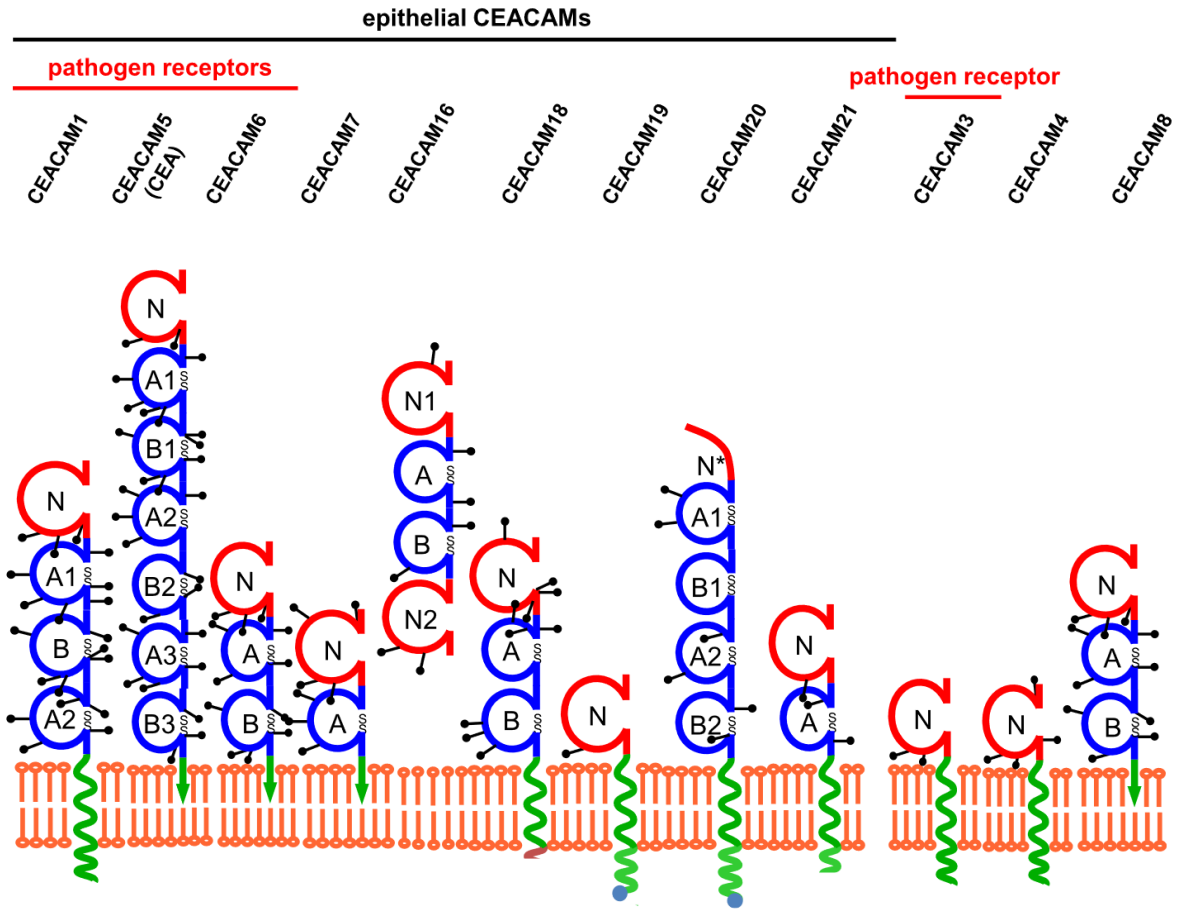

Figure 3: Members of the human CEACAM family. The human CEACAM family consists of twelve members that share structural similarities. All possess an N-terminal immunoglobulin variable-like (IgV) domain (shown in red) and between zero and six immunoglobulin constant-like (IgC) domains (shown in blue) that form disulfide bridges (S-S). Except for CEACAM16, all members are membrane-associated, either via a GPI anchor (green arrow) or via a transmembrane domain (green membrane-spanning spiral line). Glycosylation of CEACAMs is shown as black sticks. Most CEACAMs are found on epithelial cells (and in some cases other cells), whereas CEACAM3, CEACAM4, and CEACAM8 are expressed only on granulocytes. CEACAM1, CEACAM3, CEA, and CEACAM6 are used as receptors by several human-specific pathogens (Tchoupa et al., 2014).

The biological functions of the CEACAM family members are manifold (Hammarström, 1999; Kuespert et al., 2006). For example, CEACAM1, CEA, CEACAM6 and CEACAM8 engage in homophilic and/or heterophilic CEACAM interactions and thus play a role in cell-cell adhesion (Benchimol et al., 1989; Oikawa et al., 1991; Teixeira et al., 1994). CEACAM1 isoforms carrying the immunoreceptor tyrosine-based inhibitory motif (ITIM) in the cytoplasmic part of the receptor (CEACAM1 occurs in a total of 11 isoforms) have been shown to mediate inhibitory signals in the cell (Chen, Zimmermann, et al., 2001; Gray-Owen & Blumberg, 2006). In addition, numerous studies on CEACAM1 have shown that this receptor also plays a role in

angiogenesis, insulin homeostasis, apoptosis, and tumour development, as well as in the modulation of innate and adaptive immune responses (Gray-Owen & Blumberg, 2006). Furthermore, CEACAM1 and several other CEACAM members (CEACAM3, CEA, and CEACAM6) are known to function as receptors for several human-specific pathogens (Tchoupa et al., 2014).

CEACAMs are ideal anchor points for successful host colonization from a pathogen perspective: they are expressed on mucosal tissues that are known sites of entry for bacterial pathogens. For example, the gram-negative pathogens *Neisseria gonorrhoeae*, *Neisseria meningitidis*, *Haemophilus influenzae*, *Moraxella catarrhalis*, several pathogenic *Escherichia coli* strains and *Heliobacter pylori* possess distinct CEACAM-binding adhesins that facilitate their colonization of the human host (Berger et al., 2004; Chen et al., 1997; D. J. Hill & Virji, 2003; Königer et al., 2016; Tchoupa et al., 2014; Virji et al., 2000; Virji, Makepeace, et al., 1996). In the case of *N. gonorrhoeae* and *N. meningitidis*, CEACAM binding is achieved via the β-barrel shaped opacity-associated (Opa) proteins (Chen et al., 1997; Virji, 2009; Virji, Makepeace, et al., 1996). For *N. gonorrhoeae*, it is furthermore known that its ability to interact with epithelial CEACAMs also allows the suppression of an important host defense mechanism (Muenzner et al., 2005). The close Opa-CEACAM mediated contact between host cells and these bacteria, enables the short-lived gas nitric oxide (NO), produced by *N. gonorrhoeae* as an intermediate of anaerobic respiration, to reach the epithelial cell and to stimulate the NO-responsive sGC-PKG host signalling pathway. The induction of this pathway results in the upregulation of the host surface protein CD105, which by activating the matrix-binding integrin proteins prevents the exfoliation of infected epithelial cells, that is normally initiated by the host to eliminate tissue-associated bacteria (Muenzner et al., 2005, 2010; Muenzner & Hauck, 2020). However, CEACAM binding is not in all cases associated with exclusively positive aspects for the pathogen. Rather, the consequences depend on the identity of the bound CEACAM receptor (Bonsignore et al., 2020). Recognition by the granulocyte-expressed CEACAM3 receptor is detrimental to the pathogen, leading to its CEACAM3-mediated phagocytosis and destruction (Bonsignore et al., 2020).

1.3 The phagocytic receptor CEACAM3

In 1996, it was first shown that CEACAM3 functions as a receptor for Opa-expressing gonococci and that this interaction leads to the internalization of the bound bacteria (Chen & Gotschlich, 1996). Today, the role of CEACAM3 as an innate phagocytic receptor that in addition to phagocytosis controls reactive oxygen species (ROS) generation is well established (Bonsignore et al., 2020; Sarantis & Gray-Owen, 2007; Schmitter et al., 2004). CEACAM3 is found exclusively on granulocytes, more specifically on granulocytes of higher primates, and thus on a cell type specialized for the defence against invading pathogens (Adrian et al., 2019; Nagel et al., 1993; Pils et al., 2008). In the cytoplasmic tail, CEACAM3 possesses an immunoreceptor tyrosine-based activation (ITAM)-like motif containing two tyrosine residues that are phosphorylated upon CEACAM3 receptor engagement, subsequently serving as docking sites for several downstream signalling molecules (Buntru et al., 2012; Chen, Bolland, et al., 2001). Classical ITAM motifs possess two tyrosine residues embedded in the sequence YxxI/L$x_{(6\text{-}12)}$YxxI/L (Underhill & Goodridge, 2007). In CEACAM3, these ITAM tyrosine residues are located at the amino acid sequence positions 230 and 241, its sequence, however, deviates from the classical ITAM consensus motif in that it contains a methionine instead of the carboxy-terminal leucine or isoleucine residue (**Y**EE**L**LKHDTNI**Y**CR**M**) (Buntru et al., 2012; McCaw et al., 2003).

1.3.1 CEACAM3 signalling leading to phagocytosis and bacterial elimination

CEACAM3 signal transduction is initiated by binding of the receptor to its bacterial ligand. The receptors rapidly accumulate and assemble at the bacterial contact site, causing the intracellular recruitment and activation of Src family kinases (SFK), which phosphorylate the tyrosine residues of the CEACAM3-ITAM-like motif (**Figure 4A**) (Bonsignore et al., 2020; Hauck et al., 1998; McCaw et al., 2003; Schmitter, Pils, Weibel, et al., 2007). Studies in which the CEACAM3-ITAM motif was affected by replacement of either tyrosine residue with the amino acid phenylalanine have clearly demonstrated that the presence and phosphorylation of both ITAM tyrosine residues are important for CEACAM3-mediated phagocytosis (Chen, Bolland, et al., 2001; McCaw et al., 2003; Schmitter et al., 2004). In their phosphorylated state they serve as anchor points for CEACAM3 effector proteins allowing the assembly of a transient signalling complex (Buntru et al., 2012). One protein that interacts directly with the phosphorylated

CEACAM3 tyrosine residue Y230 is the guanine nucleotide exchange factor (GEF) Vav, which binds to the receptor through its SH2 domain (Schmitter, Pils, Sakk, et al., 2007). Vav facilitates the GTP loading of the small Rho GTPase Rac, thereby tiggering the activation of Rac proteins in the vicinity of the clustered CEACAM3 molecules (Schmitter, Pils, Sakk, et al., 2007). The adapter protein Nck also interacts with the CEACAM3-ITAM-like motif via the phosphorylated tyrosine residue Y230 (Pils et al., 2012). Its interaction with the WAVE complex protein Nck-associated protein 1 (Nap1) allows Nck to direct the proteins of the WAVE complex to the bacteria-engaged CEACAM3 receptor (Pils et al., 2012). An interaction between the protein cytoplasmic FMR1-interacting protein (CYFIP; also known as Sra-1), which is also part of the WAVE complex, with the small GTPase Rac, is considered as one of the prerequisites for the activation of the WAVE complex (Kobayashi et al., 1998; Lebensohn & Kirschner, 2009). The activated WAVE complex activates the Arp2/3 complex, which controls the nucleation of new actin filament branches forming the local actin-containing lamellipodia that establish the phagocytic cup around the CEACAM3-bound pathogen (**Figure 4B**) (Buntru et al., 2012; Rougerie et al., 2013).

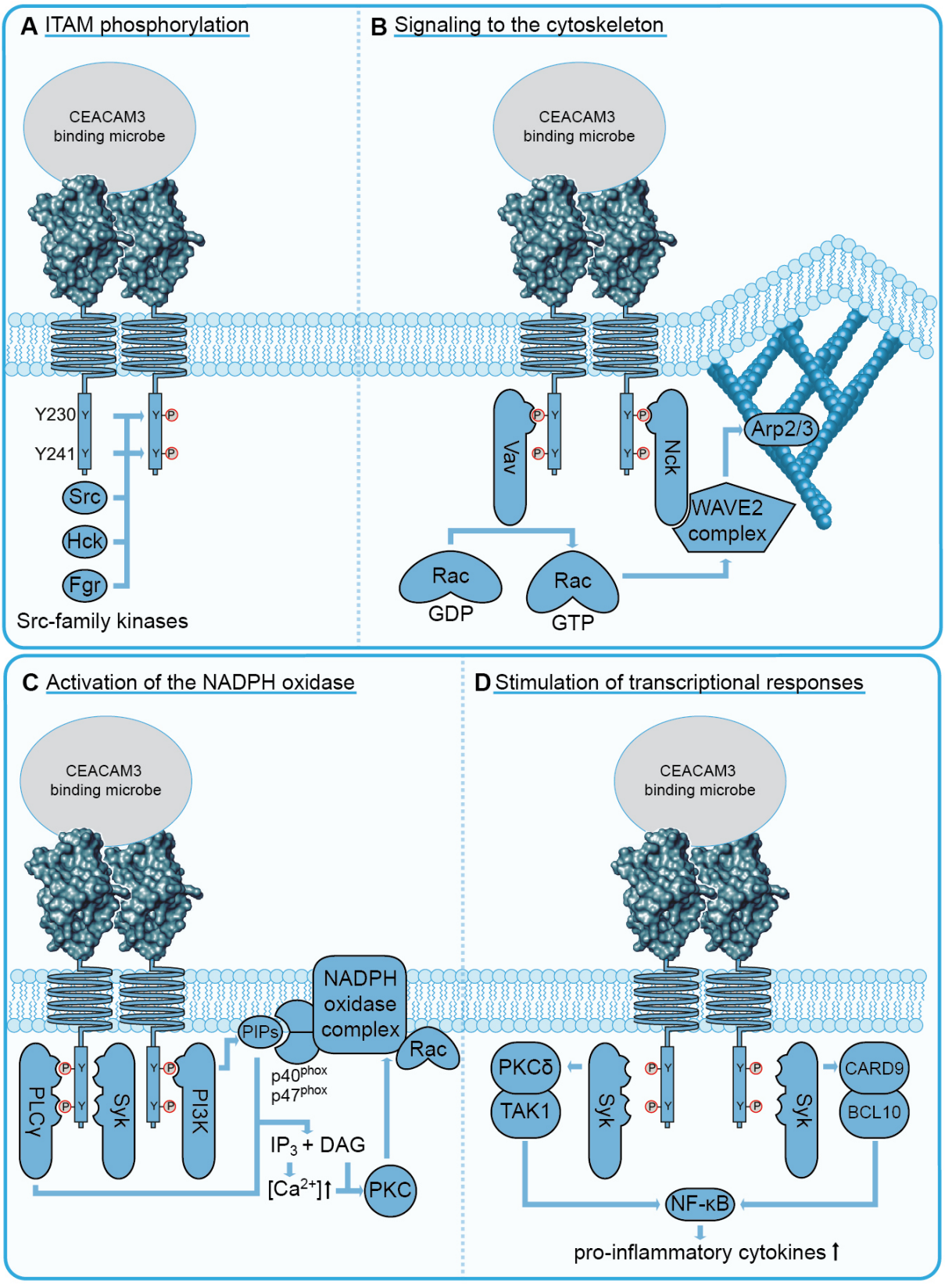

Figure 4: Overview of the signalling connections of the CEACAM3-ITAM-like motif. (A) Phosphorylation of the ITAM-like motif of CEACAM3. Binding of CEACAM3 receptors to a pathogen result in clustering of the receptors at the host-pathogen contact site. This leads to activation of Src family kinases (Src, Fgr, Hck), which subsequently phosphorylate the two tyrosine residues (Y230 and Y241) of the CEACAM3-ITAM-like motif. The phosphorylated

tyrosine residues act as docking sites for CEACAM3 effector proteins and are thus essential for the induction of CEACAM3 signal transduction. **(B)** CEACAM3 signalling to the actin cytoskeleton. After phosphorylation of the CEACAM3-ITAM-like motif by Src family kinases, the GEF Vav and the adapter protein Nck can bind to phosphorylated pY230 tyrosine residues of CEACAM3 receptors via their SH2 domains. By facilitating GTP loading of the small GTPase Rac, Vav promotes local activation of Rac proteins. GTP-loaded Rac promotes activation of the WAVE2 complex, which is recruited to the CEACAM3 receptor via Nck. The active WAVE2 complex activates the Arp2/3 complex, which, by mediating the nucleation of new actin filament branches, enables the formation of lamellipodia that lead the uptake of the pathogen. **(C)** CEACAM3 signaling connections leading to the activation of the NADPH oxidase complex. The lipid kinase PI3K, the phospholipase C γ (PLCγ) and the kinase Syk are also part of the CEACAM3 signalling complex. PI3Ks generate phosphatidylinositides (PIPs) that serve as docking sites for the NADPH oxidase subunits $p40^{phox}$ and $p47^{phox}$. The PLCγ cleaves PIPs into diacylglycerol (DAG) and inositol triphosphates (IP_3), thereby indirectly promoting PKC activation. The PKC kinase (activated by DAG and Ca^{2+}) contributes to the activation of the NADPH oxidase complex by phosphorylating several NADPH oxidase subunits. The active NADPH oxidase complex mediates the oxidative burst response that leads to the killing of the internalized bacteria. **(D)** CEACAM3 signalling leading to the production of pro-inflammatory cytokines. Syk, which is recruited to the CEACAM3 signalling complex after CEACAM3 phosphorylation, stimulates the activation of the transcription factor NFκB via signalling pathways involving PKCδ and TAK1 or CARD9 and BCL10. The active transcription factor NFκB controls transcriptional regulation of several pro-inflammatory cytokines. Thus, CEACAM3 signaling connections may also contribute to the production of pro-inflammatory cytokines (Bonsignore et al., 2020).

Intracellular pathogens internalized by CEACAM3 are subsequently eliminated via the CEACAM3-induced activation of reactive oxygen species (ROS)-generating NADPH oxidases that ultimately cause the destruction of the pathogens (Buntru et al., 2011, 2012; Sarantis & Gray-Owen, 2012). NADPH oxidase systems are multicomponent complexes consisting of, among others, the small GTPase Rac and the $p40^{phox}$ and $p47^{phox}$ subunits (Bedard & Krause, 2007). Certain 3'-phosphorylated phosphoinositides serve as binding sites for the NADPH oxidase subunits $p40^{phox}$ and $p47^{phox}$, allowing the assembly of the NADPH oxidase complex at the phagosome membrane (Kanai et al., 2001; Zhan et al., 2002). Phosphatidylinositol 3'-kinases (PI3Ks), known to catalyse the phosphorylation of phosphoinositides on the 3' position of the inositol ring, can bind directly to phosphorylated CEACAM3-pY230 via their SH2 domain located in the regulatory subunit of the kinases (Buntru et al., 2011). Indeed, studies assessing the concentration of 3'-phosphorylated phosphatidyl inositol phosphates (PIPs) during CEACAM3-mediated bacterial uptake by CEACAM3-transfected HeLA cells, have demonstrated the accumulation of phosphatidylinositol 3,4,5-trisphosphate (PI(3,4,5)P) at phagocytic cups (Booth et al., 2003). Aside from these, other phosphoinositides also play a role in the induction of the CEACAM3-mediated oxidative bust response. Phosphatidylinositol-(4,5)-bisphosphate ($PI(4,5)P_2$) serves as a substrate for the phospholipase C γ (PLCγ), which is

recruited to the receptor after CEACAM3 engagement (McCaw et al., 2003). It converts $PI(4,5)P_2$ to diacylglycerol (DAG) and inositol trisphosphate (IP_3) (Kaiser et al., 1990). DAG and Ca^{2+}, that is released by the action of IP_3, are in turn activators of the protein kinase C (PKC), which contributes to activation of the NADPH oxidase systems by phosphorylating several NADPH oxidase subunits (**Figure 4C**) (Belambri et al., 2018; Bonsignore et al., 2020).

In addition to phagocytosis and the oxidative burst, microbial recognition by CEACAM3 also leads to the activation of the transcription factor NFκB and NFκB-associated cytokine production. Studies by Heinrich et al. and Sintsova et al. demonstrate a role for the tyrosine kinase Syk in the CEACAM3-stimulated activation of this transcription factor (Heinrich et al., 2016; Sintsova et al., 2014). The investigations by Heinrich et al. furthermore suggest that the CARD9 adapter protein is involved in the CEACAM3-mediated stimulation of NFκB in response to recognition of *Moraxella catarrhalis* by CEACAM3 (Heinrich et al., 2016). Besides the role of Syk, the studies by Sintsova et al. demonstrate the involvement of the protein kinase C delta (PKCδ) and the serin/threonine kinase Tak1 in *N. gonorrhoeae*-triggered CEACAM3-mediated stimulation of NFκB (**Figure 4D**) (Sintsova et al., 2014). Proinflammatory cytokines generated upon CEACAM3 activation via the stimulation of NFκB cause the recruitment and activation of additional neutrophils which promote the bacterial clearance of the invading pathogens at the site of infection. Overall, CEACAM3 thus functions as a bacteria-binding receptor that mediates bacterial uptake by phagocytosis, bacterial killing by the induction of the NADPH oxidase system, and the initiation of a cytokine response via the activation of the transcription factor NFκB (Bonsignore et al., 2020).

1.3.2 Negative regulators of CEACAM3-mediated signalling

CEACAM3-mediated antimicrobial responses can protect the human body from harmful pathogens. With the aim of understanding these CEACAM3-mediated processes, numerous factors important for the induction of phagocytosis, the inflammatory response, and the oxidative burst have been identified in the past (Bonsignore et al., 2020). In contrast, only little is known about negative regulators of CEACAM3 signalling. Possible excessive CEACAM3-mediated production of pro-inflammatory cytokines that promote the recruitment and

activation of neutrophils, or CEACAM3-mediated massive production of reactive oxygen species, however, could also pose a risk to the human body and potentially lead to severe cell and tissue damage (Bonsignore et al., 2020; Stevens & Criss, 2018). To date, only the adapter protein growth factor receptor-bound protein 14 (Grb14) is known to negatively regulate CEACAM3-mediated signalling (Kopp et al., 2012). This non-enzymatic protein contains an SH2 domain that, like most proteins interacting directly with CEACAM3, binds the phosphorylated tyrosine residue 230 of the CEACAM3-ITAM-like motif. By interacting with this phospho-residue, Grb14 most likely prevents the binding of proteins to the receptor that are important for the CEACAM3 signalling, thereby attenuating the induction of CEACAM3-mediated activities (Kopp et al., 2012). Apart from this non-enzymatic protein, however, no other CEACAM3 regulator has yet been described that could limit CEACAM3 effector functions. Consequently, also the protein phosphatase(s) that reverse the phosphorylation of the CEACAM3-ITAM motif and thus prevent CEACAM3 signaling is/are unknown.

For other ITAM motif-containing molecules, such as the ζ-chain of the T cell receptor (TCR) or the phagocytic receptor Dectin-I, the receptor-type protein tyrosine phosphatases (PTPRs) PTPRJ (CD148) and PTPRC (CD45) have been shown to dephosphorylate the tyrosine residues of the ITAM motif (Baker et al., 2001; Cordoba et al., 2013; Furukawa et al., 1994; Goodridge et al., 2011). To investigate whether PTPRs might also play a role in the regulation of the CEACAM3-mediated signal transduction, J. Adrian recently performed a genetic screen as part of his PhD research in the laboratory of Prof. Dr. C. R. Hauck (Dissertation J. Adrian, 2019). Using lentiviral transduction of Cas9 and specific single guide RNAs (sgRNAs), he generated a total of 20 different PTPR-deficient HL60 cell populations to evaluate the role of all 20 human PTPRs in the CEACAM3-mediated bacterial internalization (Dissertation J. Adrian, 2019). The results of these infection studies suggest that several PTPRs, including PTPRF, PTPRG, PTPRJ, and PTPRS, interfere with CEACAM3-mediated phagocytosis (**Figure 5**) (Dissertation J. Adrian, 2019; Goob et al., 2022). However, further research is required to address which of these phosphatases reverse CEACAM3 phosphorylation and which of these enzymes are important for CEACAM3-mediated bacterial uptake.

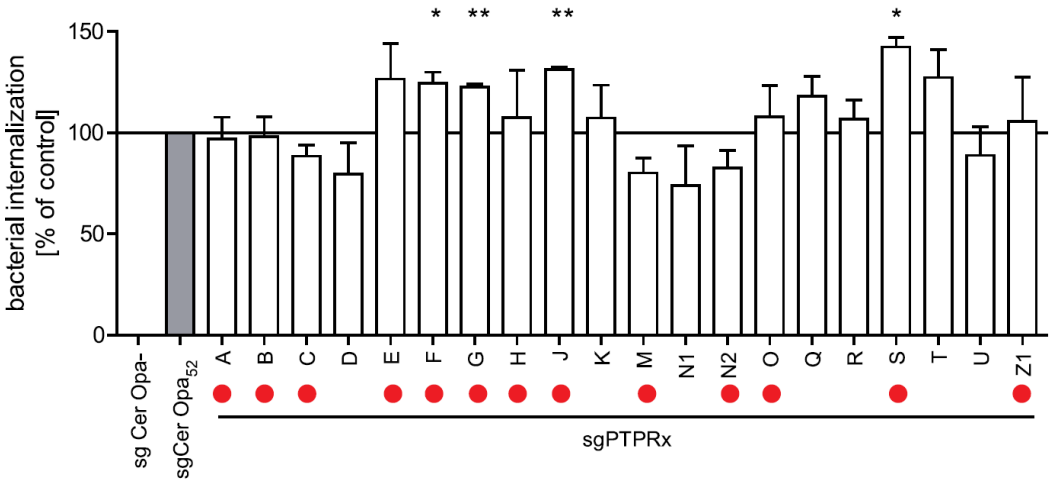

Figure 5: Knockout of the receptor-type protein tyrosine phosphatases PTPRF, PTPRG, PTPRJ and PTPRS promotes phagocytosis of *N. gonorrhoeae* in CEACAM3-mKate-expressing HL60 cells. HL60-CEACAM3-mKate cells transduced with the indicated PTPR-targeting sgRNA (sgPTPRx) or HL60-CEACAM3-mKate cells in which only cerulean is knocked out (sgCer; control cells) were infected with CSFE-labeled non-opaque (Opa-) or Opa_{52}-expressing *N. gonorrhoeae* (Opa_{52}). Fifteen minutes after infection, CFSE signals of extracellular bacteria were quenched with trypan blue, and CSFE fluorescence derived from the intracellular bacteria was measured by flow cytometry. Shown is the quantification of three independent uptake experiments performed by J. Adrian (Dissertation J. Adrian, 2019). Data are normalized to the CFSE fluorescence of control cells (sgCer) infected with *N. gonorrhoeae* expressing Opa_{52} (sgCer Opa_{52}) or no Opa adhesin (sgCer Opa-). The bars correspond to the mean values ± SEM of the three experiments. Bars showing significantly increased bacterial uptake compared to control cells (grey bar) according to Student's t-tests are marked with asterisks. *$p < 0.05$; **$p < 0.01$. PTPRs expressed by HL60 cells are indicated by red dots (Rincon et al., 2018). This figure was taken and modified from the dissertation of J. Adrian (Dissertaion J. Adrian, 2019) and can be found in the publication of (Goob et al., 2022) of which J. Adrian is a co-author.

1.3.3 CEACAM3-Pathogen co-evolution

Pathogen recognition is a prerequisite for immune receptors to trigger elimination of invading pathogens. CEACAM3, due to the high sequence similarity of its bacteria-binding IgV domain with the IgV domains of other pathogen-binding CEACAMs, is able to recognize various bacteria that use epithelial CEACAMs as docking sites for initial host colonization (Pils et al., 2008). While its extracellular domain resembles that of pathogen-binding CEACAM members, the intracellular domain of CEACAM3 shows high sequence similarity to the intracellular sequence of the orphan receptor CEACAM4, the only other CEACAM member that possesses an ITAM motif. Based on these similarities, it has been suggested that CEACAM3 may have arisen by recombination between a *CEACAM* gene encoding a pathogen-binding receptor (possibly CEACAM1 or CEA) and a precursor of the *CEACAM4* gene (Pils et al., 2008). Given the

ability of CEACAM3 to facilitate rapid phagocytosis and destruction of recognized bacteria, CEACAM-binding bacteria appear to respond to the existence of CEACAM3 by adapting their adhesins to bind to epithelial CEACAMs but not to be recognized by CEACAM3 (Bonsignore et al., 2020). Indeed, for Opa proteins of gonococci and meningococci, and for the CEACAM-binding adhesin Omp1 of *H. influenzae*, interaction studies have demonstrated that most of the adhesins enable CEACAM1 or CEA binding, but comparatively few, or none (as in the case of the meningococcal Opa proteins tested) are recognized by CEACAM3 (Bonsignore et al., 2020; De Jonge et al., 2003; Muenzner et al., 2000; Roth et al., 2013; Tchoupa et al., 2015).

At the same time, CEACAM3 also appears to adapt to counteract the loss of recognition of these pathogens and to keep pace with the evolution of the pathogen adhesins. Indeed, it has been shown that CEACAM3 is one of the most rapidly evolving genes in the human genome (Adrian et al., 2019). A recently described CEACAM3 polymorphism present in populations of African ancestry shows an expanded binding spectrum for several gonococcal Opa proteins, which are not recognized by the common CEACAM3 variant (Adrian et al., 2019). The four amino acid changes of this CEACAM3 allele are all located in the pathogen-binding domain of the receptor, and, interestingly, correspond exactly to the amino acids carried by CEACAM1 at the corresponding sites (Adrian et al., 2019; Bonsignore et al., 2020). These are the substitutions S43R, L44Q, V49A, and T69P, based on which we refer to this CEACAM3 allele as the CEACAM3-RQAP variant in this work. The discovery of this CEACAM1-approximating IgV polymorphism in CEACAM3 and its potential to bind *N. gonorrhoeae* Opa adhesins that are not recognized by the common receptor suggests that not only pathogens modify their adhesins to escape binding to CEACAM3, but that CEACAM3 co-evolves to catch up with pathogens and maintain its function as an innate immune receptor (Adrian et al., 2019; Zimmermann, 2019). Whether and to what extent this CEACAM3 polymorphism affects the interaction with other CEACAM-binding pathogens such as *N. meningitidis*, has not yet been investigated. Given the striking clustering of this CEACAM3 variant in African populations (Adrian et al., 2019), the continent with still the highest incidence of meningococcal disease and death (Mazamay et al., 2021), it would be particularly interesting to study the ability of the CEACAM3-RQAP allele in relation to the recognition of different *N. meningitidis* serogroups or other human-restricted pathogens responsible for severe disease in this part of the world. Such studies would allow us to better understand the significance of this CEACAM3-

RQAP polymorphism as a possible example of coevolution between human-restricted pathogens and their human immune receptors.

1.4 *Neisseria gonorrhoeae*

The gram-negative diplococcus *Neisseria gonorrhoeae* (*Ngo*) belongs to the genus *Neisseria* and is the causative agent of the sexually transmitted disease gonorrhoea (Quillin & Seifert, 2018). This pathogen, also known as gonococcus, is uniquely adapted to humans as its exclusive host and primarily colonizes the mucous membranes of the human genital tract and, less commonly, the mucous membranes of the rectum, mouth, or eye (Chan et al., 2016; Hunte et al., 2010; Noble et al., 1979; Quillin & Seifert, 2018; Wan et al., 1986).

With more than 86 million infections annually, gonorrhoea remains one of the most common sexually transmitted diseases worldwide (Rowley et al., 2019). One of the reasons for this high incidence may be the fact that the disease is often asymptomatic, especially in women, but to a lesser extent also in men (Edwards & Apicella, 2004), allowing for an unconscious transmission of the pathogen. In most cases, gonococcal colonization remains confined to the lower genital tract, where it frequently causes inflammation of the urethra (urethritis) in men and inflammation of the cervix (cervicitis) in women (Unemo et al., 2019). A common sign of gonococcal infection of the lower genital tract is a purulent discharge accompanied by pain during urination, especially in men. This purulent discharge, which consists largely of neutrophils and the pathogen itself, results from the massive influx of granulocytes into the site of infection, a typical characteristic of symptomatic gonococcal infections (Quillin & Seifert, 2018). Left untreated, gonococcal infections can spread to the upper genital tract, often causing more serious consequences, especially in women. Ascending infections are considered to cause pelvic inflammatory disease (PID) and can lead to ectopic pregnancies or infertility (Quillin & Seifert, 2018). In rare cases, when gonococci invade the tissues of the genital tract, enter the bloodstream, and spread throughout the body, severe systemic (disseminated) gonococcal infections, such as septic arthritis or infective endocarditis may occur (Bowmer et al., 1982; Suzaki et al., 2011). Moreover, women who are infected at the time of their child's birth are at risk for gonococcal transmission to the child's ocular mucosa

in the birth canal, formerly a common cause of new-born blindness (Alexander, 1988; Sandstrom, 1987). Gonococcal infections also increase the risk of transmitting or acquiring other sexually transmitted diseases. For example, the presence of gonococci may increase HIV shedding in HIV-infected persons, facilitating transmission of the virus (Fleming & Wasserheit, 1999; Ghys et al., 1997), and because gonococcal colonization often results in damage to the genital tissue, gonococci may also increase the susceptibility to HIV infection (Jarvis & Chang, 2012).

In most cases, our immune system is able to contain the gonococcal infection and prevent severe consequences. However, as the mentioned complications indicate, *N. gonorrhoeae* has strategies to evade immune system recognition and to modulate responses of the immune system (Quillin & Seifert, 2018). These strategies include the secretion of IgA proteases that disrupt IgA antibodies preventing an Fcα receptor-mediated immune response (Mistry & Stockley, 2006; Plaut et al., 1975). In addition, gonococci increase their colonization success by suppressing the host-mediated exfoliation of infected epithelial cells via surface expression of so-called opacity-associated (Opa) adhesion proteins that bind epithelial-expressed receptors of the CEACAM family. This close Opa-mediated binding to the host epithelial cells allows *N. gonorrhoeae* to stimulate the expression of the host protein CD105, which promotes the increased attachment of the cell to the extracellular matrix (Muenzner et al., 2005, 2010). Furthermore, via Opa-mediated interaction with immunoreceptor tyrosine-based inhibitory motif (ITIM)-containing CEACAM1 receptors on DCs or T cells, *N. gonorrhoeae* is able to suppress DC maturation and the inhibition of T cell activation, hindering the establishment of an adaptive immune response (Boulton & Gray-Owen, 2002; Yu et al., 2013). An effective and characteristic way for *N. gonorrhoeae* to evade the immune system lies also in their rapid antigen- and/or phase variation of surface proteins. Important adhesion or virulence factors, including Opa proteins, type IV pili and lipooligosaccharides (LOS) change their appearance with high frequency, a property that also massively complicates the development of *N. gonorrhoeae*-vaccines (Apicella et al., 1987; S. A. Hill & Davies, 2009; Jerse & Deal, 2013; Stern et al., 1986). Since no effective vaccine against *N. gonorrhoeae* is available to date, the treatment of gonococcal infections is still exclusively based on the use of antibiotics (WHO, 2016). However, due to the increasing emergence of multidrug-resistant *N. gonorrhoeae* strains, treatment options have declined rapidly in recent decades, making *N. gonorrhoeae* a

serious health threat to the human population (da Costa-Lourenco et al., 2017; Unemo et al., 2016).

1.4.1 *N. gonorrhoeae* opacity-associated (Opa) proteins

To attach to and invade human epithelial cells, *N. gonorrhoeae* utilizes several surface-expressed virulence factors. These include type IV pili that establish initial contact with the host, opacity-associated (Opa) adhesion proteins that subsequently mediate tight binding to epithelial cells and transcytosis into subepithelial tissues, and lipooligosaccharides (LOS) that promote the gonococcal invasion of host cells (Gray-Owen, 2003; Song et al., 2000; Swanson, 1973; Virji, Makepeace, et al., 1996; Wang et al., 1998).

Opa proteins are integral membrane proteins that owe their name to their characteristic of giving *N. gonorrhoeae* colonies an opaque appearance (Swanson, 1982). Most Opa proteins enable *N. gonorrhoeae* to interact with epithelial-expressed members of the human CEACAM family (Gray-Owen, Dehio, et al., 1997; Roth et al., 2013). However, a limited number of Opa adhesins are known not to bind to CEACAMs but to mediate interaction with heparansulphate proteoglycans (HSPG) also expressed on the host surface (Chen et al., 1995; Roth et al., 2013; van Putten & Paul, 1995).

In general, about 11 genes encoding Opa proteins are found in the genome of *N. gonorrhoeae* (Bhat et al., 1992). In most cases, however, not all Opa proteins are present on the surface of a single bacterium, which is due to the fact that the expression of each Opa protein can be independently switched on and off by phase variation, resulting in significant differences in the diversity and number of expressed Opa variants within *N. gonorrhoeae* populations (Mayer, 1982; Stern et al., 1986). This phase-variable expression of Opa adhesins is enabled by the presence of identical repeats of the pyrimidine-sequence CTCTT located in the coding region of *opa* genes. Mismatch of the pentameric repeat units during replication alters the number of the repeats that determines whether an *opa* gene is in the correct reading frame or in a shifted frame. Consequently, strand mismatch can either lead to expression of the Opa protein or can prevent its expression (Murphy et al., 1989; Stern et al., 1986).

Studies on the genetic variability of *opa* genes show that they are largely conserved but contain two highly variable (HV) regions. Most of this variation appears to be due to homologous recombination between the HV regions of different *opa* genes (Bilek et al., 2009; Connell et al., 1988). These HV regions are located in two of the total four extracellular loops of the Opa proteins and have been shown to be involved in host interaction (Bos et al., 2002). Together, these four surface-exposed loops connect the eight conserved β-strands that give the Opa proteins their membrane-spanning β-barrel shape. One of the two non-hypervariable loops is highly conserved, the other one shows moderate variability, which is why it is often referred to as the semi-variable loop (Bos et al., 2002; Malorny et al., 1998).

1.5 *Neisseria meningitidis*

Besides *N. gonorrhoeae*, *Neisseria meningitidis* (*Nme*) is the only other pathogen within the genus *Neisseria*. However, unlike *N. gonorrhoeae*, *N. meningitidis* usually occurs as a harmless inhabitant of its ecological niche, the nasopharynx of humans. Up to 10% of the population are unnoticed carriers of this diplococcus, which is transmitted from person to person by droplet infection (Caugant & Maiden, 2009; Pizza & Rappuoli, 2015). Yet, *N. meningitidis* is also known to cause the most severe infections of the meninges (meningitis) when it crosses the blood-brain barrier (Coureuil et al., 2012). Among the total of twelve *N. meningitidis* serogroups, which are distinguished by the composition of their polysaccharide capsules, invasive meningococcal diseases are almost exclusively caused by meningococci of the serogroups A, B, C, W, X, and Y (Caugant & Brynildsrud, 2020; Pizza & Rappuoli, 2015). While nasopharyngeal colonization by *N. meningitidis* is mostly without consequences, invasive courses of infection are fatal in up to 15% of infected individuals (Rouphael & Stephens, 2012), and survivors often have to cope with severe lifelong impairments. These include damage of the cranial nerves, mental retardation, inner ear damage leading to hearing loss, seizures, or hemiplegia (Vyse et al., 2013). Although effective vaccines against all invasive meningococcal strains are now available, sporadic to epidemic outbreaks of meningitis continue to occur worldwide. In particular, the African continent and especially the countries of the "meningitis belt," which extends south of the Sahara from Senegal in the west to Ethiopia and Somalia in the east, have been affected by large meningococcal serogroup A epidemics in the past (Crum-

Cianflone & Sullivan, 2016; Mazamay et al., 2021; Stephens et al., 2007). Although these cases declined significantly after 2010 as a result of large-scale vaccination with an *N. meningitidis* serogroup A vaccine, an increase in outbreaks caused by other invasive meningococcal strains was observed instead. In particular, strains from serogroups X, C, and W have been responsible for meningitis outbreaks in the meningitis belt in recent years (**Figure 6**) (Mazamay et al., 2021).

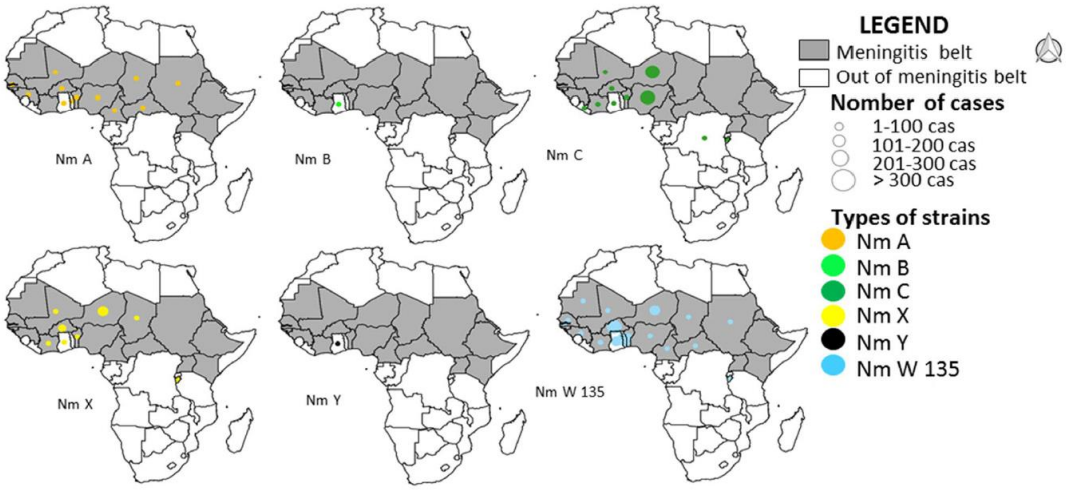

Figure 6: Spatial distribution of the major meningitis-causing *N. meningitidis* strains in Africa from 2011 to 2017. The countries in Africa that belong to the "meningitis belt" are marked in gray. This area stretches from Senegal in the west to Ethiopia and Somalia in eastern Africa and is considered the region with the highest incidence of bacterial meningitis worldwide. Shown are the cases caused in each country by the serogroups A, B, C, X, Y, and W-135 for the period 2011 to 2017. This figure was modified from (Mazamay et al., 2021).

Isolated cases or smaller local meningococcal outbreaks also occur outside Africa, although less frequently. In the past, these were often caused by meningococci of serogroups B or C (Stephens et al., 2007). In recent years, the number of cases associated with meningococci of serogroup C has declined, but instead, an increase in cases caused by bacteria of the serogroups Y and W has been described, particularly in parts of America and in Europe (Abad et al., 2014; Broeker et al., 2015; Krone et al., 2019).

Although meningococci may be encapsulated or non-encapsulated, the capsule appears to be almost always present in cases of disseminated courses, indicating its central role as a virulence factor in meningococcal pathogenesis. It protects the pathogen against recognition by antibodies and the complement-mediated immune response, facilitating its survival in the

bloodstream (Tzeng et al., 2016; Uria et al., 2008; Vogel & Frosch, 1999). In addition to the polysaccharide capsule, the virulence of *N. meningitidis* is influenced by several colonization factors. Like *N. gonorrhoeae*, *N. meningitidis* expresses type IV pili that mediate initial contact with the epithelial tissue (Nassif et al., 1997; Virji, Alexandrescu, et al., 1992), as well as Opa proteins that enable tight host binding to members of the CEACAM family (Virji, Makepeace, et al., 1996). However, unlike *N. gonorrhoeae*, *N. meningitidis* expresses additional adhesins, such as the β-barrel-shaped adhesin Opc. This protein facilitates invasion into epithelial and endothelial cells by binding to HSPGs and the integrin-binding extracellular matrix proteins vitronectin and fibronectin (de Vries et al., 1998; Sa et al., 2010; Unkmeir et al., 2002; Virji, Makepeace, et al., 1992). In addition, the adhesin and penetration protein App (Hadi et al., 2001; Serruto et al., 2003) and the coiled-coil adhesin NadA (Neisseria adhesin A) (Capecchi et al., 2005), among others, enable *N. meningitidis* to colonize humans and penetrate deeper tissues.

2. Aims of the study

Since the discovery that CEACAM3 controls the efficient phagocytosis and elimination of a number of human-restricted bacterial pathogens, numerous factors involved in the execution of CEACAM3-initiated responses have been deciphered. The importance of tyrosine phosphorylation of the CEACAM3-ITAM-like sequence as the initial event triggering CEACAM3 signalling is well described. In contrast, little is known about the cellular factors, in particular protein phosphatases, that dephosphorylate the CEACAM3 cytoplasmic tail and thus prohibit CEACAM3 signalling in the absence of ligands. Preliminary studies indicated that several receptor-type protein tyrosine phosphatases, including PTPRF, PTPRG, PTPRJ, and PTPRS, could counteract CEACAM3-mediated signaling. However, it remained unclear, which of these candidates opposes CEACAM3 phosphorylation and which of these enzymes is relevant for CEACAM3-mediated phagocytosis. Moreover, while it has been realized that CEACAM3 is one of the most rapidly evolving proteins in humans, the extent to which CEACAM3 polymorphisms affect the interaction with major CEACAM-binding microbial pathogens, such as *N. meningitidis*, has not been investigated. To further clarify these urgent questions and to further elucidate the evolutionary arms race between humans and specialized human-restricted pathogens, we addressed the following questions in this work:

(1) A CEACAM3 polymorphism, the CEACAM3-RQAP allele, is common in different ethnicities in sub-Saharan Africa, yet is not present in European or Asian populations. The distribution of this allele coincides with the so-called meningitis belt, a region affected by recurring *N. meningitidis* epidemics. We wondered if the CEACAM3-RQAP allele is an adaptation to cope with meningococcal Opa proteins that escape recognition by the common CEACAM3 allele. To address this question, we analysed the CEACAM-binding spectrum of a *N. meningitidis* strain-collection covering different serogroups. Furthermore, we determined the interaction of individual meningococcal Opa proteins and the CEACAM3-RQAP allele and investigated the consequences of this interaction in functional assays of phagocytosis (Project I).

(2) Which of the candidate receptor-type protein tyrosine phosphatases (PTPRF, PTPRG, PTPRJ, or PTPRS) is involved in regulating CEACAM3-mediated phagocytosis? Along these lines, we have created defined genetic knock-outs in human myeloid cells and

studied the consequences in uptake assays with CEACAM3-binding *N. gonorrhoeae*. Detailed biochemical and functional studies were conducted to clearly delineate the role of specific PTPR family member(s) for CEACAM3-mediated phagocytosis (Project II).

The development of new treatment strategies against gonococcal infections is urgently needed due to the growing number of multidrug-resistant gonococcal strains. However, research approaches in this regard require the usability of an animal model that can replicate *N. gonorrhoeae* colonization in humans as closely as possible. A major limitation in modelling vaginal tract gonococcal infections in female mice has already been overcome by the use of transgenic mice expressing the human CEA protein as a mucosal receptor for Opa-adhesin-expressing gonococci. However, even in this optimized infection model, vaginal colonization by *N. gonorrhoeae* can so far only be maintained for a limited duration due to the strong adaptation of this pathogen to humans. Therefore, in this work, we aimed to optimize the CEAtg mouse model to extend the observation beyond the 24-hour infection period studied previously. In doing so, we addressed the question:

(3) Can we extend the duration of infection in CEAtg female mice to 48 hours by modifying the previously established 24h-infection-protocol? Several areas of optimization, either affecting the pathogen or directed against the microbiota of the host, were identified. First, we wanted to investigate, whether anaerobically cultured *N. gonorrhoeae* have a colonization advantage in the mouse vagina compared to aerobically cultured gonococci. Second, we wanted to investigate whether mouse passage of the *N. gonorrhoeae* has a positive effect on their colonization success. Moreover, we observed that CEAtg mice, despite treatment with the antibiotic trimethoprim, were strongly colonized by commensal bacteria in the vaginal tract, which may negatively affect gonococcal colonization. Therefore, we also decided to test the use of additional antibiotics as a pre-conditioning of the mice prior to infection with gonococci as a further optimization approach (Project III).

3. Results

3.1 Project I: The interaction of CEACAM3 and its polymorphic variant with Opa proteins of *N. meningitidis*

3.1.1 *N. meningitidis* strains bind to epithelial CEACAM1 and CEA, but are not recognized by granulocyte CEACAM3

Previous studies have indicated a lack of CEACAM3-binding Opa proteins in individual *N. meningitidis* serogroup A, B, and C strains (Johswich et al., 2013; Muenzner et al., 2000). To test the CEACAM-binding profile of a broader range of *N. meningitidis* serogroups, we produced the soluble amino-terminal IgV-like domains of human CEACAM1, CEACAM3, CEA, CEACAM6 and CEACAM8 in the form of GFP fusion proteins (**Figure 7A**). We also selected opaque colony variants of meningococci from serogroups A, B, C, and W. Western blotting with a monoclonal anti-Opa antibody revealed that all strains expressed at least one Opa protein (**Figure 7B**). As controls with known CEACAM-binding profiles we included Opa-negative as well as Opa_{52}-expressing *Neisseria gonorrhoeae* strains (**Figure 7B**). The microbes were incubated with the different soluble CEACAMs, extensively washed, and bacteria-bound receptor domains were detected by Western blot analysis with anti-GFP antibodies as schematically outlined (**Figure 7C**). In line with previous studies, Opa_{52}-expressing gonococci associated with CEACAM1, CEACAM3, CEA, and CEACAM6, but not CEACAM8, while non-opaque gonococci did not interact with any of the tested CEACAM domains (Roth et al., 2013) (**Figure 7D**). In contrast to opaque gonococci, none of the tested opaque *N. meningitidis* strains from the different serogroups was able to bind the granulocyte receptor CEACAM3 (**Figure 7D**). This was in sharp contrast to the uniform binding of all Opa protein-expressing meningococci to CEACAM1 (**Figure 7D**). Furthermore, several meningococci associated with CEA, which is exclusively expressed by epithelial cells (**Figure 7D**). As meningococci usually encode four distinct Opa genes (Stern & Meyer, 1987), we wondered if the various strains might by chance express an Opa protein without CEACAM3 binding properties *in vitro*, while the additional encoded Opa alleles might be recognized by CEACAM3, if their expression could be switched on. Therefore, we used *E. coli* expressing each individual Opa protein encoded by serogroup B strain MC58 (Kuespert et al., 2011) and *N. gonorrhoeae* expressing each individual

Opa protein encoded by serogroup C strain C1938 (Muenzner et al., 2000) (**Figure 7E**). In binding assays with soluble CEACAM IgV-like domains almost all meningococcal Opa proteins (7 out of 8) showed association with CEACAM1 and/or CEA, while none of the meningococcal Opa protein was bound by CEACAM3 (**Figure 7F**). There was a single Opa protein in the serogroup C strain (OpaC4), which did not bind to CEA or CEACAM1 (**Figure 7F**). This is in agreement with a previous report, which also showed the same situation for a serogroup A strain with 4 out of 5 tested Opa proteins binding to epithelial CEACAM1 or CEA, but none binding to CEACAM3 (Muenzner et al., 2000). In summary, our results combined with previous reports indicate a strongly biased receptor binding spectrum of the Opa protein repertoire encoded by *N. meningitidis* (**Figure 7F,G**). The vast majority of meningococcal Opa proteins is able to bind the monomeric, soluble IgV-like domain of epithelial CEACAM1 or CEA, but none of these bacterial adhesins is interacting with CEACAM3. This implies that *N. meningitidis* exploits CEACAM1 and CEA as initial docking sites for successful mucosal colonization by CEACAM1-optimized adhesins, thereby evading the opsonin-independent recognition afforded by granulocyte CEACAM3.

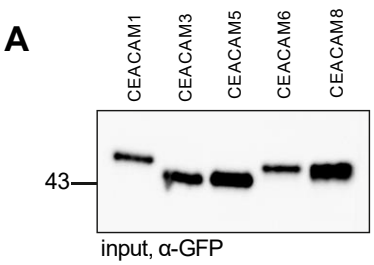
A
CEACAM1
CEACAM3
CEACAM5
CEACAM6
CEACAM8
43
input, α-GFP

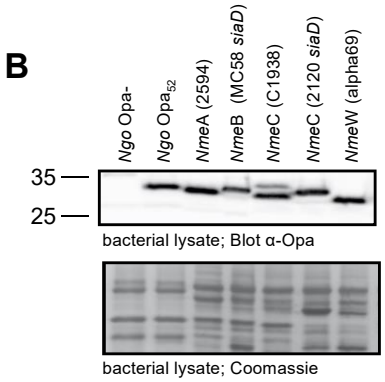
B
Ngo Opa-
Ngo Opa52
NmeA (2594)
NmeB (MC58 siaD)
NmeC (C1938)
NmeC (2120 siaD)
NmeW (alpha69)
35
25
bacterial lysate; Blot α-Opa
bacterial lysate; Coomassie

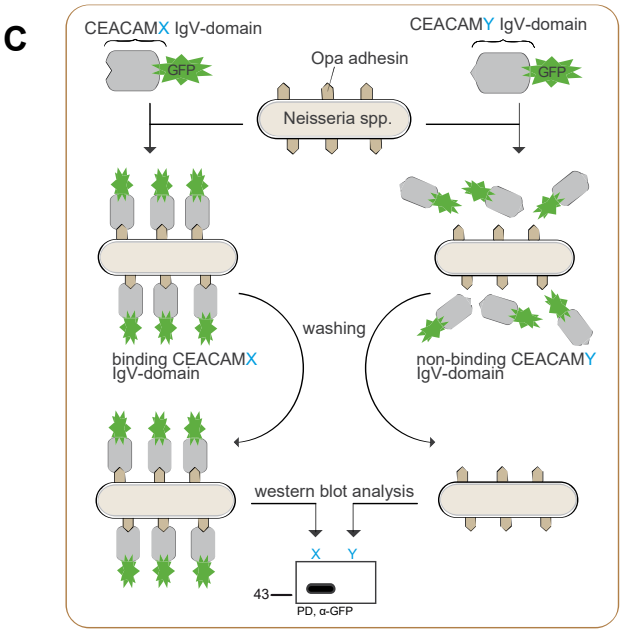
C
CEACAMX IgV-domain
CEACAMY IgV-domain
GFP
Opa adhesin
Neisseria spp.
washing
binding CEACAMX IgV-domain
non-binding CEACAMY IgV-domain
western blot analysis
X
Y
43
PD, α-GFP

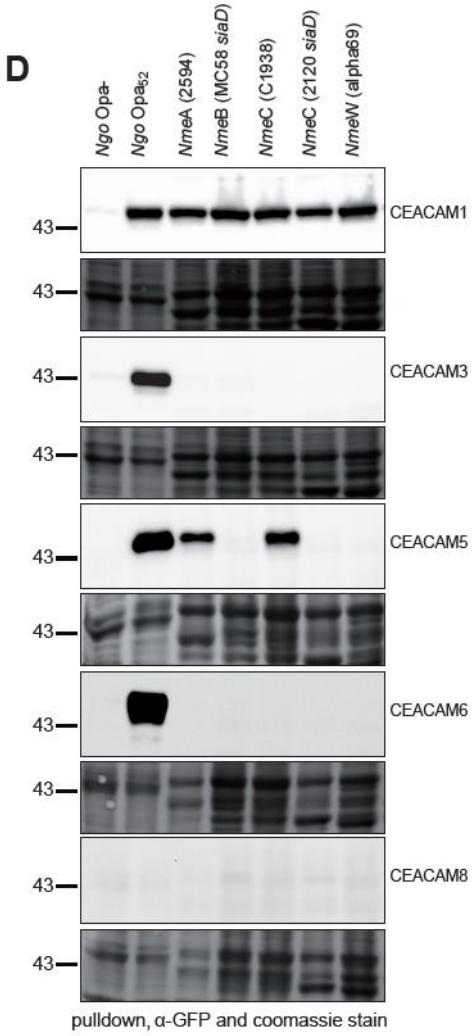
D
Ngo Opa-
Ngo Opa52
NmeA (2594)
NmeB (MC58 siaD)
NmeC (C1938)
NmeC (2120 siaD)
NmeW (alpha69)
43
CEACAM1
CEACAM3
CEACAM5
CEACAM6
CEACAM8
pulldown, α-GFP and coomassie stain

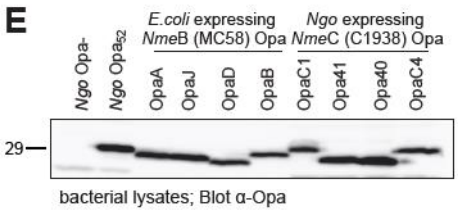
E
E.coli expressing NmeB (MC58) Opa
Ngo expressing NmeC (C1938) Opa
Ngo Opa-
Ngo Opa52
OpaA
OpaJ
OpaD
OpaB
OpaC1
Opa41
Opa40
OpaC4
29
bacterial lysates; Blot α-Opa

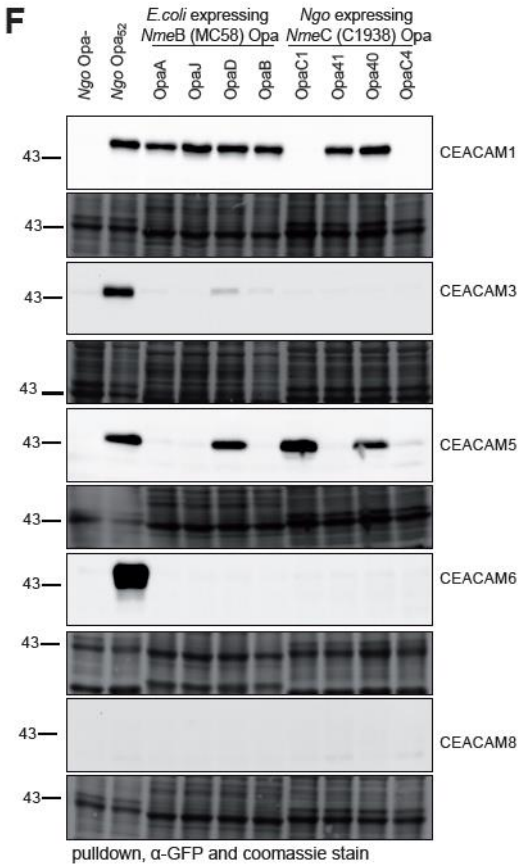
F
E.coli expressing NmeB (MC58) Opa
Ngo expressing NmeC (C1938) Opa
Ngo Opa-
Ngo Opa52
OpaA
OpaJ
OpaD
OpaB
OpaC1
Opa41
Opa40
OpaC4
43
CEACAM1
CEACAM3
CEACAM5
CEACAM6
CEACAM8
pulldown, α-GFP and coomassie stain

G

Strain/ Adhesin / CEACAM	NgoOpa$_{52}$	NmeA 2594	NmeB MC58 *siaD*	NmeC 1938	NmeC 2120 *siaD*	NmeW alpha69	*E.coli* expressing *Nme*B (MC58) Opa: OpaA	OpaJ	OpaD	OpaB	*Ngo* expressing *Nme*C (C1938) Opa: OpaC1	Opa41	Opa40	OpaC4	*E.coli* expressing (*) *Nme*A (00170/F6124) Opa: OpaA132	OpaB92	OpaB94	OpaD100	OpaJ101
CEACAM1	+	+	+	+	+	+	+	+	+	+	-	+	+	-	+	+	+	+	-
CEACAM3	+	-	-	-	-	-	-	-	-	-	-	-	-	-	-	-	-	-	-
CEA	+	+	-	+	-	-	-	-	+	-	+	-	+	-	+	+	+	-	-
CEACAM6	+	-	-	-	-	-	-	-	-	-	-	-	-	-	+	-	-	-	-
CEACAM8	-	-	-	-	-	-	-	-	-	-	-	-	-	-	ND	ND	ND	ND	ND

Figure 7: *N. meningitidis* strains bind to epithelial CEACAM1 and CEA, but are not recognized by granulocyte CEACAM3. (A) The amino-terminal domains of CEACAM1, 3, 5, 6, and 8 were produced as soluble GFP-fused proteins in 293T cells. Supernatants containing high amounts of soluble CEACAM fusion proteins were diluted to equalize the amounts of soluble CEACAM-GFP proteins in the different supernatants. Equalization of CEACAM-GFP amounts was confirmed by immunoblotting analyses with α-GFP antibodies. **(B)** Opa protein expression of the indicated *N. gonorrhoeae* and *N. meningitidis* strains was analysed by immunoblotting using α-Opa antibodies (upper panel). Coomassie staining demonstrates protein loading of the lanes (lower panel). **(C)** Schematic outline of bacterial pulldown experiments. Soluble GFP-tagged CEACAM domains from the supernatants in (A) are incubated with the different *N. meningitidis* strains or, with *N. gonorrhoeae* expressing the adhesin Opa$_{52}$ or lacking Opa protein expression (Opa-). The CEACAMX IgV domain represents an N-terminal CEACAM domain capable of binding the Opa protein(s) expressed by the example bacterium, and the CEACAMY IgV domain a CEACAM domain incapable of doing so. Unbound CEACAM domains are washed out by multiple washing steps. Bacteria-associated CEACAM domains are visualized by Western blotting with α-GFP antibodies. **(D)** Soluble GFP-tagged CEACAM domains were incubated with the indicated *N. meningitidis* strains, or with *N. gonorrhoeae* expressing no Opa proteins (Opa-) or expressing Opa$_{52}$. To detect bacteria-CEACAM interactions, bacterial pulldown assays were performed and bound CEACAM domains were determined by western blotting using α-GFP antibodies. Coomassie staining demonstrates protein loading of the lanes. **(E)** Opa protein expression of bacteria used in (F) was verified by immunoblotting using α-Opa antibodies. **(F)** Soluble amino-terminal CEACAM-GFP fusion proteins were incubated with *E. coli* expressing the indicated meningoccocal serogroup B (MC58 *siaD*) Opa proteins (OpaA, OpaJ, OpaD or OpaB) or with *N. gonorrhoeae* expressing the meningoccocal serogroup C (C1938) Opa proteins OpaC1, Opa41, Opa40 or OpaC4. Bacterial pulldowns were performed and bacteria bound-CEACAMs were analysed by immunoblotting using α-GFP antibodies. Coomassie staining demonstrates protein loading of the lanes. **(G)** Binding profiles of CEACAMs to Opa$_{52}$-expressing *N. gonorrhoeae* (*Ngo*), the indicated *N. meningitidis* (*Nme*) strains and the indicated meningococcal Opa proteins expressed by *E. coli* or *N. gonorrhoeae*. Binding is indicated by "+". No binding is indicated by "-". ND, not determined. (*) The binding profiles of CEACAM family members to *E. coli* expressing the *N. meningitidis* serogroup A (00170/F6124) Opa proteins were analysed in a study by Muenzner et al. (Muenzner et al., 2000). Experiments shown in A, D and F were performed by Alena Kress during her Master thesis in the laboratory of Prof. Dr. C. R. Hauck.

3.1.2 A polymorphism in human CEACAM3 enables recognition of *N. meningitidis* Opa proteins

The innate immune receptor CEACAM3 is one of the most rapidly evolving human proteins and several major single nucleotide polymorphisms (SNPs) have been localized to the

extracellular, bacteria-binding IgV domain (Adrian et al., 2019). In particular, we located 4 non-synonymous SNPs in the coding region of human CEACAM3, which alter the amino acid composition of the CEACAM3 IgV domain (Adrian et al., 2019). These SNPs result in the primary sequence alterations S43R, L44Q, V49A, and T69P and co-occur in most individuals, suggesting the existence of a CEACAM3-RQAP allele (**Supplementary Table 1**). From here on, we refer to the previously known CEACAM3 sequence as the common CEACAM3 allele, and to the CEACAM3 variant incorporating the four amino acid substitutions as the CEACAM3-RQAP allele. Interestingly, the CEACAM3-RQAP allele was exclusively found in populations of African descent and was absent in genomes of European or Asian descent (**Figure 8A**). The CEACAM3-RQAP allele has an extraordinary high prevalence in sub-Saharan African, where this allele was found in 37% of Gambians in the Western Division, 30% of the Yoruba in Nigeria, 27% of the Esan in Nigeria, and 21% of the Luhya in Kenya (Ensemble Database; 1000 Genomes Project Phase 3; last accessed 07/2022) (**Figure 8A** and **Supplementary Table 1**). In the Mende in Sierra Leone, the CEACAM3-RQAP allele was even present in the majority of the population (58%). In this population, the allele frequency of the RQAP allele was 33%, while this allele occurred only once in 500 European genomes, reflecting an allele frequency of 0,1% (**Figure 8A** and **Supplementary Table 1**). We noted that all four amino acid substitutions found in CEACAM3-RQAP resemble the CEACAM1 sequence at these positions (**Figure 8B**). The coincidence of a CEACAM1-mimicking polymorphism in CEACAM3 and its limited regional distribution along the meningitis belt suggested that the CEACAM3-RQAP allele might be an adaptation to recognize CEACAM1-optimized meningococcal Opa adhesins.

Accordingly, we set out to analyse the functional significance of the CEACAM3-RQAP variant for meningococcal recognition by producing the soluble extracellular IgV-like domain of CEACAM3-RQAP as well as the common CEACAM3 in the form of GFP fusion proteins (**Figure 8C**). Strikingly, the CEACAM3-RQAP protein was able to bind to six out of the eight individual Opa proteins derived from the serogroup B and C strains, while the common allele of CEACAM3 again did not recognize any of the tested Opa proteins (**Figure 8D,E**). To further confirm these remarkable binding differences, we investigated the interaction of the GFP-labeled CEACAM3 and CEACAM3-RQAP domains with individual Opa adhesins by flow cytometry. In agreement with the immunoblotting analyses, the amino-terminal IgV-like domain of the common CEACAM3 protein showed no association with meningococcal

adhesins, but strongly bound to the gonococcal Opa_{52} adhesin (**Figure 8F**). In contrast to the common CEACAM3 allele, CEACAM3-RQAP again was able to bind 6 of the 8 individual meningococcal Opa proteins (**Figure 8F**). The 6 Opa proteins recognized by CEACAM3-RQAP were identical to the 6 individual meningococcal Opa adhesins associating with CEACAM1 (**Figure 7F, Figure 8F,G**). As the binding assays had been conducted with meningococcal Opa proteins expressed in a heterologous background, we also tested opaque meningococci for CEACAM3-RQAP binding. Importantly, CEACAM3-RQAP, but not the common CEACAM3 allele, was able to recognize meningococci of serogroup B and C expressing CEACAM1-binding Opa proteins (**Figure 8H**). Thus, our data suggest that CEACAM3-RQAP, which is a polymorphism found in sub-Saharan Africa, allows recognition of *N. meningitidis*-Opa adhesins that are optimized for CEACAM1 binding and that evade recognition by the common CEACAM3 allele. Since pathogen recognition is the prerequisite for CEACAM3-mediated bacterial uptake into granulocytes, these results indicate that CEACAM3-RQAP, in contrast to the common CEACAM3 receptor, may enable opsonin-independent uptake of *N. meningitidis*.

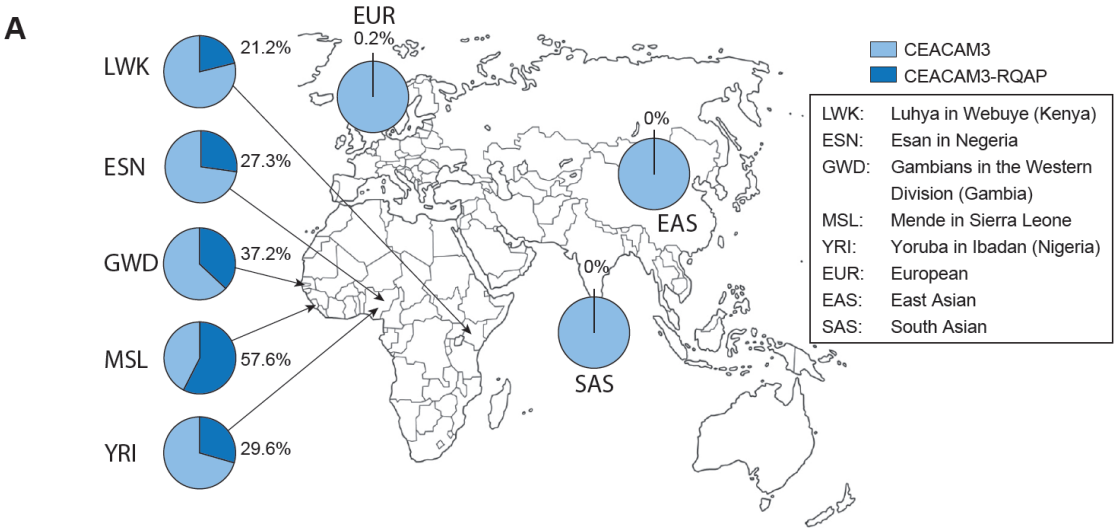

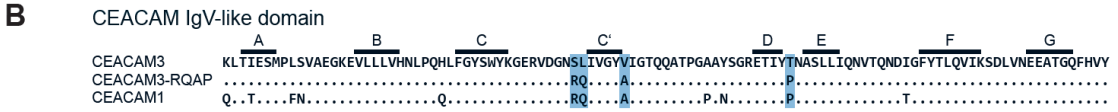

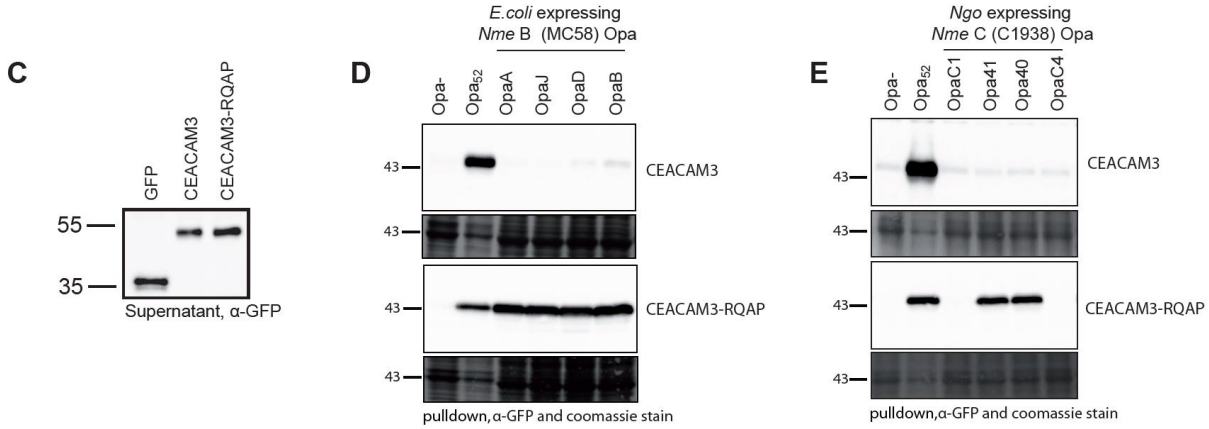

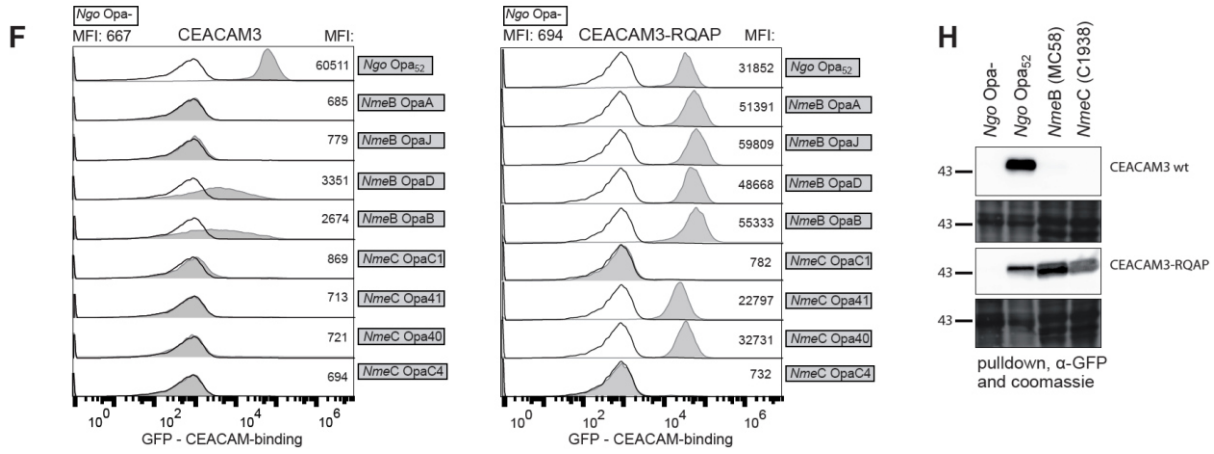

G

Strain/Adhesin / CEACAM	NgoOpa52	NmeB MC58 siaD	NmeC C1938	E.coli expressing NmeB (MC58) Opa: OpaA	OpaJ	OpaD	OpaB	Ngo expressing NmeC (C1938) Opa: OpaC1	Opa41	Opa40	OpaC4
CEACAM1	+	+	+	+	+	+	+	-	+	+	-
CEACAM3	+	-	-	-	-	-	-	-	-	-	-
CEACAM3-RQAP	+	+	+	+	+	+	+	-	+	+	-

Figure 8: A polymorphism in human CEACAM3 enables recognition of *N. meningitidis* Opa proteins. (A) The pie charts indicate the frequency with which the four SNPs found in the CEACAM3-RQAP variant occur together in the genomes of the respective population. While CEACAM3-RQAP is common in populations of African origin, the four SNPs are absent or extremely rare in the genomes of individuals of European or Asian origin. **(B)** Amino acid sequence alignment of the human IgV-like domains of CEACAM3, CEACAM3-RQAP, and CEACAM1. The black bars with the letters A to G label the β-strand regions within the IgV domain. **(C)** GFP or GFP-fused N-terminal domains of CEACAM3 or CEACAM3-RQAP were generated as soluble proteins in 293T cells. Amounts of GFP and CEACAM-GFP proteins in supernatants were adjusted and equalization was confirmed by immunoblotting analyses with α-GFP antibodies. **(D, E)** Soluble IgV-like domains of CEACAM3 and CEACAM3-RQAP were incubated with *E. coli* expressing the indicated meningococcal serogroup B MC58 *siaD* Opa protein (D) or with *N. gonorrhoeae* expressing the indicated meningococcal serogroup C (C1938) Opa protein (E). As controls, the soluble constructs were incubated with *N. gonorrhoeae* lacking Opa protein expression (Opa-) or expressing Opa_{52}. CEACAM-bacteria interactions were analysed by bacterial pulldown and immunoblotting with α-GFP antibodies. Comparable amounts of bacteria used in the experiments were verified by Coomassie staining of the respective membranes. **(F)** Supernatants containing the N-terminal IgV domain of CEACAM3 or CEACAM3-RQAP were incubated with *E. coli* expressing the indicated *Nme* serogroup B MC58 Opa protein or with *N. gonorrhoeae* expressing the indicated *Nme* serogroup C (C1938) Opa protein. As controls, supernatants were incubated with *N. gonorrhoeae* expressing the gonococcal adhesin Opa_{52} or lacking Opa expression (Opa-). After incubation and bacterial pulldown, CEACAM binding was determined by flow cytometry. MFI indicates the median GFP fluorescence intensity of fluorescence values ≥ 2. **(G)** Summary of the CEACAM3, CEACAM3-RQAP and CEACAM1 binding profiles to Opa_{52}-expressing *N. gonorrhoeae*, *N. meningitidis* MC58 *siaD* and C1938, and bacteria individually expressing the Opa proteins of the MC58 *siaD* or C1938 meningococci. Binding is shown by "+". No binding is indicated by "-". **(H)** Soluble N-terminal CEACAM3-GFP constructs were incubated with serogroup B MC58 *siaD* or serogroup C C1938 *N. meningitidis*, or with *N. gonorrhoeae* lacking Opa expression (Opa-) or expressing the adhesin Opa_{52}. Binding of CEACAM3 or CEACAM3-RQAP to bacteria was determined by bacterial pulldown followed by Western blot analysis with α-GFP antibodies. Comparable amounts of bacteria used in the pulldowns were verified by Coomassie staining. Experiments shown in D, E, F and H were performed by Alena Kress during her Master thesis in the laboratory of Prof. Dr. C. R. Hauck.

3.1.3 CEACAM3-RQAP recognizes and initiates the internalization of a broad spectrum of meningococcal Opa proteins

To determine whether CEACAM3-RQAP-mediated recognition of *N. meningitidis* Opa adhesins can lead to internalization of the bacteria, we expressed full length CEACAM3 or CEACAM3-RQAP in 293T cells. Both receptors were expressed at equivalent levels and localized to the membrane of transfected cells (**Figure 9A**). Next, transfected 293 cells were infected with *N. gonorrhoeae* expressing either the *N. meningitidis* serogroup C Opa proteins Opa41 or Opa40, or the gonococcal adhesin Opa_{52}. As a further control, Opa-negative (Opa-) bacteria were used. After 45 minutes of infection, gentamicin was added to kill non-internalized, extracellular bacteria. Upon lysis of the 293 cells, the intracellular bacteria were released and plated to allow quantification of internalized bacteria (gentamicin protection assay). As expected, Opa-negative gonococci were not internalized, and Opa_{52}-expressing bacteria were

recovered in large numbers from CEACAM3- as well as CEACAM3-RQAP-expressing cells (**Figure 9B**). In contrast, bacteria expressing the meningococcal Opa proteins were selectively taken up by CEACAM3-RQAP expressing cells, while cells expressing the common CEACAM3 allele barely internalized these strains (**Figure 9B**). These results were confirmed by confocal microscopy of infected samples, which were differentially stained for intracellular and extracellular bacteria (**Suppl. Figure S1**). Again, a substantial number of bacteria expressing meningococcal Opa41 and Opa40 were internalized by CEACAM3-RQAP-transfected cells, whereas this was not the case for CEACAM3-expressing cells (**Suppl. Figure S1**). Moreover, uptake of fluorescently labeled bacteria by CEACAM3 and CEACAM3-RQAP-expressing cells was measured by flow cytometry, which further demonstrated the unique ability of CEACAM3-RQAP to recognize and internalize bacteria with meningococcal Opa proteins (**Figure 9C,D**). Given this gain-of-function phenotype of the CEACAM3-RQAP protein with regard to recognition of Opa proteins from serogroups B and C meningococci, we wondered whether this specific capability also applies to a broader range of *N. meningitidis* serogroups. Therefore, we incubated the soluble amino-terminal domain of CEACAM3-RQAP as well as that of the common CEACAM3 receptor with different Opa-expressing *Neisseria meningitidis* strains, including serogroups A, B, C, W and Y (**Figure 9E**). Interestingly, the binding assays revealed a clear black-and-white pattern: while CEACAM3 did not recognize any of the tested meningococci, CEACAM3-RQAP bound to each Opa protein-expressing *N. meningitidis* strain (**Figure 9F**). These results demonstrate that CEACAM3-RQAP not only recognizes a very broad spectrum of *N. meningitidis* strains, but that CEACAM3-RQAP-mediated recognition of *N. meningitidis* Opa adhesins can also lead to internalization of the bacteria. It is quite conceivable that recognition of Opa protein-expressing meningococci by CEACAM3-RQAP could be a critical advantage in an environment where meningitis epidemics remain a major public health concern (Mazamay et al., 2021).

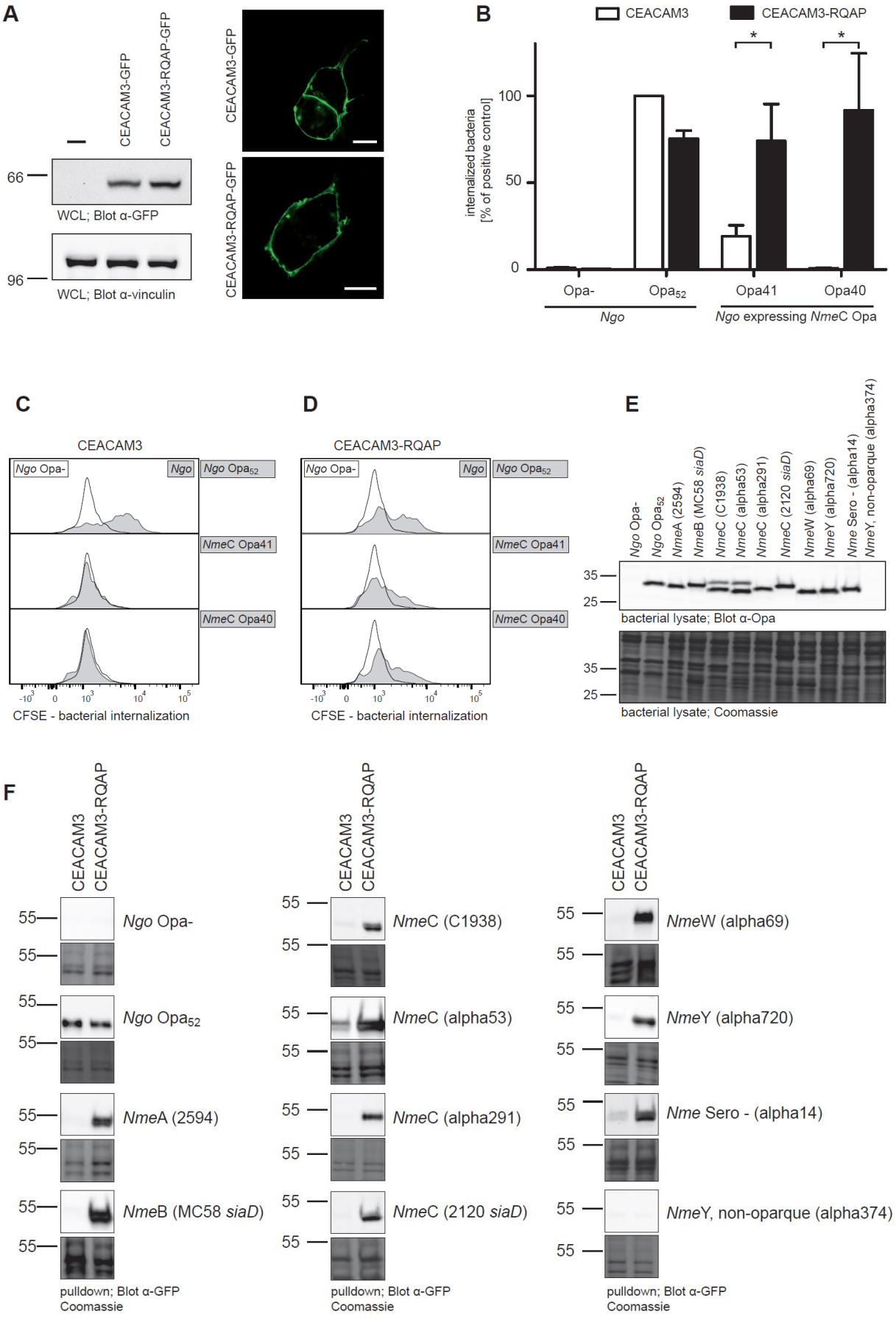
A
CEACAM3-GFP
CEACAM3-RQAP-GFP
66
WCL; Blot α-GFP
96
WCL; Blot α-vinculin
CEACAM3-GFP
CEACAM3-RQAP-GFP
B
CEACAM3
CEACAM3-RQAP
internalized bacteria [% of positive control]
100
50
0
*
*
Opa-
Opa52
Opa41
Opa40
Ngo
Ngo expressing NmeC Opa
C
CEACAM3
Ngo Opa-
Ngo
Ngo Opa52
NmeC Opa41
NmeC Opa40
CFSE - bacterial internalization
D
CEACAM3-RQAP
Ngo Opa-
Ngo
Ngo Opa52
NmeC Opa41
NmeC Opa40
CFSE - bacterial internalization
E
Ngo Opa-
Ngo Opa52
NmeA (2594)
NmeB (MC58 siaD)
NmeC (C1938)
NmeC (alpha53)
NmeC (alpha291)
NmeC (2120 siaD)
NmeW (alpha69)
NmeY (alpha720)
Nme Sero - (alpha14)
NmeY, non-oparque (alpha374)
35
25
bacterial lysate; Blot α-Opa
35
25
bacterial lysate; Coomassie
F
CEACAM3
CEACAM3-RQAP
55
Ngo Opa-
Ngo Opa52
NmeA (2594)
NmeB (MC58 siaD)
pulldown; Blot α-GFP
Coomassie
NmeC (C1938)
NmeC (alpha53)
NmeC (alpha291)
NmeC (2120 siaD)
NmeW (alpha69)
NmeY (alpha720)
Nme Sero - (alpha14)
NmeY, non-oparque (alpha374)

Figure 9: CEACAM3-RQAP recognizes and initiates the internalization of a broad spectrum of meningococcal Opa proteins. (A) (Left) 293T cells were transfected to express CEACAM3-GFP or CEACAM3-RQAP-GFP or were left untransfected. Comparable expression of the GFP fusion proteins was verified by Western blotting with α-GFP antibodies (upper panel). Equal loading of lysates was confirmed using an α-Tubulin antibody (lower panel). To determine the membrane localization of the two receptors, cells were fixed and analyzed by confocal microscopy (Right). Bars represent 10 µm. **(B)** 293T cells transiently expressing CEACAM3-GFP or CEACAM3-RQAP-GFP were infected for 45 min at an MOI of 30 with *N. gonorrhoeae* expressing no Opa adhesin (Opa-), expressing Opa_{52}, or expressing the meningococcal serogroup C C1938 adhesins Opa41 or Opa40. Subsequently, extracellular bacteria were killed with gentamicin and 293T cells were lysed to determine the number of intracellular bacteria released. Bars represent means ± SEM of five independent experiments done in triplicates. Statistical significance was determined with a two-tailed Student's t test. ns: not significant, *$p < 0.01$. **(C, D)** 293T cells transiently expressing CEACAM3-mKate2 (C) or CEACAM3-RQAP-mKate2 (D) were infected for 60 minutes (MOI60) with CFSE-stained *N. gonorrhoeae* expressing no Opa protein (Opa-), Opa_{52}, or the Opa41 or Opa40 protein of *N. meningitidis* serogroup C (C1938). CFSE signals of extracellular bacteria were subsequently quenched by exposing the cells to Trypan blue and CFSE fluorescence of the internalized bacteria was determined by flow cytometry. Unfilled histograms show signals of cells infected with *N. gonorrhoeae* lacking Opa expression (Opa-), whereas filled histograms show signals of cells infected with *N. gonorrhoeae* expressing the indicated Opa protein. **(E)** Opa protein expression of the indicated *N. gonorrhoeae* and *N. meningitidis* strains was analysed by immunoblotting using α-Opa antibodies (upper panel). Coomassie staining demonstrates protein loading of the lanes (lower panel). **(F)** Soluble GFP-fused IgV domains of CEACAM3 or CEACAM3-RQAP were incubated with the indicated *N. meningitidis* strains. Interaction between the amino-terminal CEACAM3 or CEACAM3-RQAP domains and the meningococcal strains was determined via bacterial-pulldown and subsequent immunoblotting with α-GFP antibodies. Comparable amounts of bacteria used in the experiments were verified by Coomassie staining of the respective membranes. Alisia Gärtner and Katharina v. Werthern contributed to the experiments shown in A-D in the context of the advanced course "Cell biology" of Prof. Dr. C. R. Hauck. The experiments were designed by Griseldis Goob and were conducted by Alisia Gärtner, Katharina v. Werthern and Griseldis Goob.

3.2 Project II: The role of receptor-type protein tyrosine phosphatases for CEACAM3-mediated phagocytosis

Major parts of the following chapter have been published in:

Phagocytosis mediated by the human granulocyte receptor CEACAM3 is limited by the receptor-type protein tyrosine phosphatase PTPRJ

Goob G., Adrian J., Cossu C., Hauck C. R. (2022) Journal of Biological Chemistry, 298(9), 102269. https://doi.org/10.1016/j.jbc.2022.102269.

3.2.1 Overexpression of active PTPRJ, but not of PTPRF and PTPRS diminishes CEACAM3-mediated phagocytosis

Preliminary studies by J. Adrian suggest that several receptor-type protein tyrosine phosphatases, including PTPRF, PTPRG, PTPRJ, and PTPRS, suppress CEACAM3-mediated signalling (Dissertation J. Adrian, 2019). However, further studies are needed to determine which of these phosphatases counteract CEACAM3 phosphorylation and which are relevant to CEACAM3-mediated phagocytosis. To directly test a potential negative role of PTPRF, PTPRG, PTPRJ, and PTPRS, we overexpressed these enzymes together with CEACAM3 using 293T cells, which lack endogenous expression of any CEACAM. We used the catalytic domains of the distinct phosphatases fused to a myristoylation signal directing the enzyme to the inner leaflet of the plasma membrane (**Figure 10A**). With the exception of PTPRG, all phosphatase domains were expressed at equivalent levels and also a uniform expression of CEACAM3 was confirmed by Western blotting (**Figure 10B**). CEACAM3-expression allowed efficient uptake of Opa_{52}-expressing *N. gonorrhoeae* by 293T cells, while nonopaque gonococci were not internalized (**Figure 10C**). Strikingly, only expression of myr-PTPRJ resulted in a strong reduction in CEACAM3-mediated bacterial internalization, while expression of myr-PTPRS, myr-PTPRF, or myr-PTPRG did not interfere with CEACAM3-mediated uptake (**Figure 10C**). Myristoylated PTPRJ was indeed found associated with the plasma membrane, where it co-localized with CEACAM3 and CEACAM3-bound gonococci (**Figure 10D**). In summary, these

results suggested that in particular the receptor protein tyrosine phosphatase PTPRJ could constitute a negative regulator of CEACAM3-mediated phagocytosis.

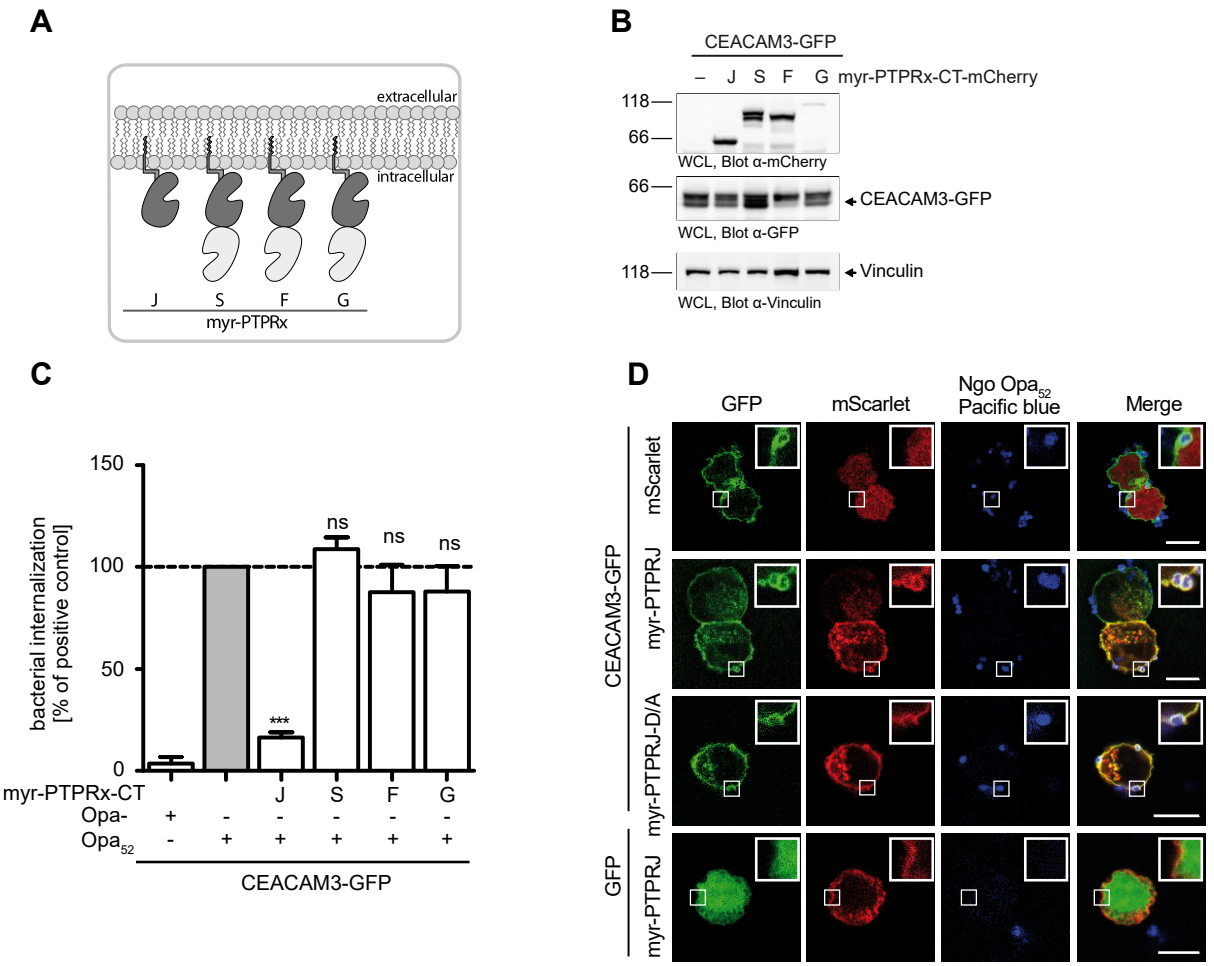

Figure 10: Overexpression of active PTPRJ diminishes CEACAM3-mediated phagocytosis. (A) Schematic representation of myristoylated (myr-) protein phosphatase domains lacking the extracellular and the transmembrane domain. PTPRS, PTPRF, and PTPRG harbor, in addition to the catalytically active phosphatase domain (dark gray), a second catalytically inactive domain (light gray). **(B)** 293T cells were cotransfected to express CEACAM3-GFP together with the indicated phosphatase domains fused to mCherry. Equal CEACAM3-GFP expression levels and expression of the different myr-phosphatase-mCherry constructs were analyzed by Western blotting using α-GFP (upper panel) and α-mCherry (middle panel) antibodies. Probing of the samples with α-vinculin (lower panel) served as loading control. **(C)** Cells from (B) were infected with Opa_{52}-expressing (Opa_{52}) or Opa-negative (Opa-) *N. gonorrhoeae* (MOI 30) for 45 min. Internalized bacteria were enumerated by gentamicin protection assays. Bars show mean ± SEM of three independent experiments performed in triplicates. Statistical significance was determined with a two-tailed Student's t test. n.s., not significant; ***$p < 0.001$. **(D)** 293T cells were cotransfected with plasmids encoding GFP-tagged CEACAM3 or GFP alone together with the indicated mScarlet-tagged myristoylated phosphatase domain or mScarlet alone. Cells were infected with PacificBlue-labeled Opa_{52}-expressing *N. gonorrhoeae* for 30 min, fixed, and analyzed by confocal microscopy. Insets show 3× magnification of boxed areas. Bars represent 10 µm (corresponding to 3.3 µm for insets). This figure is published in (Goob et al., 2022).

3.2.2 PTPRJ diminishes CEACAM3 tyrosine phosphorylation

Upon bacterial engagement, the CEACAM3 cytoplasmic domain is rapidly tyrosine phosphorylated at the HemITAM sequence by active Src family kinases (McCaw et al., 2003; Schmitter, Pils, Weibel, et al., 2007). To examine if PTPRJ affects bacterial uptake by diminishing CEACAM3 phosphorylation or by interfering with Src kinase activity, we co-transfected 293T cells with constructs encoding CEACAM3-GFP or GFP together with either myr-PTPRJ wildtype or the catalytically inactive mutant myr-PTPRJ-D/A. Western blot analysis confirmed the equivalent expression of CEACAM3-GFP and GFP (**Figure 11A**). Likewise, myr-PTPRJ and myr-PTPRJ-D/A were expressed at similar levels (**Figure 11A**). A low basal tyrosine phosphorylation of immunoprecipitated CEACAM3 could be observed, both in the absence of CEACAM3-binding bacteria and after infection with Opa-negative *N. gonorrhoeae* (**Figure 11B**). As expected, infection with CEACAM-binding *N. gonorrhoeae* Opa_{52} resulted in a marked increase in CEACAM3 tyrosine phosphorylation (**Figure 11B**). However, receptor phosphorylation was completely abolished, when the truncated, active myr-PTPRJ was co-expressed together with CEACAM3, whereas co-expression of the catalytically inactive myr-PTPRJ-D/A variant showed the opposite effect (**Figure 11B**). Interestingly, although PTPRJ has been reported to dephosphorylate the carboxy-terminal tyrosine residue of Src, thereby promoting Src kinase activity (Boggon & Eck, 2004; Hermiston et al., 2009; Stepanek et al., 2011), expression of myr-PTPRJ did not alter the tyrosine phosphorylation state of c-Src, neither at the activation loop tyrosine residue Y-419 nor at the carboxy-terminal negative regulatory tyrosine residue Y-530 (**Figure 11C**). The Y-530 residue of c-Src is dephosphorylated upon serum stimulation of cells, which is known to correspond to increased c-Src activity (**Figure 11D**). In agreement with a negligible effect on c-Src phosphorylation and activity, the expression of myr-PTPRJ did also not abrogate the increased tyrosine phosphorylation of the c-Src substrate $p130^{Cas}$ (**Figure 11E**). These data demonstrated that the presence of active PTPRJ selectively altered the phosphorylation state of CEACAM3, while PTPRJ did not influence c-Src tyrosine phosphorylation or c-Src activity, suggesting that PTPRJ might directly act on CEACAM3.

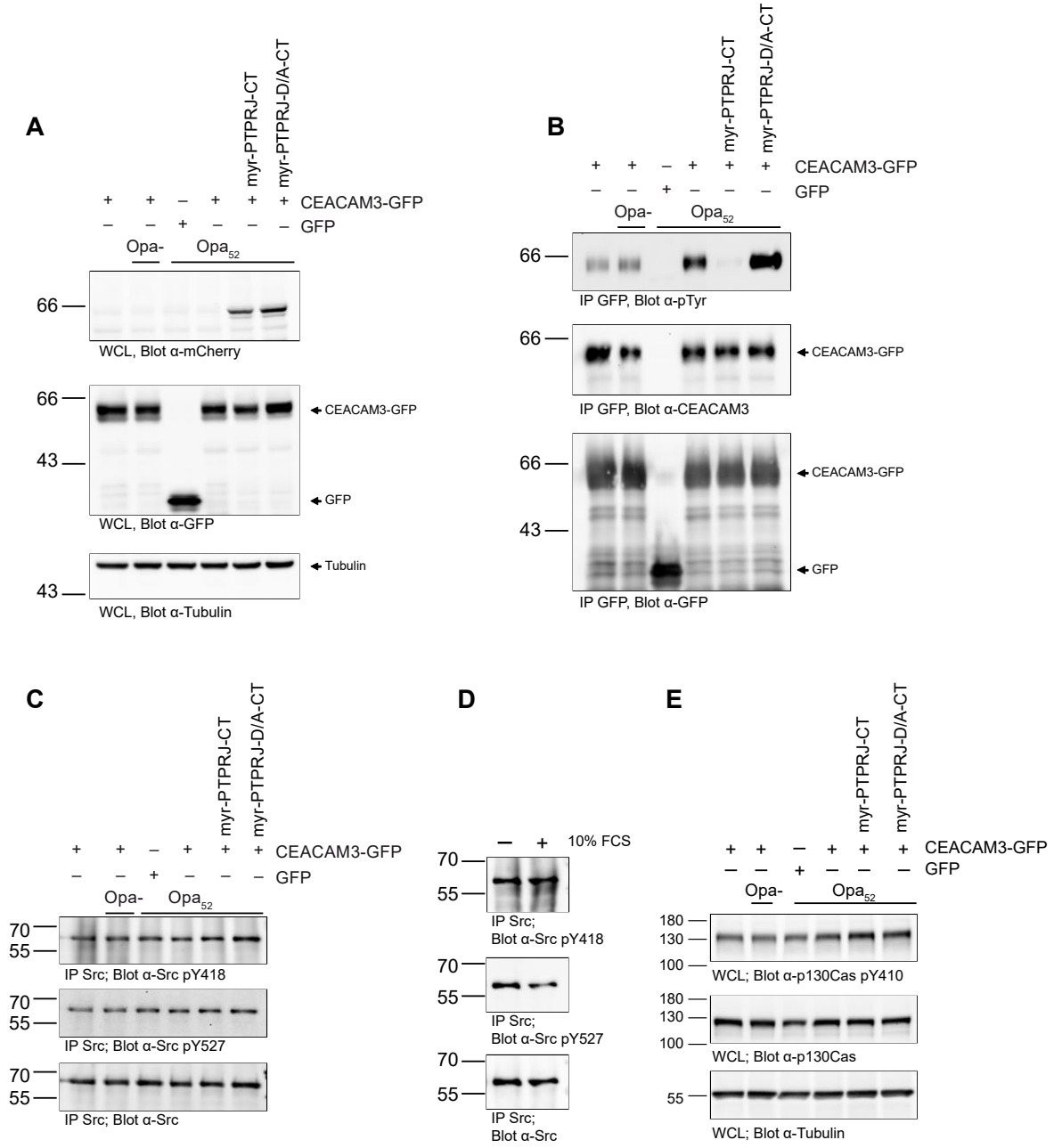

Figure 11: PTPRJ diminishes CEACAM3 tyrosine phosphorylation. (A) 293T cells were transfected to express CEACAM3-GFP or GFP. Where indicated, cells were additionally transfected with constructs encoding the mCherry-tagged myristoylated phosphatase domain of PTPRJ or the inactive mutant (PTPRJ-D/A). Transfected cells were infected with Opa$_{52}$-expressing (Opa$_{52}$) or Opa-negative (Opa-) *N. gonorrhoeae* (MOI of 30) for 15 min or remained uninfected. Subsequently, WCL were prepared, and expression of PTPRJ-mCherry (upper panel) and CEACAM3-GFP or GFP (middle panel) was confirmed by immunoblotting with appropriate antibodies. Lysates were probed with α-tubulin antibodies to confirm equal loading (lower panel). **(B)** Lysates from (A) were incubated with GFP-binding nanobodies and GFP or CEACAM3-GFP was immunoprecipitated. Tyrosine phosphorylation of CEACAM3 in the precipitates was analyzed by Western blotting with α-phospho-tyrosine (pTyr) antibodies (upper panel). Equal immunoprecipitation from the samples was verified by probing with α-CEACAM3 (middle panel) and α-GFP antibodies (lower panel). **(C)** c-Src was immunoprecipitated from cell lysates as in (A). The tyrosine phosphorylation status of c-Src was determined by Western blotting with antibodies directed against phosphorylated Y418 (pY418; upper panel; corresponds to pY419 in human c-Src) or pY527

(middle panel; corresponds to pY530 in human c-Src). Probing with α-c-Src antibodies confirmed equal loading (lower panel). **(D)** c-Src was immunoprecipitated from lysates of serum-starved (-) or serum-stimulated (+) murine embryonic fibroblasts, and the samples were probed as in (C). **(E)** The tyrosine phosphorylation status of $p130^{Cas}$ was determined by Western blotting with antibodies directed against phosphorylated Y410 of $p130^{Cas}$ (pY410; upper panel), while probing with α-$p130^{Cas}$ antibody (middle panel) and α-tubulin (lower panel) confirmed equal loading. This figure is published in (Goob et al., 2022).

3.2.3 Recombinant PTPRJ dephosphorylates the CEACAM3 tyrosine residues Y230 and Y241

While overexpression of PTPRJ resulted in reduced tyrosine phosphorylation of CEACAM3, this might be an indirect effect mediated by PTPRJ acting on another protein phosphatase or protein kinase. Therefore, we tested the ability of PTPRJ to directly dephosphorylate tyrosine residues within the CEACAM3 ITAM-like motif. To this end, we recombinantly expressed and purified the phosphatase domains of wildtype human PTPRJ and of the inactive PTPRJ-D/A mutant (PTPRJ-D/A) in the form of His-tagged proteins in *E. coli* (**Figure 12A**). The enzymatic activity of the recombinant proteins was confirmed by *in vitro* phosphatase assay with the generic substrate 4-methylumbelliferyl phosphate (4-MUP). Importantly, wildtype PTPRJ dephosphorylated 4-MUP, while the PTPRJ-D/A mutant did not show catalytic activity (**Figure 12B**). Next, we incubated the recombinant phosphatase with synthetic phospho-peptides spanning the CEACAM3 ITAM-like motif and bearing a phospho-tyrosine residue at either position Y230 or Y241 (**Figure 12C**). While wildtype PTPRJ readily dephosphorylated each phospho-tyrosine-containing peptide in a dose-dependent manner, PTPRJ-D/A showed no activity (**Figure 12D**). Phosphate release from both tyrosine residues by PTPRJ was linear over the course of 60 minutes and occurred with comparable efficiency (**Figure 12E**). Taken together, these results show that recombinant PTPRJ is able to directly catalyze the hydrolysis of both phosphorylated tyrosine residues of the CEACAM3 ITAM-like motif *in vitro*. To investigate if PTPRJ also dephosphorylates both residues in the context of the native CEACAM3 protein, we expressed GFP-tagged CEACAM3 in 293T cells in the presence or absence of v-Src. As reported previously, co-expression of v-Src leads to strong, constitutive tyrosine phosphorylation of the CEACAM3 ITAM-like motif (Buntru et al., 2011; Kopp et al., 2012; Pils et al., 2012) (**Figure 12F**). Upon precipitation of CEACAM3-GFP from whole-cell lysates, the protein was incubated with recombinant wildtype PTPRJ or the inactive PTPRJ-D/A mutant for

5 to 45 minutes (**Figure 12F**). Clearly, incubation of tyrosine phosphorylated CEACAM3 with the wildtype phosphatase led to an almost complete dephosphorylation in the course of 30 to 45 minutes, while PTPRJ-D/A did not affect the phosphorylation state of CEACAM3 (**Figure 12F**). Moreover, we transfected 293T cells with either CEACAM3 wildtype or CEACAM3 mutants with a single phosphorylatable tyrosine residue in the ITAM-like motif (CEACAM3-Y230F and CEACAM3-Y241F). All constructs were expressed at similar levels (**Figure 12G**). Following infection with CEACAM3-binding *N. gonorrhoeae*, CEACAM3 proteins were precipitated from cells and incubated or not with recombinant PTPRJ for 45 minutes. As expected, CEACAM3-Y230F and CEACAM3-Y241F showed reduced tyrosine phosphorylation levels compared to wildtype CEACAM3 (**Figure 12H**). However, upon incubation with recombinant PTPRJ all proteins were completely dephosphorylated (**Figure 12H**). These findings confirm the ability of PTPRJ to directly dephosphorylate both tyrosine residues embedded within the CEACAM3 ITAM-like motif, suggesting that PTPRJ can limit CEACAM3-initiated, tyrosine phosphorylation-dependent processes such as phagocytosis of human restricted pathogens.

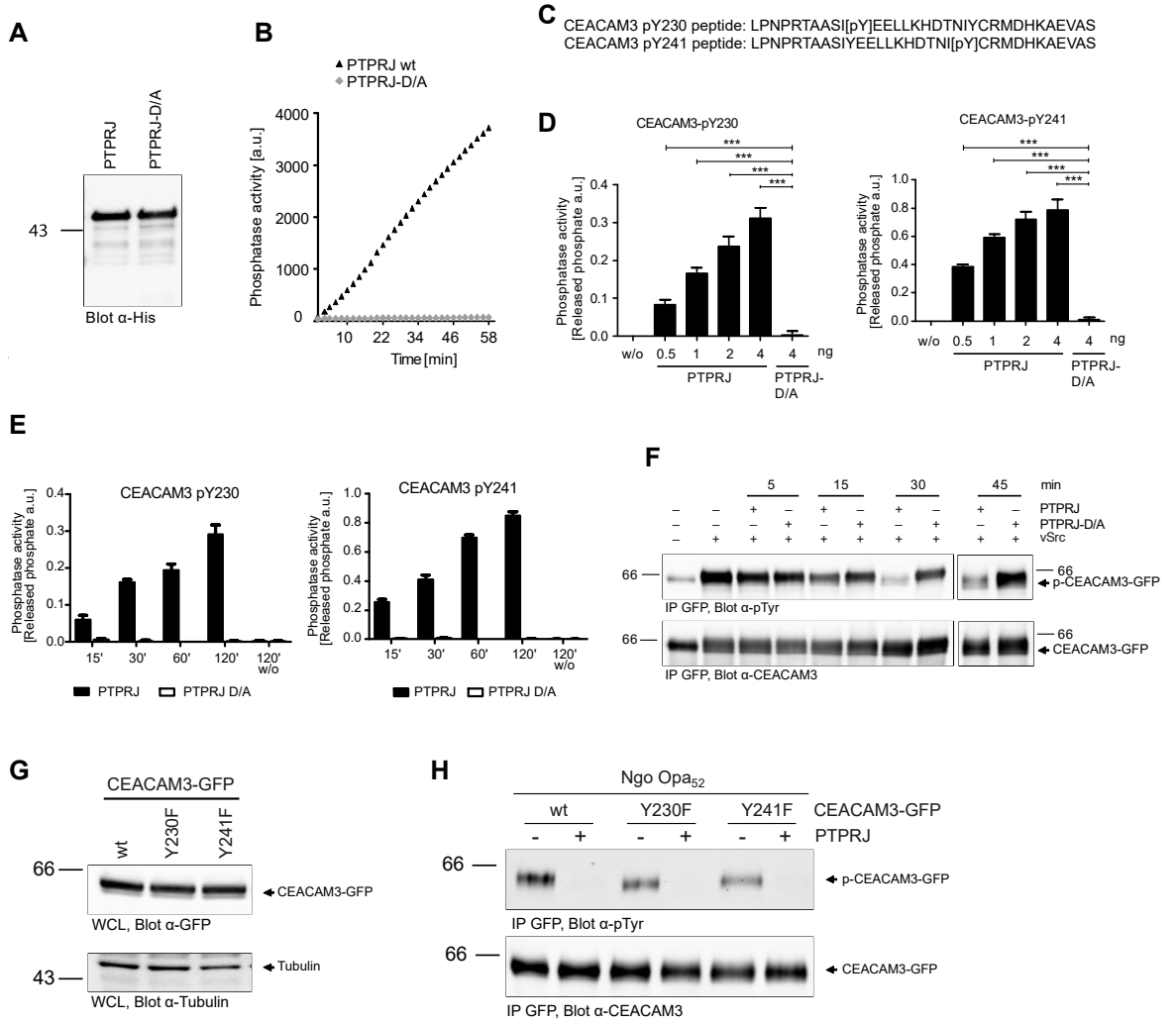

Figure 12: Recombinant PTPRJ dephosphorylates the CEACAM3 tyrosine residues Y230 and Y241. (A) Recombinant phosphatase domains of His-PTPRJ and His-PTPRJ-D/A were expressed in *E. coli*, purified, and analyzed by Western blotting using an α-His antibody. **(B)** 12.5 ng recombinant PTPRJ or PTPRJ-D/A phosphatase domains were incubated with 500 µM of 4-MUP. Shown is the increase in 4-MU fluorescence of a representative experiment over a 60-min period. **(C)** Synthetic phospho-peptides spanning the carboxy-terminus of CEACAM3. Either tyrosine residue 230 (pY230) or 241 (pY241) of the ITAM-like sequence is phosphorylated. **(D)** CEACAM3 phospho-peptides were incubated at 30 °C without phosphatases (w/o) or with the indicated amounts of recombinant PTPRJ or PTPRJ-D/A phosphatase domains. Released phosphate was determined by malachite green. Background values (buffer plus malachite green) were subtracted. Bars represent mean ± SD of three independent experiments. Statistically significant differences were determined by one-way ANOVA followed by Dunnett's posttest. **p < 0.01; ***p < 0.001. **(E)** CEACAM3 phospho-peptides were incubated with or without 1 ng of recombinant PTPRJ or PTPRJ-D/A for the indicated time at 30 °C. Released phosphate was determined as in (D). Bars show mean ± SD from three technical replicates. **(F)** CEACAM3-GFP was co-expressed or not with the active tyrosine kinase v-Src in 293T cells. CEACAM3-GFP immunoprecipitates were incubated with 200 ng recombinant His-PTPRJ or His-PTPRJ-D/A phosphatase domains for the indicated times at 30 °C. CEACAM3 tyrosine phosphorylation was monitored by Western blot analysis using α-phospho-tyrosine antibodies (upper panels). Probing of the membrane with α-CEACAM3 antibodies (lower panels) confirmed equal precipitation of CEACAM3-GFP. **(G)** 293T cells were transfected to express CEACAM3-GFP wildtype, CEACAM3-GFP Y230F, or CEACAM3-GFP Y241F. Immunoblotting with α-GFP antibodies (upper panel) and α-tubulin (lower panel) confirmed equal expression of CEACAM3 variants as well as equal loading of the samples. **(H)** 293T cells transfected as in (G) were infected at an MOI of 30 with Opa_{52}-expressing (Opa_{52}) *N. gonorrhoeae* for 15 min.

Cells were lysed, and wildtype CEACAM3-GFP and CEACAM3 mutants were immunoprecipitated. Immunoprecipitates were incubated for 45 min at 30 °C with or without recombinant PTPRJ phosphatase (400 ng). Samples were examined by Western blot analysis with α-phospho-tyrosine antibodies (upper panel). Equivalent amounts of immunoprecipitated CEACAM3 were verified by probing with α-CEACAM3 (lower panel). This figure is published in (Goob et al., 2022).

3.2.4 PTPRJ deletion in human phagocytes results in elevated phagocytosis

As CEACAM3 is expressed exclusively by human granulocytes (Buntru et al., 2012), we wondered about the functional interaction of this phagocytic receptor and PTPRJ in myeloid cells. Accordingly, we generated PTPRJ-deficient clonal HL60 cell lines by lentiviral transduction of HL60 CEACAM3-mKate2 cells with Cas9 and sgRNAs targeting PTPRJ (HL60-CEACAM3-mKate2 sgPTPRJ clone 6 and clone 12). As a control, HL60-CEACAM3-mKate2 cells were transduced with Cas9 and sgRNAs targeting Cerulean (HL60-CEACAM3-mKate2 sgCer). Western blotting, flow cytometry, and immunofluorescence staining confirmed that the derived HL60-CEACAM3-mKate2 sgPTPRJ cells completely lacked PTPRJ expression (**Figure 13A,B** and **Suppl. Figure S2**). Expression of PTPRC, a related receptor protein tyrosine phosphatase expressed in immune cells, was not affected (**Figure 13C**), and HL60-CEACAM3-mKate sgCer and HL60-CEACAM3-mKate sgPTPRJ clone 6 cells showed equivalent surface expression of CEACAM3 (**Figure 13D**). The clonal PTPRJ-deficient HL60-CEACAM3 cells exhibited increased CEACAM3-mediated uptake of Opa_{52}-expressing *N. gonorrhoeae* (**Figure 13E,F**). Importantly, increased uptake by PTPRJ-deficient cells was not seen for nonopaque, non-CEACAM-binding gonococci, demonstrating that enhanced phagocytosis depended on Opa-protein-CEACAM3-interaction (**Figure 13E,F**). Together, these findings corroborate the idea that PTPRJ action limits CEACAM3-mediated phagocytosis by human myeloid cells.

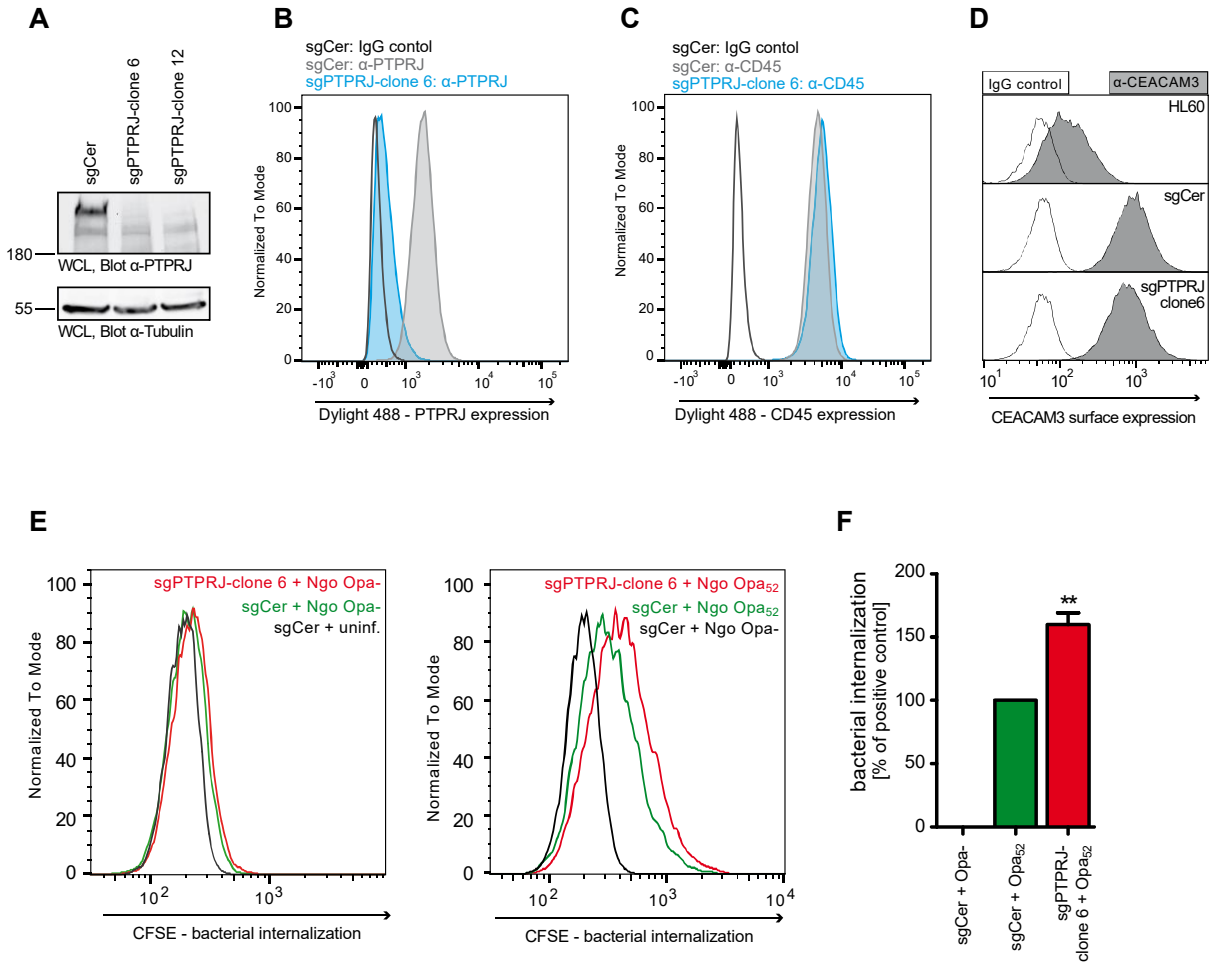

Figure 13: PTPRJ deletion in human phagocytes results in elevated phagocytosis. (A) HL60 CEACAM3 mKate Cerulean cells were treated with sgRNAs against cerulean (HL60 CEACAM3-mKate control) or a combination of sgRNAs against cerulean and PTPRJ (HL60 CEACAM3-mKate sgPTPRJ). PTPRJ expression in whole cell lysates (WCLs) of the indicated clonal cell lines was analyzed by Western blotting with α-PTPRJ antibodies (upper panel). Equal loading was confirmed by probing with α-tubulin (lower panel). **(B)** PTPRJ expression in HL60 CEACAM3-mKate control (gray filled curve) or HL60 CEACAM3-mKate sgPTPRJ clone 6 cells (blue filled curve) was analyzed by surface staining with α-PTPRJ antibodies and flow cytometry. A sample of HL60 CEACAM3-mKate control cells was also stained with an isotype-matched primary control antibody (IgG control, open curve). **(C)** PTPRC expression in cells as in (B) was analyzed by surface staining with α-PTPRC antibodies and flow cytometry. A sample of HL60 CEACAM3-mKate control cells was also stained with an isotype-matched primary control antibody (IgG control, open curve). **(D)** CEACAM3 expression in HL60 cells, HL60 CEACAM3-mKate control cells, and HL60 CEACAM3-mKate sgPTPRJ clone 6 cells was analyzed by staining with α-CEACAM3 antibodies and flow cytometry (gray filled curve). Each cell line was also stained with an isotype-matched primary control antibody (IgG control, open curve). **(E)** HL60 CEACAM3-mKate sgPTPRJ cells or HL60 CEACAM3-mKate control cells were infected for 10 min at an MOI of 10 with CFSE-labeled *N. gonorrhoeae* expressing either Opa_{52} (Ngo Opa_{52}) or no Opa-adhesin (Ngo Opa-). After quenching the fluorescence of extracellular bacteria with trypan blue, the CSFE signal of internalized bacteria was measured by flow cytometry. Shown is a representative experiment. **(F)** Quantification of bacterial internalization assays performed as in (E). Bars represent median fluorescent intensities (MFIs) ± SEM from five independent experiments and are normalized to the CFSE fluorescence detected upon infection of HL60 CEACAM3-mKate control cells with Opa_{52}-expressing *N. gonorrhoeae*. Statistically significant increases in bacterial internalization were determined by Student's t test and indicated by asterisks; **$p < 0.01$. This figure is published in (Goob et al., 2022).

3.2.5 PTPRJ deletion in human phagocytes leads to a gain-of function phenotype

As CEACAM3-initiated responses are accompanied by phenotypic changes of the phagocytes, such as remodeling of the actin cytoskeleton and induction of prominent cell protrusions, we investigated infected samples by scanning electron microscopy (SEM). Clearly, uninfected HL60-CEACAM3-mKate sgCer and HL60-CEACAM3-mKate sgPTPRJ cells showed small filopodia-like protrusions throughout the cell body (**Figure 14A**). Upon infection with CEACAM-binding gonococci, lamellipodia with a length of 1 to 2 µm emerged locally in HL60 CEACAM3-mKate sgCer cells (**Figure 14A**). However, lamellipodia formation by infected PTPRJ-deficient HL60 cells was markedly magnified with wider and larger (>2 µm) lamellipodia formed (**Figure 14A**). Based on 10 distinct SEM images of each sample, we estimated the area covered by individual lamellipodia. While lamellipodia in wildtype cells extended on average over around 7 μm^2 in response to infection with CEACAM-binding bacteria, in PTPRJ knock-out cells this area was doubled (**Figure 14B**). Together, these findings illustrate that PTPRJ is a negative regulator of CEACAM3-initiated phagocyte functions and that PTPRJ action on CEACAM3 prevents exaggerated phagocyte responses.

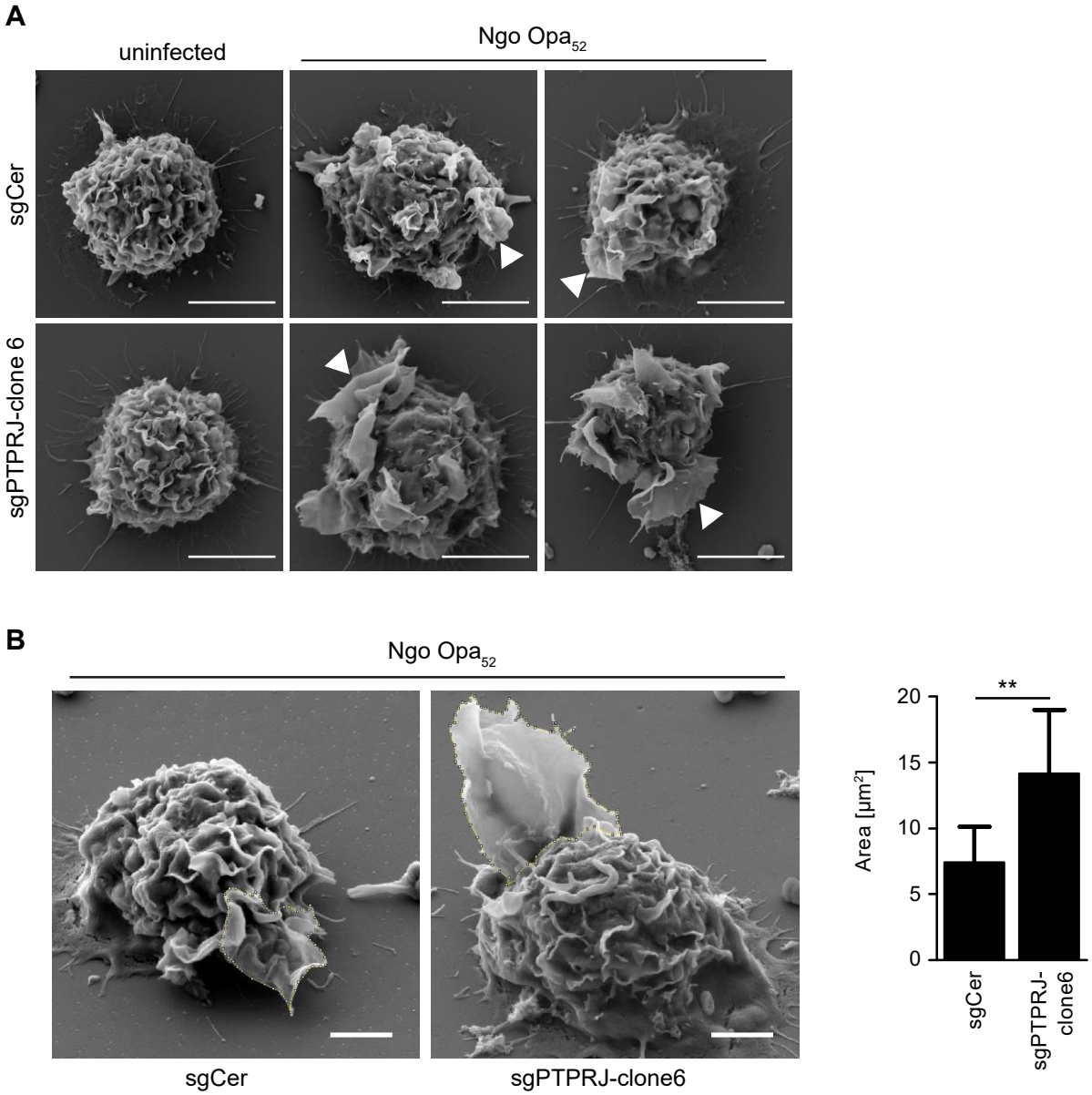

Figure 14: Deletion of PTPRJ in human phagocytes results in a gain-of-function phenotype. (A) HL60 CEACAM3-mKate sgPTPRJ clone 6 (sgPTPRJ-clone 6) and HL60-CEACAM3-mKate2 control cells (sgCer) were left uninfected or were infected with Opa_{52}-expressing *N. gonorrhoeae* for 30 min (MOI 30). Cells were fixed and analyzed by scanning electron microscopy. Arrowheads point to lamellipodia involved in phagocytosis. Scale bars represent 5 µm. **(B)** In samples from (A), the extension of bacteria-induced lamellipodia was determined by manual determination of the circumference and calculation of the area in NIH ImageJ as in the depicted examples. Scale bars represent 2 µm. The broken line indicates the circumference of the lamellipodia. Bars in the right panel represent mean lamellipodial area in μm^2 ± SD of 10 individual cells for each condition. Statistically significant differences were determined by two-tailed Student's t test and indicated by asterisks. **p < 0.01. The SEM images shown in (A) and (B) were acquired with the assistance of Michael Laumann (Electron Microscopy Service of the Department of Biology, University of Konstanz). This figure is published in (Goob et al., 2022).

3.3 Project III: Optimization of experimental *N. gonorrhoeae* genital tract infections in CEA transgenic estradiol-treated mice

N. gonorrhoeae is a human-specific pathogen and the causative agent of the sexually transmitted disease gonorrhoea (Quillin & Seifert, 2018). Every year, around 80 million people become infected with this pathogen, that mainly colonizes the genital mucosa (Quillin & Seifert, 2018). Consequences of gonococcal infection are most often local inflammatory reactions, but in a minority of the cases, the disease can develop a severe course that may lead to infertility or ectopic pregnancies in women (Stevens & Criss, 2018; Unemo et al., 2019). Infections with *N. gonorrhoeae* can also increase the risk of HIV infection (Cohen, 1998), underscoring the importance of testing new therapeutic approaches to prevent or treat gonococcal infections in humans. Though these microbes are highly adapted to humans as their sole natural host, animal models that mimick at least critical aspects of the disease in man, are urgently needed for pre-clinical evaluation of drug candidates or vaccine studies. Female mice expressing the gonococcal Opa-adhesin-binding human CEA receptor have been used by several groups to study the initial colonization of and inflammatory responses in the murine vaginal tract mucosa (Islam et al., 2018; Muenzner et al., 2010; Muenzner & Hauck, 2020). However, in our laboratory, the gonococcal mouse model has been used and established only for short-term infections of 24 hours, a time window in which some questions, such as the sexual transmissibility of the bacteria to male mice or the evaluation of the efficacy of potential antibiotics can be assessed only to a limited extent. The aim of the work described here was to optimize the CEAtg mouse infection model also in our laboratory to allow stable vaginal colonization by gonococci over a period of at least 48 hours.

3.3.1 CEAtg Balb/c mice, but not CEAtg C57BL6/J mice show gonococcal colonization for 48 hrs

As two inbred strains expressing human CEA, CEAtg C57BL6/J (Eades-Perner et al., 1994) and CEAtg Balb/c mice were available, we first investigated whether either mouse line was more suitable for establishing prolonged vaginal infections. It is known that the susceptibility of female mice to gonococci can be improved by pre-treating the mice with estradiol, which stabilizes the mouse cycle in the proestrus/oestrus phase (Taylor-Robinson et al., 1990).

Similar to the established 24-hour infection model (Muenzner et al., 2010), we treated the mice subcutaneously with 17β-estradiol 4 days before infection and added trimethoprim to the drinking water to prevent excessive growth of the commensal vaginal tract flora, which is enhanced under the influence of estradiol (Furr & Taylor-Robinson, 1991) (**Figure 15A**). Four days after the estradiol-treatment, the CEAtg mice were vaginally infected with 10^8 Opa_{52}-expressing *N. gonorrhoeae* (Ngo Opa_{52}) in a vitamin-rich solution, additionally containing iron and other nutrients beneficial for gonococcal survival (vitamin solution). In the case of the 48-hour infection period, mice were treated again with the vitamin solution 24 hours after inoculation by vaginal application to avoid deficiencies of essential nutrients (**Figure 15A**). To determine the bacterial load, mice were sacrificed 24 hours or 48 hours after infection and the bacteria were re-isolated by urogenital swabs. For accurate enumeration of *N. gonorrhoeae*, re-isolated bacteria were plated on GC plates containing the antibiotics chloramphenicol (Cam) and erythromycin (Erm), to which the used Opa_{52}-expressing *N. gonorrhoeae* strain is resistant (Kupsch et al., 1993, 1996). In addition, dilutions of the re-isolates were also plated on GC plates without antibiotics to detect the entire vaginal flora remaining under the treatment of trimethoprim. In the re-isolates collected 24 hours after infection, we detected *N. gonorrhoeae* on the antibiotic-containing GC plates in one of three CEAtg Balb/c mice and one of three CEAtg C57BL6/J mice (**Figure 15B**). In contrast, after 48 hours of infection, all three CEAtg Balb/c mice but none of the CEAtg C57BL6/J mice showed gonococcal colonization (**Figure 15B**). Based on this clearly better infection rate of the CEAtg Balb/c mice 48 hours after inoculation, we decided to establish the 48-hour infection model in this inbred mouse line. A striking observation in this experiment was that both CEAtg mouse strains showed an unexpectedly high background growth of commensal bacteria in the vaginal tract despite the trimethoprim treatment (data not shown). It was noticeable that mice that had a strong vaginal colonization by commensal bacteria were more likely to have poor gonococcal colonization than mice whose vaginal swabs indicated a lower commensal flora (data not shown).

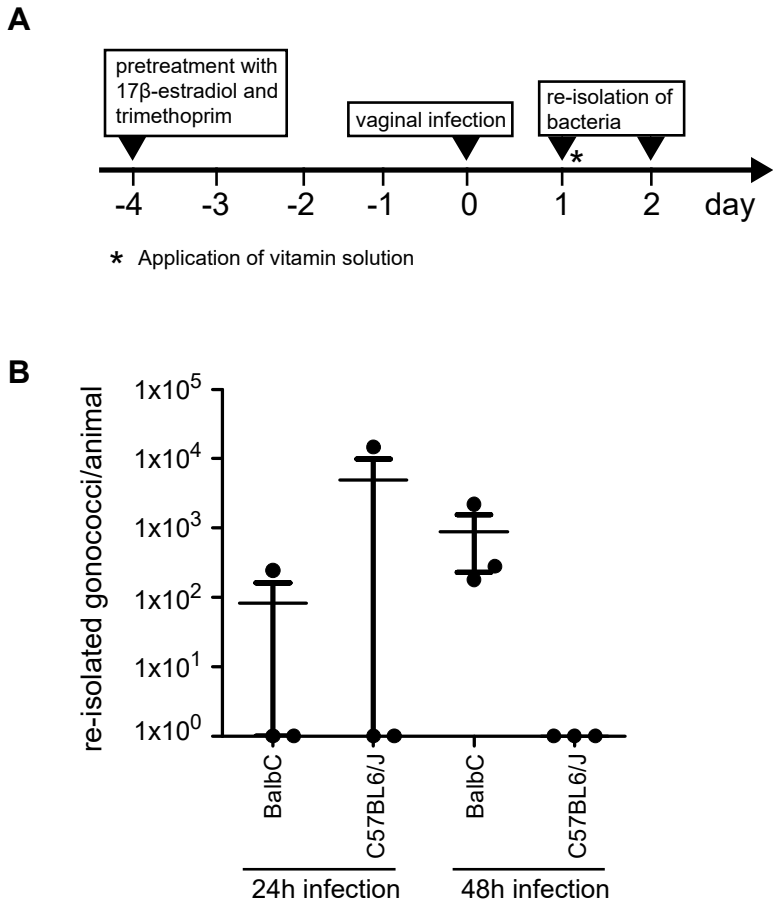

Figure 15: CEAtg Balb/c mice, but not CEAtg C57BL6/J mice show gonococcal colonization for 48 hrs. (A) Schematic representation of the treatment and infection protocol. CEAtg mice were treated subcutaneously with 17β-estradiol four days prior to infection (day -4) and received drinking water supplemented with trimethoprim (40 mg/100ml). On day 0, vaginal inoculation was performed with 10^8 Opa_{52}-expressing *N. gonorrhoeae* in vitamin supplements-containing PPM medium. One or two days after infection, the mice were killed and the bacteria were re-isolated by urogenital swabs. Mice infected for two days were treated intravaginally with PPM medium containing vitamin supplements one day after infection (*). **(B)** Female CEAtg Balb/c or CEAtg C57BL6/J mice were treated as described in (A) and vaginally infected with 10^8 Opa_{52}-expressing *N. gonorrhoeae*. Mice were killed 24 or 48 hours after infection, bacteria were re-isolated from the genital tract and plated on GC plates with and without antibiotics. Each dot indicates the number of bacteria re-isolated from a single mouse on the Erm/Cam-containing GC plates. Indicated is the mean number of *N. gonorrhoeae* isolated from all mice in an experimental group (black line). The error bars indicate the SEM.

3.3.2 Intraperitoneal administration of vancomycin HCl and streptomycin sulfate improve vaginal tract colonization with *N. gonorrhoeae* in CEAtg Balb/c mice

Since administration of trimethoprim via the drinking water did not sufficiently reduce the commensal vaginal flora, we tested the use of additional antibiotics. For this purpose, CEAtg Balb/c female mice were either treated as before, or were additionally treated intraperitoneally with the antibiotics vancomycin HCl and streptomycin sulfate, which have been reported to improve gonococcal colonization in estradiol-treated mice by supressing the commensal vaginal flora (Jerse, 1999). The antibiotics were administered four days and two days before infection and on the day of infection (**Figure 16A**). Indeed, CEAtg mice treated with vancomycin HCl and streptomycin sulfate showed lower vaginal tract colonization with commensal bacteria than CEAtg animals not subjected to additional antibiotic treatment (data not shown). Nevertheless, even among the vancomycin HCl/streptomycin sulfate-treated animals, not all mice were free of commensal bacteria. Comparison of re-isolated *N. gonorrhoeae* from infected CEAtg mice and infected CEAtg mice treated with vancomycin HCl and streptomycin sulfate indicated that additional antibiotic treatment indeed promoted gonococcal colonization (**Figure 16B**). The strong colonization of the vaginal tract with commensal bacteria in the trimethoprim-only treated animals (data not shown) could be a possible explanation for why no *N. gonorrhoeae* colonies at all could be re-isolated from the mice not treated with the additional antibiotics in this experiment (**Figure 16B**). We therefore decided to use vancomycin HCl and streptomycin sulfate for all further experiments.

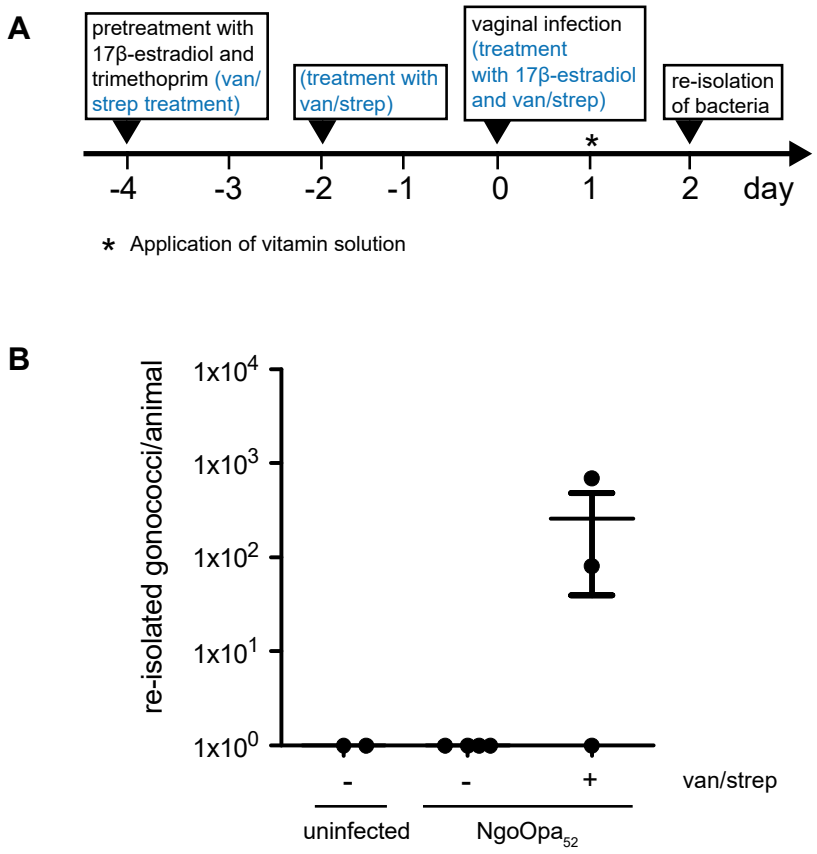

Figure 16: Intraperitoneal administration of vancomycin HCl and streptomycin sulfate improves vaginal tract colonization with *N. gonorrhoeae* in CEAtg Balb/c mice. (A) Schematic illustration of the treatment and infection protocol. Female mice were treated subcutaneously with 17β-estradiol on day -4 and received drinking water supplemented with trimethoprim (40 mg/100 ml). Mice were intraperitoneally treated or not with the antibiotics vancomycin HCl (van) and streptomycin sulfate (strep) on days -4, -2, and 0 (blue font). On day 0, mice were vaginally inoculated with 10^8 Opa_{52}-expressing *N. gonorrhoeae*. Mice treated with van/strep also received an additional subcutaneous injection of 17β-estradiol on day 0. One day after infection (day 1), mice were treated intravaginally with vitamin supplements-enriched PPM medium (*). Re-isolation of the bacteria was performed by urogenital swabs on day 2 post-infection. **(B)** Female CEAtg mice were pre-treated as described in (A). On day 0, mice were vaginally infected with 10^8 Opa_{52}-expressing *N. gonorrhoeae*. At 48 hours post infection, mice were killed, vaginal *N. gonorrhoeae* were re-isolated and plated on GC-Erm/Cam plates (Erm: erythromycin; Cam: chloramphenicol) and GC plates. Each dot indicates the number of bacteria re-isolated from a single mouse on the Erm/Cam-containing GC plates. Indicated is the mean number of *N. gonorrhoeae* isolated from all mice in an experimental group (black line). The error bars indicate the SEM.

3.3.3 Anaerobically cultured Opa_{52}-expressing *N. gonorrhoeae* show no colonization advantage in CEAtg mice compared with aerobically grown bacteria

The natural habitat of *N. gonorrhoeae*, the genital tract, has low oxygen levels. Because *N. gonorrhoeae* can switch to anaerobic respiration in low-oxygen environments, they are ideally adapted to growth under these conditions (Knapp & Clark, 1984). However, in the experiments described so far, the gonococci used were grown under microaerophilic rather than anaerobic conditions. It cannot be ruled out that gonococcal factors important for colonization are not expressed or are greatly reduced in the presence of oxygen. In this case, pre-culturing *N. gonorrhoeae* under anaerobic conditions could potentially improve the colonization of the genital tract of female mice. To investigate this, we first tested in preliminary experiments how rapidly gonococci in anaerobic environments express the nitrite reductase AniA, which is expressed only under oxygen-limited conditions (Mellies et al., 1997). Culturing *N. gonorrhoeae* for 24 hours under oxygen-limited conditions (0.5% O_2) proved sufficient to induce significant expression of AniA (**Figure 17A**). A longer anaerobic incubation period did not further increase the AniA expression level (**Figure 17A**). To next test the effect of oxygen conditions on infection success, in the subsequent experiment, gonococci were cultured either under microaerophilic conditions as before or under anaerobic conditions for 24 hours and administered to CEAtg female mice treated with vancomycin HCl and streptomycin sulfate (**Figure 17B**). A conformation that the anaerobically cultured *N. gonorrhoeae* used for infection indeed had significantly higher AniA expression than the aerobically cultured bacteria is shown in **Figure 17C**. Enumeration of the *N. gonorrhoeae* re-isolated from the CEAtg mice 48 hours after inoculation, however, showed no advantage for colonization of the vaginal tract by anaerobically cultured bacteria compared with aerobically cultured bacteria (**Figure 17D**). Since no overall improvement of the mouse model for *N. gonorrhoeae* infections could be achieved with the anaerobically cultured *N. gonorrhoeae*, we decided to return to using aerobically grown gonococci for future experiments.

It is worth noting that in this experiment, the effect of the additional antibiotics on reducing the natural vaginal flora was confirmed, which was evident by comparing the number of re-isolated bacteria on GC plates without antibiotics (GC) and the number of re-isolated *N.*

gonorrhoeae on the GC plates containing erythromycin and chloramphenicol (GC-Erm/Cam) (**Figure 17D**). The two plates belonging to one animal showed approximately the same colony count, which was observed in almost all re-isolates.

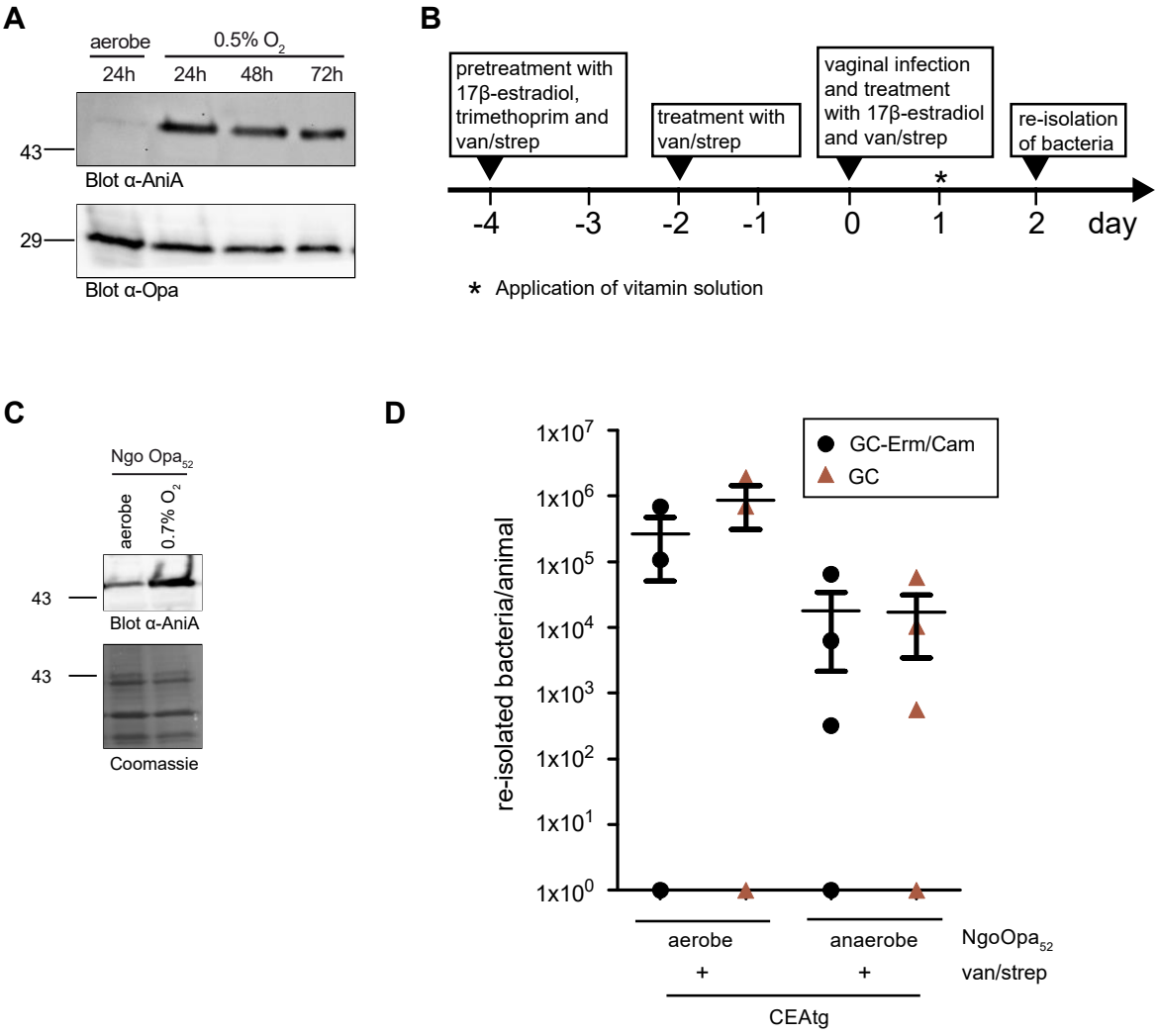

Figure 17: Anaerobically cultured Opa$_{52}$-expressing *N. gonorrhoeae* show no colonization advantage in CEAtg mice compared with aerobically grown bacteria. (A) Opa$_{52}$-expressing *N. gonorrhoeae* were cultured under microaerophilic growth conditions or under anaerobic growth conditions (0.5% O_2) in the presence of 2 mM $NaNO_2$ for the indicated periods. Bacterial lysates were prepared and analysed by Western blotting using polyclonal antibodies against AniA (upper panel) or monoclonal antibodies against Opa proteins (lower panel). **(B)** Schematic representation of the treatment protocol. CEAtg Balb/c mice received drinking water supplemented with trimethoprim (40 mg/100 ml) from day -4 and were treated subcutaneously with 17β-estradiol on day -4 and day 0. Mice were intraperitoneally injected with vancomycin HCl (van) and streptomycin sulfate (strep) in PBS on day -4, -2, and 0. Vaginal inoculation with 10^8 anaerobically or aerobically cultured Opa$_{52}$-expressing *N. gonorrhoeae* was performed on day 0. The following day (day 1), mice were treated intravaginally with PPM medium containing vitamin supplements (*). Bacteria were re-isolated on day 2 post-infection by vaginal swabs. **(C)** Opa$_{52}$-expressing *N. gonorrhoeae* were grown for 24 hours under anaerobic or aerobic conditions. Bacteria were lysed and analysed for expression of AniA by Western blotting using polyclonal

antibodies against AniA. Coomassie staining demonstrates even protein loading of the two lanes (lower panel). **(D)** CEAtg mice were pre-treated as described in (B) and infected with anaerobically or aerobically cultured Opa_{52}-expressing *N. gonorrhoeae* grown as in (C). Two days after infection, bacteria were re-isolated from the genital tract and plated on GC plates containing chloramphenicol and erythromycin (GC-Erm/Cam) and on GC plates without antibiotics (GC). The number of re-isolated bacteria counted on GC plates without antibiotics are shown as brown triangles, those counted on GC plates containing Erm/Cam are shown as black dots. Each dot/triangle represents the number of bacteria re-isolated from a single animal. The mean value of re-isolated bacteria for each experimental group (n = 3-4) is indicated by a black line. Error bars indicate the SEM.

3.3.4 Mouse-passaged Opa_{52}-expressing *N. gonorrhoeae* demonstrate successful 48-hour vaginal colonization of CEAtg mice

In several inoculation experiments, we were unable to re-isolate gonococci from individual CEAtg mice 48 hours after intravaginal infection with Opa_{52}-expressing *N. gonorrhoeae* despite the same pre-treatment. We wondered whether passage of gonococci in the vaginal tract of CEAtg mice could enhance the ability of these bacteria to colonize the mouse vaginal tract, potentially allowing for a more reliable and less variable 48-hour infection in terms of bacterial numbers. To test this, female CEAtg mice were infected with *N. gonorrhoeae* that had been passaged twice in CEAtg female mice. Indeed, gonococci could be re-isolated from all three infected CEAtg mice 48 hours after intravaginal inoculation (**Figure 18A**). The number of colonies recovered from the infected mice and grown on the GC-Erm/Cam plates was between $7.2x10^3$ and $8.8x10^4$, which is a much smaller range than in the previously performed infection studies. Furthermore, by preparing lysates of the re-isolated bacteria, we were able to confirm that the bacteria grown on the GC-Erm/Cam plates were indeed Opa-expressing bacteria (**Figure 18B**). As before, treatment with vancomycin HCl and streptomycin sulfate showed successful inhibition of commensal vaginal tract bacteria in the CEAtg mice (**Figure 18A**). Again, the numbers of colony-forming units (cfu) counted on the GC plates (GC) were similar to the colony numbers counted on the corresponding Erm/Cam-containing GC plates (GC-Erm/Cam) (**Figure 18A**). Overall, these results demonstrate that mouse-passaged Opa_{52}-expressing *N. gonorrhoeae* can successfully colonize the vaginal mucosa for at least 48 hours when introduced into CEAtg mice following the aforementioned treatment regimen. Thus, in addition to treatment of CEAtg mice with vancomycin HCl and streptomycin sulfate, the use of mouse-passaged *N. gonorrhoeae* represents the second optimization of the CEAtg mouse

model for gonococcal infections, which together enable successful 48-hour colonization of the vaginal tract.

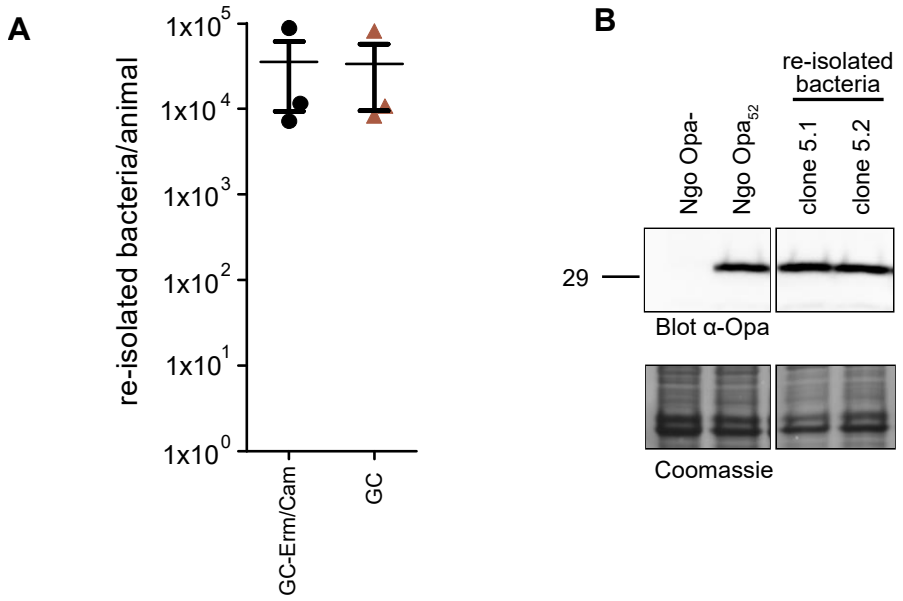

Figure 18: Mouse-passaged Opa_{52}-expressing *N. gonorrhoeae* demonstrate successful 48-hour vaginal colonization of CEAtg mice. (A) CEAtg female mice treated with 17β-estradiol, vancomycin HCl, streptomycin sulfate and trimethoprim were vaginally infected with 10^8 mouse-passaged Opa_{52}-expressing *N. gonorrhoeae*. 48 h after infection, bacteria were re-isolated and plated on GC plates containing chloramphenicol and erythromycin (GC-Erm/Cam) and GC plates without antibiotics (GC). The number of re-isolated bacteria counted on GC plates without antibiotics are shown as brown triangles, and those counted on GC plates with Erm/Cam are shown as black dots. Each dot/triangle represents the number of bacteria re-isolated from a single animal. The mean value of the re-isolated bacteria in each experimental group (n = 3) is shown as a black line. The error bars indicate the SEM. **(B)** Single bacterial colonies re-isolated in (A) were grown on GC plates and subsequently lysed. The bacterial lysates (clones 5.1 and 5.2) were analyzed together with lysates from non-mouse-passaged *N. gonorrhoeae* (*N. gonorrhoeae* lacking Opa proteins (Ngo Opa-) and Opa_{52}-expressing *N. gonorrhoeae* (Ngo Opa_{52})) by Western blotting with anti-Opa monoclonal antibodies.

4. Discussion

4.1 CEACAM3-RQAP – a CEACAM3 polymorphism that directs opsonin-independent recognition of *Neisseria meningitidis*

In the first part of this thesis, we analysed the binding spectrum of Opa-expressing meningococci of different serogroups for members of the CEACAM family and describe the finding that the CEACAM3 polymorphism CEACAM3-RQAP, which is widely distributed in populations of sub-Saharan Africa, allows opsonin-independent recognition of *N. meningitidis*.

4.1.1 *N. meningitidis* strains bind to epithelial CEACAM1 and CEA, but are not recognized by granulocyte CEACAM3

Colonization of the human nasopharyngeal mucosa, the only natural habitat of *N. meningitidis*, occurs by direct attachment of the bacteria to host surface structures (Virji, 2009). While the receptors for most of the meningococcal adhesins, such as PilC, NadA, NhhA, or NspA, are not well characterized, the phase-variable Opa proteins are intensely studied outer membrane proteins of meningococci. Indeed, Opa proteins allow these pathogens to bind to members of the CEACAM family expressed on epithelial cells of the nasopharynx, which not only facilitates initial host colonization but also promotes their invasion into subepithelial tissues (Sadarangani et al., 2011; Virji, 2009). In contrast, CEACAM3, the only pathogen-binding member of the CEACAM family that is not expressed on mucosal surfaces, but exclusively found on granulocytes directs the opsonin-independent phagocytosis and destruction of CEACAM-binding pathogens (Bonsignore et al., 2020). Given these opposing consequences for CEACAM-binding pathogens, it would be reasonable to assume that *N. meningitidis* prefer binding to epithelial CEACAMs but avoid recognition by CEACAM3. Indeed, the bacterial pull-down experiments in which we tested the interaction of five *N. meningitidis* strains with the CEACAM receptors CEACAM1, CEACAM3, CEACAM5, CEACAM6, and CEACAM8 revealed that all *N. meningitidis* strains expressed Opa proteins that allowed binding to the epithelial-expressed receptor CEACAM1 (**Figure 7D**). This is consistent with reports by Virji and colleagues who in studies with 32 *N. meningitidis* strains, including members of serogroups A, B, C, X, Y, Z, and W, demonstrated binding to CEACAM1 for 27

strains (84%) and reported non-significant Opa expression in most cases for the few non-CEACAM1-binding bacteria (Virji, Watt, et al., 1996). In contrast to the uniform binding of the Opa protein-expressing *N. meningitidis* to CEACAM1, we did not find a single CEACAM3-binding meningococcal strain in our analyses, in which we examined a total of 9 Opa-expressing meningococcal strains for their ability to interact with CEACAM3 (**Figure 9F**). By analysing the CEACAM-binding spectrum of each of the four Opa proteins encoded by *N. meningitidis* of the serogroup B strain MC58 and the serogroup C strain C1938 individually, we were for these meningococcal strains furthermore able to exclude the possibility that they only by chance did not express CEACAM3-interacting Opa proteins (**Figure 7F**,**Figure 8D,E**). In fact, the absence of CEACAM3-binding Opa proteins in the *N. meningitidis* strains MC58 and C1938 was already observed in previous studies by Muenzner et al. and Johswich et al. (Johswich et al., 2013; Muenzner et al., 2000) and could be confirmed by us in this work. Furthermore, studies examining the CEACAM-binding spectrum of individual meningococcal Opa proteins of strains not included in this work have demonstrated the absence of CEACAM3-binding Opa proteins in additional *N. meningitidis* strains. For example, all four Opa proteins of the serogroup B strain H44/76 were observed to bind to CEACAM1, but none of the Opa proteins was shown to interact with CEACAM3 (De Jonge et al., 2003). For the Opa proteins encoded by the serogroup A strain F6124, three of the four Opa proteins have been shown to bind to CEACAM1, but likewise none of the Opa proteins interacted with CEACAM3 (Muenzner et al., 2000). It is also worth mentioning that not only Opa proteins of *N. meningitidis* show a preference for binding to epithelial CEACAMs and an avoidance of binding to CEACAM3, corresponding binding tendencies have also been described for the CEACAM-binding adhesins of *Neisseria gonorrhoeae* and *Haemophilus influenzae* (Gray-Owen, Lorenzen, et al., 1997; Roth et al., 2013; Tchoupa et al., 2015). Obviously, *N. meningitidis* and other CEACAM-binding bacteria appear to adapt their CEACAM-binding structures to allow binding to epithelial CEACAMs such as CEACAM1 and CEA but avoid binding to the phagocytic CEACAM3 receptor.

4.1.2 CEACAM3-RQAP recognizes and initiates the internalization of a broad spectrum of meningococcal Opa proteins

It has been suggested that CEACAM3 may also adapt to maintain its function as an effective decoy receptor of the immune system (Adrian et al., 2019; Zimmermann, 2019). Indeed, our

data show that the CEACAM3 polymorphism CEACAM3-RQAP, which is widely distributed in sub-Saharan African populations, recognizes all meningococcal Opa proteins for which we have demonstrated binding with CEACAM1 (**Figure 8D,E,G**). As we have shown, CEACAM3-RQAP is not only capable of recognizing CEACAM1-optimized meningococcal Opa proteins that escape recognition by the common CEACAM3 receptor, but also mediates rapid internalization of the bound Opa-expressing bacteria (**Figure 9B,D**). Furthermore, our results highlight the striking geographic coincidence of the CEACAM3-RQAP polymorphism with the exceptionally high burden of invasive meningococcal disease in the meningitis belt and provide a plausible scenario, which selective advantage might have driven the fixation and spread of such a CEACAM3 variant in this area. Indeed, the recognition of Opa protein expressing meningococci afforded by CEACAM3-RQAP might be a vital advantage in an environment, where epidemics of meningitis during the annual dry season can reach attack rates of 1 in 10 in local communities (Greenwood, 1999). The finding of a gain-of-function polymorphism in a phagocytic receptor also implies that granulocyte-mediated opsonin-dependent and –independent phagocytosis might help to limit meningococcal colonization and spread. Indeed, ablation of granulocytes in a humanized mouse model of meningococcal nasal colonization is accompanied by elevated numbers and prolonged presence of meningococci in the nasopharynx (Johswich et al., 2013).

Although we cannot date the ancestry of the CEACAM3-RQAP allele with certainty, the extended haplotype homozygosity with an integrated haplotype score (iHS) >2 for each of the four single nucleotide polymorphisms and the remarkable allele frequency in most sub-Saharan populations suggests a strong positive selection (Maclean et al., 2015). It has been argued that epidemic meningitis is a rather recent phenomenon in sub-Saharan Africa based on the lack of anecdotal reports of this devastating disease from this region before the 19th century (Greenwood, 1999). If capsulate meningococci have indeed been absent in sub-Saharan Africa only a few generations ago, the emergence and regional distribution of the CEACAM3-RQAP allele cannot be explained by its gain-of-function in *N. meningitidis* detection. Therefore, other CEACAM-binding pathogens, including *Neisseria gonorrhoeae*, *Haemophilus influenzae*, or *Helicobacter pylori* might serve as driving forces behind this apparent positive selection. A recent paper from our group has already shown that CEACAM3-RQAP also allows binding to Omp P1, the CEACAM-binding adhesin of *H. influenzae*, and to Opa proteins of

gonococci that interact with CEACAM1 but are not recognized by the common CEACAM3 receptor (Adrian et al., 2019).

Interestingly, a CEACAM3 allele (CEACAM3-AP) harbouring two of the four sequence alterations contained in CEACAM3-RQAP and, therefore, also partially mimicking CEACAM1, is found in a *Homo neanderthalensis* sample from the Vindija Cave in Croatia (Prüfer et al., 2017; https://bioinf.eva.mpg.de/jbrowse). This remarkable discovery suggests that gene conversions between CEACAM1 and CEACAM3 and the creation of CEACAM1-mimicking CEACAM3 alleles might have occurred previously in other hominid populations. Whatever the microbial driver behind the evolution of major CEACAM3 polymorphisms might be, the fact that CEACAM1-mimicking CEACAM3 alleles appear as a recurring theme in human evolution points to an important role of opsonin-independent detection of bacterial pathogens by the granulocyte-expressed CEACAM3 receptor.

4.2 PTPRJ is a negative regulator of CEACAM3 signaling that acts directly on the receptor protein

Parts of this discussion section have been published in:

Phagocytosis mediated by the human granulocyte receptor CEACAM3 is limited by the receptor-type protein tyrosine phosphatase PTPRJ

Goob G., Adrian J., Cossu C., Hauck C. R. (2022) Journal of Biological Chemistry, 298(9), 102269. https://doi.org/10.1016/j.jbc.2022.102269.

In the second part of this thesis, I focused on the identification of a negative regulator of the granulocyte-expressed innate immune receptor CEACAM3. CEACAM3 is a specialized phagocytic receptor, enabling primate granulocytes to detect and eliminate a restricted set of host-adapted bacterial pathogens (Adrian et al., 2019). CEACAM3 downstream signalling is initiated by tyrosine phosphorylation of a characteristic sequence motif in the cytoplasmic domain of this receptor (Bonsignore et al., 2020). Here, we reveal that CEACAM3 signalling is controlled by the receptor-type tyrosine phosphatase PTPRJ (also known as CD148 and DEP-

1). PTPRJ activity is directed towards the phosphorylated tyrosine residues of CEACAM3, thereby constraining CEACAM3-initiated cellular responses.

In this regard, PTPRJ appears as the second negative regulator of CEACAM3 signalling, which acts directly on the receptor protein. Grb14, a SH2 domain-containing adaptor protein, has previously been shown to associate with the phosphorylated tyrosine residue Y230 of CEACAM3 and thereby prohibits access of functionally important binding partners (Kopp et al., 2012). Indeed, pY230 is the major binding site of SH2 domains encoded by Src family kinases, the GEF Vav and the adapter protein Nck, which together orchestrate the cytoskeletal rearrangements required for efficient phagocytosis (Buntru et al., 2012). By competitive binding to pY230, Grb14 interferes with CEACAM3 downstream signalling and reduces bacterial uptake. In a similar manner, PTPRJ achieves a comparable outcome, by slightly different means: this enzyme readily dephosphorylates the tyrosine residues embedded in the ITAM-like motif (**Figure 12F,H**), thereby completely abrogating the phosphorylation-dependent, SH2-domain-mediated binding by multiple interaction partners.

A direct action of PTPRJ on CEACAM3 is supported by the *in vitro* dephosphorylation of phospho-peptides derived from the CEACAM3 ITAM-like motif by recombinant PTPRJ (**Figure 12D,E**). Moreover, the reduced CEACAM3 phosphorylation observed in intact cells overexpressing active PTPRJ, which do not show changes in the phosphorylation pattern of Src family kinases, is further strong evidence that CEACAM3 is a direct substrate of PTPRJ (**Figure 11**). The lack of an effect of PTPRJ on Src family kinases might appear surprising given the known positive role of PTPRJ for Src PTK activation in platelets, but this might be different in human myeloid cells, where absence of PTPRJ has been linked to increased activity of receptor protein tyrosine kinases (Arora et al., 2011) and where the activation of Src family kinases can be mediated by distinct PTPRs, such as PTPRC (CD45) (Hermiston et al., 2003, 2009).

Similar to other PTPRs, PTPRJ is characterized by the possession of a large, multidomain extracellular part (Hermiston et al., 2009). This spacious extracellular part of the enzyme is functionally relevant during phagocytosis, as it leads to the displacement of PTPRJ by a surfacebound particle (Goodridge et al., 2011). A similar situation can be envisioned in the case of gonococci associating with CEACAM3. The tight binding of the bacteria to CEACAM3

leads to a close apposition of the particle and the phagocyte membrane as observed by scanning electron microscopy (Billker et al., 2002; Schmitter et al., 2004). Accordingly, the steric hindrance of the large extracellular domain of PTPRJ would result in a lateral displacement of the protein phosphatase away from the clustered, pathogen-bound receptor. As a consequence of this microscale spatial separation, the local absence of PTPRJ could give way to elevated tyrosine phosphorylation of the CEACAM3ITAM-like motif, whenever the receptor is engaged by a particle. In line with this elegant concept of a phagocytic synapse formation (Goodridge et al., 2011), truncation of the large extracellular domain of PTPRJ results in a constitutive-active form of the protein phosphatase, which cannot get displaced by a bound particle and therefore, diminishes CEACAM3-mediated phagocytosis. Another mode of PTPRJ regulation, which depends on the generation of reactive oxygen by the NADPH oxidase has been reported from human acute myeloid leukaemia (AML) cells (Godfrey et al., 2012). As CEACAM3-initiated signals trigger strong GTP-loading of Rac and NADPH oxidase assembly, PTPRJ could also become enzymatically silenced via reactive oxygen species acting on critical cysteine residues in the phosphatase domain (den Hertog et al., 2008). In this way, NADPH oxidase action might generate a positive feedback loop to promote sustained tyrosine phosphorylation of CEACAM3 by dampening PTPRJ activity.

Together, our results indicate that human granulocytes possess multiple, independent means of regulating the phosphorylation state of the CEACAM3 ITAM-like motif. This finding implies that tight control of this receptor is needed to prevent unintended activity. Indeed, by triggering the release of proinflammatory cytokines and inducing massive stimulation of reactive oxygen production (Buntru et al., 2011; Heinrich et al., 2016; Schmitter et al., 2004; Sintsova et al., 2014), uncontrolled CEACAM3 signaling has the potential to cause severe cell and tissue damage. On the other hand, the action of this granulocyte receptor can protect our body from harmful microbes suggesting that the negative regulation by PTPRJ or Grb14 has to be finely tuned to allow maximum effectivity of CEACAM3 at infection sites.

4.3 Optimization of experimental *N. gonorrhoeae* genital tract infections in CEA transgenic estradiol-treated mice

Despite the strict adaptation of *N. gonorrhoeae* to humans, it has long been known that gonococci can at least temporarily colonize mice treated with 17β-estradiol (Taylor-Robinson et al., 1990). The generation of mice expressing the human CEA receptor (Eades-Perner et al., 1994) opened the possibility to investigate the role of the Opa-CEA interaction in human gonococcal colonization and pathogenesis, and allowed prolonged colonization of the genital tract with CEA-binding *N. gonorrhoeae* compared to wild-type mice (Islam et al., 2018; Muenzner et al., 2010). Our laboratory has also been working with CEAtg mice for years to understand the mechanisms of *in vivo* colonization by this human-specific pathogen. However, the treatment and infection protocol we have used in the past has only been developed and applied to studies with an infection duration of 24 hours (Muenzner et al., 2010; Muenzner & Hauck, 2020). In the third part of this thesis, we aimed to optimize the mouse infection model used in our laboratory based on the previously followed protocol to maintain gonococcal infections in CEAtg mice for at least 48 hours. In agreement with reports from other researchers (Jerse, 1999; Jerse et al., 2011), we confirm here that treatment of estradiol-treated mice with the antibiotics vancomycin HCl and streptomycin sulfate minimizes the commensal flora of the genital tract and improves gonococcal infection. Furthermore, we observed that infection with *N. gonorrhoeae* previously passaged in female CEAtg mice help to reduce variations in gonococcal load between infected animals. Contrary to our assumptions, the use of anaerobically cultured *N. gonorrhoeae* did not improve the infection of the mouse genital tract. Since the experiments were performed only with small groups of animals, the reliability of these data is not sufficiently assured. Further experiments with more mice are needed to verify that the above adaptations are sufficient to reliably achieve gonococcal infection in female CEAtg mice over a period of at least 48 hours.

Like most microorganisms, *N. gonorrhoeae* depend on the acquisition and uptake of iron to survive and grow. In humans, *N. gonorrhoeae* use, among others, their transferrin and lactoferrin receptors to bind the human transferrin and lactoferrin proteins allowing them to acquire the iron stored by these molecules (Lee & Schryvers, 1988; Mickelsen et al., 1982). However, these gonococcal receptors are not able to bind murine iron-binding proteins, like

murine transferrin (Blanton et al., 1990; Cornelissen et al., 1993). To prevent that a possible inability of *N. gonorrhoeae* to harness sufficient iron in the mouse genital tract affects the colonization, we decided to supply iron and other nutrients to the mice 24 hours after infection by vaginal application of the vitamin solution. It has been shown that *N. gonorrhoeae* in estradiol-treated BALB/c mice can survive an average of 12 to 13 days without externally supplied iron, suggesting that gonococci in mice can use other sources of iron not restricted to the host (Jerse, 1999). However, infection studies with *N. meningitidis*, that showed higher infection numbers and longer bacterial survival in human transferrin-transgenic mice than in wild-type mice, suggest that additional iron sources can prolong infection of mice with pathogenic *Neisseriae* (Zarantonelli et al., 2007). Therefore, it would be reasonable to assume that mice expressing human CEA and human transferrin or human lactoferrin could further improve the mouse model for gonococcal infections, but so far such double-transgenic mice are not available.

A decisive advance for the usability of mice as *N. gonorrhoeae* infection models was the finding by Taylor-Robinson and colleges that female mice exhibit higher susceptibility to *N. gonorrhoeae* upon treatment with estradiol (Taylor-Robinson et al., 1990). The administration of estradiol to maintain the cycle of female mice in the estrus stage, as practiced by us and other research groups working with the gonococcal mouse model, has therefore been a long-standing practice (Islam et al., 2018; Jerse, 1999; Muenzner et al., 2010). However, it is also known that increasing estradiol levels are accompanied by increased proliferation of the endogenous genital tract flora (Furr & Taylor-Robinson, 1991). Because overgrowth of the commensal flora can negatively affect gonococcal susceptibility in estradiol-treated mice, we have previously used the broad-spectrum antibiotic trimethoprim over the course of the experiment (Muenzner et al., 2010; Muenzner & Hauck, 2020). Unexpectedly, we observed here that many CEAtg female mice had a very pronounced commensal flora in the vaginal tract even after 5 or 6 days of use of this antibacterial agent. Female mice that showed marked colonization with endogenous bacteria despite trimethorprim treatment were more likely to show poor gonococcal colonization than mice whose vaginal tract was largely free of endogenous bacteria (unquantified observation). Because trimethoprim was ingested by the mice only via the drinking water, it is likely that differences in the drinking behavior resulted in not all mice ingesting the same amount of this antibiotic. This could be an explanation for

the differences in the remaining endogenous vaginal flora. However, since the mice were kept in open cages, it is also conceivable that the vaginal flora within the mouse population changed over time or even that colonization differences occurred between mice of different cages. The spread of microorganisms with poorer sensitivity to trimethoprim can therefore not be ruled out. Individually ventilated cages (IVC) would be a possibility to better control the endogenous mouse flora, but this type of housing is very laborious and associated with significantly higher costs. We therefore decided to continue to keep the mice in open cages and test whether, as reported by Jerse, the use of additional antibiotics could minimize the endogenous flora and thus increase the susceptibility of mice to *N. gonorrhoeae* (Jerse, 1999). Although we were also partially unable to re-isolate gonococci in mice additionally treated with vancomycin HCl and streptomycin sulfate, overall, the use of these antibiotics appeared to improve the gonococcal colonization of the mouse genital tract. We cannot comment on the colonization status with strictly anaerobically growing bacteria, but at least for aerobically growing and well-culturable bacteria, intraperitoneal administration of these antibiotics resulted in a strong reduction of the vaginal flora (**Figure 17D**,**Figure 18A**). Not only trimethoprim, but also vancomycin HCl and streptomycin sulfate are reported to be commonly used in the estradiol-controlled mouse model to avoid an interference of the commensal flora during gonococcal infections (Islam et al., 2018; Jerse, 1999; Jerse et al., 2011; Li et al., 2011). The concentrations of trimethoprim (0.04 g/100 ml drinking water), streptomycin sulfate (2.4 mg/mouse) and vancomycin HCl (0.6 mg/mouse) that we used in this study were within the range of concentrations regularly reported in the literature in the context of the gonococcal mouse model (Islam et al., 2018; Jerse, 1999; Xu et al., 2018). However, with a 48-hour application frequency (four days and two days prior to infection, as well as on the day of infection), our experiments fall below commonly described antibiotic treatment frequencies. Islam and co-workers administered 0.6 mg vancomycin HCl and 2.4 mg streptomycin sulfate daily to estradiol-treated mice for a recently published study (Islam et al., 2018). Jerse states in a publication from 1999 to treat the estradiol-treated female mice twice daily with 0.6 mg vancomycin HCl and 1.2 mg streptomycin sulfate beginning on day two prior to infection (Jerse, 1999). Thus, if further experimental gonococcal infections in mice show that the 48-hour treatment scheme is not sufficient to control the commensal vaginal flora, it might be useful to test daily administration of these antibiotics.

The observation that some mice showed no or comparatively poor gonococcal colonization despite effective suppression of the endogenous vaginal flora prompted us to test further approaches to optimize the mouse infection model. One approach was based on infecting female CEAtg mice with anaerobically cultured *N. gonorrhoeae*. Initial results, however, showed no improvement in colonization compared to aerobically grown bacteria (**Figure 17**), which is why we did not pursue this optimization approach. In studies by Islam et al., 50% of the CEAtg mice were still colonized with gonococci after 7 days of infection with aerobically pre-cultured *N. gonorrhoeae*, indicating that anaerobic cultivation is not a prerequisite for long-term infection in transgenic female mice (Islam et al., 2018). However, since the genital tract is a low-oxygen environment, it would have been conceivable that bacteria that have already adapted to the anaerobic growth conditions could have a colonization advantage compared to aerobically grown bacteria. For example, some gonococcal proteins, including the nitrite reductase AniA, which converts nitrite to nitric oxide (NO) in anaerobic respiration, are known to be expressed only under anaerobic conditions (Mellies et al., 1997). Recently, NO produced by *N. gonorrhoeae* was shown to suppress shedding of infected epithelial cells in CEAtg mice and thus to promote the establishment *N. gonorrhoeae* in the urogenital tract (Muenzner & Hauck, 2020). To block exfoliation, bacterial NO must enter the host cell, which is enabled by the Opa-CEACAM-mediated close interaction between *N. gonorrhoeae* and the host cell. There, NO promotes integrin activation by inducing expression of the host transmembrane glycoprotein CD105 (Muenzner & Hauck, 2020). Increased integrin activity leads to enhanced binding of cells to the extracellular matrix and facilitates initial colonization of the mucosa by CEACAM-binding *N. gonorrhoeae* (Muenzner et al., 2010). We did not test how rapidly aerobically grown *N. gonorrhoeae* upregulate AniA expression after intravaginal inoculation of mice. However, *in vitro* gonococcal infection assays with 293T cells performed under static, non-aerated growth conditions show that aerobically cultured *N. gonorrhoeae* strongly express AniA *in vitro* within 4 hours of epithelial cell infection (Muenzner & Hauck, 2020). It is likely that *N. gonorrhoeae* respond similarly rapidly to the anaerobic conditions present in the mouse genital tract by expressing AniA. If this is the case, it could explain why aerobic culture prior to inoculation shows no disadvantage in the infection success.

While anaerobic cultivation of the bacteria did not improve the mouse infection model, the results of this work suggest that the use of mouse-passaged *N. gonorrhoeae* in experimental

mouse infections reduces the variation in the number of re-isolated bacteria 48 hours after infection (**Figure 18A**). However, because this conclusion is based only on re-isolates from three animals, the effect of *N. gonorrhoeae* passage in mice on infection success and consistency of gonococcal counts should be tested in further experiments, in which non-mouse-passaged *N. gonorrhoeae* are used for comparison. Passages in mice might contribute to the actual human-specific pathogen being better adapted for infections in mice. Furthermore, it would be possible that *in vitro* passages negatively affect the colonization ability of *N. gonorrhoeae in vivo* and that this could be increased or restored by *in vivo* passages. If it is confirmed that the use of mouse-passaged *N. gonorrhoeae*, in combination with the adapted antibiotic treatment, allows a reliable vaginal infection with a bacterial load comparable from mouse to mouse for at least 48 hours, this would be an important improvement of the transgenic mouse model of gonococcal infection that we use. This could not only contribute to a better understanding of host responses to *N. gonorrhoeae*, but also improve testing of the *in vivo* efficacy of agents such as therapeutics against *N. gonorrhoeae*.

5. Material

5.1 Buffers and solutions

Buffer or Solution	Composition
Blocking buffer (IF)	10% heat-inactivated FCS in PBS
Blotto (blocking buffer)	50 mM Tris-HCl (pH 7.5), 150 mM NaCl, 0.05% Tween 20, 2% BSA, 0.05% (w/v) NaN_3
Coomassie staining solution	50% (v/v) methanol, 7.5% (v/v) acetic acid, 1% (w/v) Coomassie blue
Coomassie destaining solution	50% (v/v) methanol, 10% (v/v) acetic acid in ddH_2O
10x Cre recombination buffer	33 mM NaCl, 50 mM Tris-HCl (pH 7.5), 10 mM $MgCl_2$
1 kb DNA-ladder	1 kb DNA-Ladder (Thermo Scientific) in 6x GEBS
ECL solution	100 mM Tris, 0.225 mM Coumaric acid, 1.25 mM Luminol, 0.012% H_2O_2, (pH 8.5)
EM-fixative	0.1 M HEPES (pH 7.2), 3% formaldehyde, 2% glutaraldehyde, 0.09 M sucrose, 0.01 M $CaCl_2$, 0.01 M $MgCl_2$
EM-wash buffer	0.1 M HEPES (pH 7.2), 0.09 M sucrose, 0.01 M $CaCl_2$, 0.01 M $MgCl_2$
FACS buffer	5% heat inactivated FCS in PBS
6x GEBS	20% (w/v) glycerol, 0.5% (w/v) Sarkosyl, 50 mM EDTA, 0.05% bromophenol blue in ddH_2O
GelRed staining solution	100 mM NaCl, 0.3 ml/l GelRed® in ddH_20
2x HBS	274 mM NaCl, 42 mM HEPES, 1.4 mM Na_2HPO_4, pH 7.05
Malachite green solution	54 mM NH_4Mo, 0.9 mM malachite green in 1 M HCl
NP40 lysis buffer	50 mM Tris-HCl (pH 7.4), 150 mM NaCl, 1% NP40, 1 mM EDTA, 50 mM NaF, protease inhibitors (5 µg/ml Leupeptin, 10 µg/ml Aprotinin, 10 µg/ml Pefabloc, 10 µM Benzamidin, 1 µM PMSF)
dNTPs	20 mM dGTP, 20 mM dATP, 20 mM dCTP, 20 mM dTTP in ddH_2O
10x PBS	1.37 M NaCl, 27 mM KCl, 14.7 mM KH_2PO_4, 6.5 mM Na_2HPO_4
4% PFA	4% (w/v) paraformaldehyde in ddH_2O (pH 7.4)

Phagocytosis buffer	0.9 mM $CaCl_2$, 0.5 mM $MgCl_2$, 5 mM glucose, 1% heat-inactivated FCS in PBS
PPM medium	see chapter 5.5
RIPA buffer	1% Triton X-100, 50 mM HEPES, 150 mM NaCl, 10% glycerol, 1.5 mM $MgCl_2$, 1 mM EGTA, 10 mM sodium pyrophosphate, 100 mM NaF, 0.1% (w/v) SDS, 1% (w/v) sodium deoxycholate, protease inhibitors (5 µg/ml Leupeptin, 10 µg/ml Aprotinin, 10 µg/ml Pefabloc, 10 µM Benzamidin, 1 µM PMSF), (phosphatase inhibitors (1 mM Na_3VO_4 and 10 mM pNPP))
SDS running buffer	3% (w/v) Tris, 14.4% (w/v) glycine, 1% (w/v) SDS
2x/4x SDS sample buffer	2%/4% (w/v) SDS, 20% (w/v) glycerol, 125 mM Tris-HCl, 10%/20% (v/v) β-mercaptoethanol, 1% (w/v) bromophenol blue (pH 6.8) in ddH_20
Separation gel buffer	1.5 M Tris-HCl (pH 8.8)
Stacking gel buffer	0.5 M Tris-HCl (pH 6.8)
TAE buffer	500 mM Tris, 50 mM EDTA, 5.7% (w/v) acetic acid
10x Taq/Pfu buffer	200 mM Tris-HCl (pH 8.8), 100 mM $(NH_4)_2SO_4$, 100 mM KCl, 1% Triton X-100, 1 mg/ml BSA, 20 mM $MgSO_4$
10x TBS	500 mM Tris-HCl, 1.5 M NaCl (pH 7.5)
TBS-T	50 mM Tris-HCl (pH 7.5), 150 mM NaCl, 0.05% Tween 20
TE buffer	10 mM Tris-HCl (pH 8), 1 mM EDTA
Vitamin solution	see chapter 5.5
Western Transfer buffer	25 mM, Trizma® base, 190 mM Glycine, 0.1% SDS, 20% MeOH

5.2 Cell lines

Cell line	Description	Source
Hek293T	Human embryonic kidney 293T cells	German collection of microorganisms and cell cultures, DSMZ, Braunschweig, Germany
HL60	Promyeloblasts from peripheral blood	American Type Culture Collection, ATCC, Manassas, Virginia
HL60-CEACAM3-mKate2-Cerulean (Cer)	HL60 cells stably expressing CEACAM3-mKate2 and Cerulean	LSH, Jonas Adrian

HL60-CEACAM3-mKate2-Cer-sgCer	HL60-CEACAM3-mKate2-Cer cells selected for CRISPR-Cas9-mediated knockout of Cerulean	LSH, Jonas Adrian
HL60-CEACAM3-mKate2-Cer-sgCer,sgPTPRJ clone 6	HL60-CEACAM3-mKate2-Cer cells selected for CRISPR-Cas9-mediated knockout of PTPRJ and Cerulean	LSH, Griseldis Goob
MEF	Murine embryonic fibroblasts	LSH, (Grimm et al., 2020)

5.3 Media and reagents for eukaryotic cells

Cell line	Medium	Composition
Hek293T cells	Culture medium	Dulbecco's modified Eagle's medium (DMEM) (Genaxxon) supplemented with 10% calf serum (CS) (Biochrom)
	Starvation medium	DMEM supplemented with 0.5% CS
	Freezing medium	DMEM supplemented with 20% CS and 10% DMSO
	Opti-MEM	Gibco
HL60 cells	Culture medium	RPMI 1640 medium (Genaxxon) supplemented with 10% fetal calf serum (FCS) (Biochrom)
	Starvation medium	RPMI 1640 medium supplemented with 0.5% FCS
	Freezing medium	RPMI 1640 supplemented with 20% FCS and 10% DMSO
MEFs	Culture medium	DMEM medium (Genaxxon) supplemented with 10% FCS, nonessential amino acids, and sodium pyruvate

5.4 Bacteria

LSH No.	Bacterial Strain	Identifier	Reference/Source
360	*E. coli* Nova blue (endA1, hsdR17 (rk12- mk12+), supE44, thi-1, recA1, gyrA96, relA1, lac [F´proA+B+ lacIqZ_M15::Tn10 (Tet^R)])	-	Novagen
09P	Non-piliated *N. gonorrhoeae* MS11-B2.1 Opa_{52}	N309	(Kupsch et al., 1993)
02P	Non-piliated *N. gonorrhoeae* MS11-B2.1 Opa^-	N302	(Kupsch et al., 1993)

54P	*N. gonorrhoeae* MS11-B1 *Nme* C OpaC1 (C1938-1)	N377	(Muenzner et al., 2000)
55P	*N. gonorrhoeae* MS11-B1 *Nme* C Opa41 (C1938-2/41)	N378	(Muenzner et al., 2000)
56P	*N. gonorrhoeae* MS11-B1 *Nme* C Opa40 (C1938-3/40)	N379	(Muenzner et al., 2000)
57P	*N. gonorrhoeae* MS11-B1 *Nme* C OpaC4 (C1938-4)	N380	(Muenzner et al., 2000)
53P	*N. meningitidis* serogroup C, C1938	N95/ C1938	T. F. Meyer (MPI for Infection Biology, Berlin, Germany)
78P	*N. meningitidis* serogroup A, clonal complex 5; mynB, IgtA	2594	U. Vogel (IHM, University of Würzburg, Würzburg, Germany)
61P	*N. meningitidis* serogroup B, MC58 (capsule-deficient mutant)	MC58 *siaD*	U. Vogel (IHM, University of Würzburg, Würzburg, Germany)
72P	*N. meningitidis* serogroup C, Carrier isolate, clonal complex (CC) 939, ST 939	alpha291	U. Vogel (IHM, University of Würzburg, Würzburg, Germany)
80P	*N. meningitidis* serogroup C, (Capsule-deficient mutant) clonal complex 11, ST 11; IgtA	2120 *siaD*	U. Vogel (IHM, University of Würzburg, Würzburg, Germany)
69P	*N. meningitidis* serogroup C, Carrier isolate, clonal complex (CC) 35, ST 35	alpha53	U. Vogel (IHM, University of Würzburg, Würzburg, Germany)
71P	*N. meningitidis* serogroup W, Carrier isolate, clonal complex (CC) 22, ST 22	alpha69	U. Vogel (IHM, University of Würzburg, Würzburg, Germany)
76P	*N. meningitidis* serogroup Y, Carrier isolate, clonal complex (CC) 92, ST 92	alpha720	U. Vogel (IHM, University of Würzburg, Würzburg, Germany)
73P	*N. meningitidis* serogroup Y, Carrier isolate, clonal complex (CC) 949, ST 949	alpha374	U. Vogel (IHM, University of Würzburg, Würzburg, Germany)
93P	*E. coli* BL21 DE3 *pET28a Nme* B OpaA (Opa1)	N/A	(Kuespert et al., 2011)
94P	*E. coli* BL21 DE3 *pET28a Nme* B OpaJ (Opa2)	N/A	(Kuespert et al., 2011)
95P	*E. coli* BL21 DE3 *pET28a Nme* B OpaD (Opa3)	N/A	(Kuespert et al., 2011)
96P	*E. coli* BL21 DE3 *pET28a Nme* B OpaB (Opa4)	N/A	(Kuespert et al., 2011)

5.5 Bacterial culture media and vitamin supplements

Medium	Composition
LB agar (solid)	5 g/l NaCl, 5 g/l yeast extract, 10 g/l Bacto-Tryptone, 10 ml/l 1M $MgCl_2$, 12 g/l Agar-Agar (pH 7)
LB medium (liquid)	5 g/l NaCl, 5 g/l yeast extract, 10 g/l Bacto-Tryptone (pH 7)
GC agar (solid)	36 g/l Difco™ GC Medium Base. The medium is autoclaved and supplemented 1:100 with vitamin supplements (see vitamin supplements listed below).
PPM medium	15 g/l proteose pepton, 1 g/l soluble starch, 5 g/l NaCl, 4 g/l KH_2PO_4, 1g/l K_2HPO_4 (pH 7.5). The medium is autoclaved and then supplemented 1:100 with Vitamin supplements (vitamin supplements listed below).
Vitamin supplements (for PPM and GC media)	100 g/l glucose, 10 g/l glutamine, 26 g/l L-cysteine, 100 mg/l Cocarboxylase, 250 mg/l Nicotinamide adenine dinucleotide (NAD), 20 mg/l $Fe(NO_3)_3$, 150 mg/l arginine, 3 mg/l vitamin B1, 10 mg/l vitamin B12, 13 mg/l p-aminobenzoic acid, 1.1 g/l cystine, 1 g/l adenine, 500 mg/l uracil, 30 mg/l guanine in ddH_2O (pH 7)
Freezing medium for *Neisseria spp.*	50% v/v PPM medium and 50% v/v 50% glycerol
Freezing medium for *E. coli*	50% v/v LB medium and 50% v/v 50% glycerol

5.6 Antibiotics

Antibiotic	Concentration	Application	Company
Ampicillin (Amp)	100 µg/ml	LB plates and liquid cultures	Roth
Kanamycin (Kan)	50 µg/ml	LB plates and liquid cultures	Roth
Puromycin dihydrochloride	1 µg/ml	Selection of transduced HL60 cells	Calbiochem
Erythromycin (Erm)	7 µg/ml	GC agar plates	AppliChem
Chloramphenicol (Cam)	10 µg/ml 30 µg/ml	GC agar plates LB agar plates	AppliChem
Gentamycin	100 µg/ml	Gentamycin protection assays	AppliChem
Vancomycin	0.6 mg/mouse	Mouse treatment	Sigma-Aldrich
Streptomycin	2.4 mg/mouse	Mouse treatment	Sigma-Aldrich

Trimethoprim (InfectoTrimet®)	0.4 mg/ml	Mouse treatment	InfectoPharm

5.7 Antibodies

5.7.1 Primary antibodies

Antigen	Clone	Species	Company/Source	Dilution
AniA	1160	Rabbit polyclonal	(Muenzner & Hauck, 2020)	WB: 1:1000
CEACAM3/CEACAM5	308/3-3	Mouse monoclonal	Immuno Tools	WB: 1:2000, FC: 1:200
GFP	JL8	Mouse monoclonal	Clontech, Mountain View, USA	WB: 1:5000
GFP		Rabbit polyclonal	tag-tools GmbH, Konstanz, Germany	1:1000
6x His	H8	Mouse monoclonal	Thermo Scientific	WB: 1:1000
Opa	4B12/C11	Mouse monoclonal	DSHB, University of Iowa, USA, a generous gift of M. Achtman	WB: 1:2000
PTPRC (CD45)	35-Z6	Mouse monoclonal	Santa Cruz	FC: 1:150
PTPRJ (DEP-1)	143-41	Mouse monoclonal	Santa Cruz	WB: 1:1000, FC: 1:150, IF: 1:100
RFP (used to detect mCherry)	6G6	Mouse monoclonal	Chromo Tek	WB: 1:2000
c-Src	SRC2	Rabbit polyclonal	Santa Cruz	WB: 1:1000
$p130^{Cas}$	P27820	Mouse monoclonal	Transduction Laboratories	WB 1:1000
phospho-$p130^{Cas}$ (pY410)	#4011	Rabbit polyclonal	Cell Signalling	WB: 1:500
phospho-Src (pY418)	Cat. # 44660G	Rabbit polyclonal	Invitrogen	WB: 1:500
phospho-Src (Tyr527)	#2105	Rabbit polyclonal	Cell Signalling	WB: 1:500

β-Tubulin	E7	Mouse monoclonal	DSHB, University of Iowa, USA	WB: 1:1000
phospho-Tyrosine	PY72	Mouse monoclonal	Upstate Biotechnology	WB: 1:1000
Vinculin	hVIN-1	Mouse monoclonal	Sigma-Aldrich	WB: 1:1000

5.7.2 Secondary antibodies

Antibody	Company	Dilution
HRP-conjugated AffiniPure goat anti-mouse IgG	Jackson ImmunoResearch Inc., Baltimore, USA	WB: 1:10.000
HRP-conjugated AffiniPure goat anti-rabbit IgG	Jackson ImmunoResearch Inc., Baltimore, USA	WB: 1:5000
Alexa Fluor (Dylight) 488-conjugated AffiniPure goat anti-mouse	Jackson ImmunoResearch Inc., Baltimore, USA	IF: 1:200 FC: 1:200

5.8 Dyes und markers

Reagent	Company
Carboxyfluorescein SE (CFSE)	Molecular Probes
Trypan blue	AppliChem
Hoechst 33342	Invitrogen
Pacific Blue	Invitrogen
EZ-Link™ Sulfo-NHS-Biotin	ThermoFischer
Alexa-Fluor 647 (Cy5)-Streptavidin	Molecular Probes

5.9 Plasmids

The following plasmids were used in this thesis.

LSH No.	Name	Insert	Resistance	Origin
353	pLPS3'-EGFP	-	Kan	Clontech
3443	pDNRdual-LIC	-	Amp	LSH
2310	pLPS3'-mCherry	-	Kan	LSH
4054	pLPS3'-mCherry_myr-PTPRF-CT	myr-PTPRF-CT	Kan	LSH

4057	pLPS3'-mCherry_myr-PTPRG-CT	myr-PTPRG-CT	Kan	LSH
4024	pLPS3'-mCherry_myr-PTPRJ-CT	myr-PTPRJ-CT	Kan	LSH
4025	pLPS3'-mCherry_myr-PTPRS-CT	myr-PTPRS-CT	Kan	LSH
4027	pLPS3'-mCherry_myr-PTPRJ-D/A-CT	myr-PTPRJ-D/A-CT	Kan	LSH
546	pLPS3'-EGFP_CEACAM3	CEACAM3 WT HA-tag	Kan	LSH
545	pLPS3'-EGFP_CEACAM-3 Y230F	CEACAM3 Y230F HA-tag	Kan	LSH
547	pLPS3'-EGFP_CEACAM3-Y241F	CEACAM3 Y241F HA-tag	Kan	LSH
321	pEGFP C1	-	Kan	Clontech
3676	pmScarlet_C1	-	Kan	Addgene
3231	pLPS3'-mScarlet_myr-PTPRJ-CT	myr-PTPRJ-CT	Kan	LSH
3232	pLPS3'-mScarlet_myr-PTPRJ-CT	myr-PTPRJ-CT-D1205A	Kan	LSH
85	pRC/CMV vSrc	vSrc	Amp	Schmidt-Ruppin
730	pLPS3'-EGFP_CEACAM1-NT	CEACAM1-NT+Leader, NEF-Epitop	Kan	LSH
731	pLPS3'-EGFP_CEACAM3-NT	CEACAM3-NT+Leader, NEF-Epitop	Kan	LSH
4634	pLPS3'-EGFP_CEACAM3-RQAP-NT	CEACAM3-RQAP-NT	Kan	LSH
751	pLPS3'-EGFP_CEACAM5-NT	CEACAM5-NT+Leader, NEF-Epitop	Kan	LSH
752	pLPS3'-EGFP_CEACAM6-NT	CEACAM6-NT+Leader, NEF-Epitop	Kan	LSH
732	pLPS3'-EGFP_CEACAM8-NT	CEACAM8-NT+Leader, NEF-Epitop	Kan	LSH
2392	pLPS3'-EGFP_CEACAM3-RQAP	CEACAM3-RQAP	Kan	LSH
4392	pLL3.7-mKate2_LIC_CEACAM3	CEACAM3	Amp	LSH
5209	pLL3.7-mKate2_LIC_CEACAM3-RQAP	CEACAM3-RQAP	Amp	LSH
4176	pLentiCRISPRv2-sgPTPRJ	PTPRJ targeting sgRNA	Amp	LSH

4308	pLentiCRISPRv2-sgCerulean-(sgCer)-w/o-Cas9	Cerulean targeting sgRNA	Amp	LSH
1256	pMD2.G	-	Amp	Addgene
1257	psPAX2	-	Amp	Addgene

5.10 Phospho-peptides

Name	Sequence	Source
CEACAM3-pY230:	Biotin-LPNPRTAASI{pY}EELLKHDTNIYCRMDHKAEVAS	Novopep, Shanghai, China
CEACAM3-pY241	Biotin-LPNPRTAASIYEELLKHDTNI{pY}CRMDHKAEVAS	Novopep, Shanghai, China

5.11 Oligonucleotides

LSH No.	Name	Forward/ Reverse	Sequence (5' – 3')
488	CEA_f	Forward	CATTTGCAACAGCTACAGTC
489	CEA_r	Reverse	AGTGCAGTGGTATCAGAAAC
4189	LIC_PTPRF_myrF	Forward	ACTCCTCCCCCGCCATGGGATGTATAAAATCAAAAGGGAAAGACAAAAGGAAAAGGACCCACTC
4190	PTPRF_LIC_rev	Reverse	CCCCACTAACCCGCGTTGCATAGTGGTCAAAGC
4191	LIC_PTPRG_myrF	Forward	ACTCCTCCCCCGCCATGGGATGTATAAAATCAAAAGGGAAAGACAGAGGGTGTAACAAAATAAAGTCC
4192	PTPRG_LIC_rev	Reverse	CCCCACTAACCCGCACTAGGGACTCCATGCTCTCAGC
2766	CEACAM3 LIC sense	Forward	ACTCCTCCCCCGCCATGGGGCCCCCCTCAGC
4042	CC3_N-C-join_for	Forward	CCAGAATGTCACCCAGAATGACATAGGATTCTACACCC
4043	4043_CC3_N-C-join_rev	Reverse	GGGTGTAGAATCCTATGTCATTCTGGGTGACATTCTGG
4115	4115_2xHA-LIC-rev	Reverse	CCCCACTAACCCGAGCGTAATCTGGAACGTCATATGG

5.12 Chemicals, reagents, recombinant proteins and enzymes

Chemical, Reagent, Protein or Enzyme	Company
Acetic acid	Roth
Acrylamide 40%	AppliChem
Agarose	Genaxxon bioscience
Aprotinin	Roth
APS (ammonium peroxydisulfate)	Roth
Benzamidine hydrochlorid	AppliChem
Bromophenol blue	Merck
BSA (bovine serum albumin)	Capricorn Scientific
$CaCl_2$	Sigma-Aldrich
Calf serum	Biochrom
Coomassie Brilliant blue R-250	AppliChem
Corn oil	Sigma-Aldrich
Coumaric acid	Sigma-Aldrich
Cre recombinase	Hauck Laboratory
dATP	Genaxxon
dCTP	Genaxxon
dGTP	Genaxxon
dTTP	Genaxxon
DMSO	Merck
DTT (dithiothreitol)	AppliChem
EDTA	AppliChem
EGTA	Roth
17β-Estradiol	Calbiochem
Ethanol	VWR
Fetal calf serum	Biochrom
GC medium base	BD
GelRed®	Genaxxon biosciences
Glutardialdehyde	Roth
Glycerol	Roth
Glycine	Roth
30% H_2O_2 (hydrogen peroxide)	Merck
Hydrochloric acid	Merck

HEPES	Roth
Hexadimethrine bromide	Sigma-Aldrich
IPTG (isopropyl-β-D-thiogalactopyranoside)	Roth
KCl (potassium chloride)	Acros organics
Leupeptin hemisulfate	AppliChem
Luminol	Sigma-Aldrich
β-Mercaptoethanol	Merck
Methanol	VWR
$MgCl_2$	Roth
$MgSO_4 \cdot 7H_2O$	AppliChem
Mounting medium	Dako
4-MUP (4-Methylumbelliferyl phosphate)	Sigma-Aldrich
NaCl	Roth
NaF	AppliChem
$NaH_2PO_4 \cdot H_2O$	Merck
Na_2HPO_4	Roth
NaN_3	AppliChem
Na_3VO_4 (sodium orthovanadate)	AppliChem
10x NEBbuffer™ 2	New England Biolabs (NEB)
$(NH_4)_2SO_2$ (Ammonium sulfate)	Roth
PFA (paraformaldehyde)	Riedel-de Haën
Pfu Polymerase	Hauck Laboratory
Pefabloc	Merck
PMSF (phenyl-methyl-sulfonyl-fluoride)	AppliChem
pNPP (disodium hexahydrate (para-nitrophenyl phosphate disodium hexahydrate)	AppliChem
Poly-L-lysine	Serva
Saponin	AppliChem
Sarcosyl (sodium lauroyl sarcosinate)	Fluka
SDS (sodium dodecyl sulfate)	Roth
FD-SmaI (XmaI)	Thermo Scientific
Sodium deoxycholate	AppliChem
Sucrose	Merck
T4 DNA polymerase	Hauck Laboratory

TCEP (Tris (2-carboxyethyl) phosphine hydrochlorid)	Sigma-Aldrich
TEMED (tetramethylethylenediamine)	AppliChem
Tris	Roth
Trizma® base	Sigma-Aldrich
Triton X-100	Roth
Trypan blue	AppliChem
Tween 20	Roth

5.13 Equipment and consumables

Equipment or consumable	Company
-80°C freezer	New Brunswick Scientific
-80°C freezer Forma 900 series	Thermo Scientific
384 well plate, PS, flat-bottom, black	Greiner Bio-One
384 well plate, PS, flat-bottom, clear, white	Greiner Bio-One
Biological safety cabinets class II	NUAIRE
CASY cell counter	Innovatis
Cell culture dishes	Greiner Bio-One
Centrifuge 5417R	Eppendorf
Centrifuge 5702	Eppendorf
ChemiDoc™ Touch imaging system	BioRad
CO_2 Incubator (cell culture)	Thermo Scientific
CO_2 Incubator Galaxy 170 R (bacteria)	New Brunswick
Confocal microscope TCS SP5	Leica
Coverslips	Marienfeld
Cryogenic vials	Thermo Scientific
Falcon Tubes (15 ml, 50 ml)	Greiner Bio-One
Gel documentation system GelDocXR	BioRad
Glass microscope slides Superfrost®	Menzel
Incubator Celsius 2005	Memmert
NanoDrop ND-1000	PeqLab
PCR Thermocycler peqStar 96 HPL Gradient	PeqLab
PCR tubes	Brand
pH Meter	Mettler Toledo

Pipettes PIPETMAN	Gilson
Pipette tips	Sarstedt
PVDF membrane	Millipore
SDS-PAGE chambers	BioRad
Spectrophotometer Libra S4	Biochrom
Sterile hood (Secuflow)	Waldner
Thermo shaker TS100	PeqLab
Varioskan Flash microplate reader	Thermo Scientific
Whatman paper	Hartenstein

5.14 Software

Software	Source
Adobe Illustrator CS4	Adobe Systems Incorporated
Adobe Photoshop CS4	Adobe Systems Incorporated
FACS Diva	Becton Dickinson
GraphPad Prism	GraphPad Software
Leica LAS AF	Leica Microsystems CMS GmbH
Clone Manager 9	Scientific and Educational Software
Image Lab 5.2.1	BioRad
ImageJ (Fiji)	NHI, Bethesda, ML, USA
FlowJo v10.6.2	FlowJo LLC

6. Methods

6.1 Polymerase chain reaction (PCR)

Amplification of the desired DNA segments was performed using appropriate primers synthesized by Sigma-Aldrich. The reaction mix contained the following components:

10x Taq/Pfu buffer	5 µl
10 µM Primer 1	1 µl
10 µM Primer 2	1 µl
Template DNA	10 ng
20 mM dNTPs	1 µl
Pfu polymerase	1 µl
ddH_20	to 50 µl

The PCR was conducted in a peqStar 96 HPL Gradient PCR thermocycler (PeqLab) according to the following program:

Denaturation	94 °C, 3 min	
Denaturation	94 °C, 20 sec	30 repetitions
Annealing	50-65 °C, 20 sec	
Elongation	72°C, 1 min per 750 bps	
Elongation	72°C, 5-10 min	
End	4°C, ∞	

6.2 Agarose gel electrophoresis

Agarose gel electrophoresis was used to separate DNA fragments or plasmids according to their size. The amount of agarose (between 0.7% and 2% agarose in TAE buffer) was adjusted according to the size of the constructs. Before loading, samples were mixed with 6x GEBs buffer. DNA was separated in TAE buffer at 100 V. To visualize the DNA, the gels were stained in GelRed staining solution. The DNA was visualized with UV light (254 nm), excised, and

purified using the PCR and Gel extraction Mini Prep Kit (Genaxxon bioscience) or analyzed in the GelDocXR documentation system (BioRad).

6.3 Ligation independent cloning (LIC)

To clone the cDNA of interest into the pDNDdual-LIC vector (LSH No. 3443) (Adrian et al., 2019) by ligation-independent cloning (LIC), the cDNA was amplified with primers that in addition to the target gene complementary sequence contained LIC overhangs (forward LIC sequence: 5'-ACTCCTCCCCCGCC(ATG)-3'; reverse LIC sequence: 5'-CCCCACTAACCCG-3'). After amplification, the PCR products were separated by agarose gel electrophoresis, the DNA was excised, and the products were purified using the PCR and Gel extraction Mini Prep Kit (Genaxxon bioscience) according to the manufacturer's protocol. The concentration of the purified DNA fragments was measured on the NanoDrop (PeqLab), and the molarity was determined using the following formula:

$$\frac{\text{pmol}}{\mu\text{l}} = \frac{\text{DNA } (\frac{\text{pg}}{\mu\text{l}})}{(660^{*} \text{ product [bps]})}$$

To generate the overhangs required for LIC cloning, the purified PCR products were treated with T4 DNA polymerase in the presence of dCTP. The T4 DNA polymerase has a 3' to 5'-exonuclease activity that removes the 3' ends of the PCR product down to the first cytosine residue, thereby generating the specific overhangs. The composition of the components used for this process is shown below:

PCR product	0.3 pmol
T4 DNA polymerase	1 µl
10x NEBbuffer™ 2	4 µl
100 mM dCTP	1 µl
100 mM DTT	2 µl
ddH20	to 40 µl

The mixture was incubated in the PCR cycler first for 30 min at 22°C and then for 20 min at 75°C. Subsequently, the T4 polymerase-treated PCR products were inserted into the pDNRdual-LIC vector (Adrian et al., 2019), which had previously been linearized with the restriction enzyme SmaI and pre-treated with the T4 polymerase (in the presence of dGTP). For insertion, 8 µl of the treated insert was incubated with 50 ng of the treated vector at RT for 10 min. The mixture was supplemented with 1 µl of 100 mM EDTA, incubated at RT for an additional 10 min, and the resulting plasmids were transformed into *E. coli* Nova blue (see 6.5). Following transformation, the bacterial suspension was plated on LB agar plates supplemented with ampicillin (100 µg/ml) and incubated overnight at 37°C. Plasmids were isolated using the Plasmid DNA Purification Mini Prep Kit (Genaxxon bioscience), and the correctness of the generated plasmids was confirmed by sequencing (LGC Genomics, Berlin, Germany).

6.4 Cre-LoxP recombination of plasmids

The components used for the recombination reactions are listed below:

1 µl 10x Cre recombination buffer
100 ng donor vector (pDNRdual-LIC-with insert)
200 ng acceptor vector (pLPS3'-mCherry or pLPS3'-EGFP)
1 µl Cre recombinase
to 10 µl ddH_20

After incubation at 37°C for two hours and heat inactivation at 70°C for 10 minutes, the resulting expression constructs were transformed into *E. coli* Nova blue (see 6.5). The transformed bacteria were plated on LB agar plates supplemented with chloramphenicol (30 µg/ml) and sucrose (7%) and incubated overnight at 37°C. The plasmids were purified using the Plasmid DNA Purification Mini Prep Kit (Genaxxon bioscience) and the correctness of the generated plasmid was verified by sequencing (LGC Genomics, Berlin, Germany).

6.5 Plasmid transformation in competent *E. coli*

For plasmid transformation, ultra-competent *E. coli* Nova blue (endA1, hsdR17 (rk12- mk12+), supE44, thi-1, recA1, gyrA96, relA1, lac [F'proA+B+ lacIqZ_M15::Tn10 (TetR)], Novagen) were used. Bacteria were thawed on ice and incubated with the desired amount of plasmid DNA for 30 minutes. Transformation was initiated by heat shock at 42°C for 75 seconds. Bacteria were cooled on ice and then incubated in 1 ml LB liquid medium for 1 hour at 37°C (220 rpm). Bacteria were pelleted by centrifugation at 3500 rpm for 4 min, the supernatant was reduced to approximately 100 µl, and the bacterial pellet was resuspended in the remaining 100 µl. The bacterial suspension was plated on LB agar plates containing the desired antibiotics and the LB agar plates were incubated at 37°C until the next day.

6.6 Generation of DNA constructs

Generation of myr-PTPRF-CT and myr-PTPRG-CT expression vectors

Expression vectors encoding the myristoylated phosphatase domains were generated as previously described (Goob et al., 2022). Briefly, to provide the PTPRF and PTPRG phosphatase domains with an N-terminal myristoylation site, the phosphatase domains were amplified from the respective full-length cDNA constructs (PTPRF: Arizona State University, DNASU Plasmid Repository # HsCD00021632 and PTPRG: Arizona State University, DNASU Plasmid Repository # HsCD00829408) with forward primers containing the myristoylation site. In addition, forward and reverse primers contained LIC overhangs that allow ligation independent cloning (LIC). The primers used are listed below:

LIC_PTPRF_myrF: 5'-ACTCCTCCCCCGCCATGGATGTATAAAATCAAAAGGGAAAGACAAAAGGAAAAGGACCCACTC-3'

PTPRF_LIC_rev: 5'-CCCCACTAACCCGCGTTGCATAGTGGTCAAAGC-3'

LIC_PTPRG_myrF: 5'-ACTCCTCCCCCGCCATGGATGTATAAAATCAAAAGGGAAAGACAGAGGGTGTAACAAAATAAAGTCC-3'

PTPRG_LIC_rev: 5'-CCCCACTAACCCGCACTAGGACTCCATGCTCTCAGC-3'.

After amplification, the PCR products were cloned into the pDNRdual-LIC vector (Adrian et al., 2019) (LSH No. 3443) by ligation independent cloning (LIC) (see 6.3). The myr-PTPRF-CT and

myr-PTPRC-CT coding sequences of the resulting pDNRdual-LIC-myr-PTPRx-CT constructs were then cloned by Cre-LoxP recombination (see 6.4) into the pLPS3'-mCherry expression vector, which connects the inserts at the carboxy terminus to the fluorescent protein mCherry.

Generation of a full length CEACAM3-RQAP expression vector

Cloning of the full-length CEACAM3-RQAP-EGFP expression construct was performed by Alena Kress under the guidance of Griseldis Goob in the laboratory of Prof. Dr. C. R. Hauck. The cDNA of the RQAP-SNPs-containing N-terminal IgV-like domain was amplified with the LIC primer 5'-ACTCCTCCCCCCCGCCATGGCCCCTCAGC-3' and the SOEing primer 5'-GGGGTGTAGAATCCTATGTCATTCTGGTGACATTCTGG-3' from the pLPS3'EGFP_CEACAM3-RQAP-NT plasmid (LSH no. 4634). In parallel, the coding sequence of the CEACAM3 transmembrane- and intracellular domain was amplified with the SOEing primer 5'-CCAGAATGTCACCCAGAATGACATAGGATTCTACCC-3' and the LIC primer 5'-CCCCACTAACCCGAGCGTAATCTGGAACGTCATGG-3' from the CEACAM3 full-length cDNA (LSH no. 546). As the SOEing primers have overlapping homologous ends, the two PCR intermediates were linked in a third PCR using the LIC primers 5'-ACTCCTCCCCCGCCATGGCCCCTCAGC-3' and 5'-CCCCACTAACCCGAGCGTAATCTGGAACGTCATATGG-3'. The resulting CEACAM3-RQAP-PCR product was cloned into the pDNRdual_LIC vector (LSH no. 3443) (Adrian et al., 2019) by ligation-independent cloning (see 6.3). The CEACAM3-RQAP cDNA was then transferred from the pDNRdual_LIC_CEACAM3-RQAP vector into the pLPS3'-EGFP vector (Clontech; LSH No. 353) by Cre-mediated recombination (see 6.4). The resulting expression construct encodes CEACAM3-RQAP-EGFP with EGFP fused to the carboxy-terminus of the protein.

6.7 Handling and cultivation of bacteria

N. gonorrhoeae MS11-B2.1 strains (non-piliated *N. gonorrhoeae* Opa_{52} (N309) and non-piliated *N. gonorrhoeae* MS11-B2.1 Opa- (N302)) (Kupsch et al., 1993) and *N. gonorrhoeae* MS11 strains expressing the individual meningococcal serogroup C (C1938) Opa proteins (Muenzner et al., 2000), were grown at 37°C and 5% CO_2 on GC agar plates supplemented with vitamin supplements and the antibiotics chloramphenicol (10 µg/ml) and erythromycin (7 µg/ml). The *N. meningitidis* serogroup C strain C1938 was a gift from T. F. Meyer (MPI for

Infection Biology, Berlin, Germany). All other *N. meningitidis* strains were kindly provided by U. Vogel (IHM, University of Würzburg, Würzburg, Germany). *Neisseria meningitidis* strains were grown on vitamin-supplemented GC plates at 37°C and 5% CO_2. *E. coli* strains expressing meningococcal serogroup B (MC58 *siaD*) Opa proteins have been described previously (Kuespert et al., 2011). These strains were grown at 37 °C on LB agar plates or in liquid LB medium supplemented with kanamycin (30 µg/ml). Opa protein expression in *E. coli* was induced with 1 mM isopropyl β-D-1-thiogalactopyranoside (IPTG). Further information on the bacterial strains used can be found in section 5.4.

6.8 Bacterial lysates

Bacteria were taken up in PBS and adjusted to an optical density (OD_{550}) of 0.8. 1 ml of the bacteria-containing solution was transferred to a new 1.5 ml Eppendorf tube and bacteria were pelleted by centrifugation at 4000 rpm for 3 min. The bacterial pellet was taken up in 120 µl 2xSDS buffer, boiled at 95 °C for 5 min, and loaded onto SDS gels.

6.9 Maintenance of HL60 cells, 293T cells and MEF cells

HL60 cells were cultured in 10% FCS-containing RPMI-1640 medium and 293T cells were cultured in 10% CS-containing DMEM and passaged every two to three days. For passage of 293T cells, the medium was aspirated, cells were washed gently with PBS and cells were detached from the cell dish with trypsin/EDTA. The detached cells were taken up in fresh 293T culture medium and pelleted at 800 rpm for 3 minutes. The supernatant was removed and the cells were distributed onto new 10 cm cell culture dishes in 293T culture medium at the desired cell density. For passage of HL60 cells, cells were pelleted by centrifugation at 800 rpm for 3 minutes and then seeded at the desired dilution in fresh FCS-containing RPMI medium. Murine embryonic fibroblasts (MEFs) (Grimm et al., 2020) were cultured in DMEM medium supplemented with 10% FCS, nonessential amino acids, and sodium pyruvate. 293T cells, MEF cells and HL60 cells were maintained at 37°C and 5% CO_2.

6.10 Cryopreservation of 293T and HL60 cells

For cryopreservation, cells of a confluent 10 cm dish were collected, pelleted at 800 rpm for 3 min and taken up in 1 ml freezing medium (HL60 cell freezing medium: RPMI-1640 medium, 20% FCS and 10% DMSO; 293T freezing medium: DMEM medium supplemented with 20% CS and 10% DMSO). Cells were transferred to cryogenic vials (Nalgene) and were frozen in appropriate freezing boxes (Mr. Frosty freezing container, Nalgene) at -80°C. After two days of storage at -80°C, the cryogenic vials were transferred to nitrogen tanks for long-term storage of the cells.

6.11 Transient transfection of 293T cells

293T cells were transfected in the adherent state and at approximately 25% confluence using calcium phosphate precipitation. For transfection, 5 µg of the desired plasmid DNA was first added to 500 µl of ddH_2O and then supplemented with 500 µl of 2xHBS buffer. During vortexing, 50 µl 2.5 M $CaCl_2$ was added, and the mixture was allowed to stand at RT for 10 min. The mixture was then applied dropwise to the 293T cell medium, and the cells were additionally treated with chloroquine to a final concentration of 25 µM. After approximately 7 hours of incubation, the transfection medium was removed and replaced with fresh 293T culture medium. The cells were incubated at 37°C and 5% CO_2 for 2 days and were then used for the desired assay/purpose.

6.12 Production of soluble CEACAM domains in 293T cells

For the production of soluble amino-terminal CEACAM protein domains, 293T cells were transfected by calcium phosphate precipitation. In deviation from the protocol described in (6.11), 6 µg of DNA was used for transfection and the cells were cultured in 5 ml serum-reduced medium (Opti-MEM, Gibco) for 3 days after 7 hours of incubation in the transfection medium. Subsequently, the medium was collected, centrifuged at 4000 rpm for 10 min, and the CEACAM-containing supernatants were either frozen at -20°C or stored at 4°C (short-term storage).

6.13 Whole cell lysates of HL60 and 293T cells

Cell lysis was performed either in NP40 lysis buffer or in RIPA buffer. In both cases, buffers were freshly supplemented with protease inhibitors and, if necessary, phosphatase inhibitors on the day of use. The composition of the buffers and the concentrations of inhibitor supplements used can be found in the material section 5.1. HL60 cells were counted prior to cell lysis. HL60 cells were pelleted (800 rpm, 3 min), resuspended in 15 µl lysis buffer/1x10^6 cells and transferred to ice for 5 min. The cell lysate was pulled through a fine needle several times to shear the DNA and then 10-30 µl sepharose beads were added. Samples were rotated for 5 min at 4°C and subsequently centrifuged for 30 min at 4°C and 13.000 rpm. The supernatant was transferred to a new 1.5 ml Eppendorf tube, mixed with appropriate amounts of 2xSDS or 4x SDS buffer, and heated at 95°C for 5-10 min. Samples were stored at -20°C or -80°C. Lysis of the 293T cells was performed in a slightly different manner. Here, the culture medium was first aspirated and the cells were carefully washed with PBS. The lysis buffer (300-500 µl/10 cm dish) was added to the cells and dishes were incubated for 5 min at 4°C. The cells were detached from the plate using a cell scraper and transferred to a 1.5 ml Eppendorf tube. Shearing of DNA, addition of sepharose beads (50 µl sepharose beads were used for 293T cells), centrifugation and heating of samples was performed as described for HL60 cells.

6.14 SDS-PAGE, Western Blotting and Coomassie Blue staining

Depending on the size of the proteins to be analyzed, SDS-PA gels with an acrylamide concentration between 7% and 12% were used. These were placed in appropriate electrophoresis chambers and the chamber was filled with running buffer. Samples were boiled at 95 °C for approximately 5 min and subsequently loaded into the gel pockets, usually in volumes between 10 µl and 20 µl. The samples were allowed to run into the gel at 80V and were then further separated at 120V.

After SDS-PAGE, the proteins were transferred from the gel to a PVDF membrane (Merck Millipore, Darmstadt, Germany) by Western blotting. The membrane was first activated in 100% (v/v) methanol for approx. 1 min. The gel was aligned on the membrane, membrane and gel were enclosed between two blotting filter papers, and the sandwich was placed in a

transfer chamber filled with western transfer buffer. The transfer was performed for 2 h at 200 mA. Subsequently, the membrane was stained in Coomassie Brilliant Blue solution for 2 min and then destained with Destain solution until the protein bands were clearly visible. After incubating the membrane in blocking solution (Blotto) for one hour at RT, the membrane was incubated overnight in the first antibody in blocking solution. The following day, the membrane was washed 3 times for 5-10 min each in TBS-T and then incubated with the HRP-conjugated secondary antibody in TBS-T for one hour at RT. After another 3 washes with TBST-T (5-10 min each), the membrane was transferred to ECL solution and the luminescence signals were detected using the Chemidoc™ Touch Imaging System (Biorad).

6.15 Production of lentiviral particles and CRISPR/Cas9-mediated knockout of PTPRJ

HL60-CEACAM3-mKate sgPTPRJ cells were generated from HL60-CEACAM3-mKate-Cerulean cells as previously described (Goob et al., 2022). Briefly, 293T cells were transfected with 3.5 µg of the packaging plasmid pMD2.G (addgene #12259; LSH No. 1256), 5 µg of the packaging plasmid psPAX2 (addgene #12260; LSH No. 1257), and 6.5 µg of the pLentiCRISPRv2-sgPTPRJ construct or the pLentiCRISPRv2-sgCerulean-(sgCer)-w/o-Cas9 plasmid (Goob et al., 2022). With the exception of the aberrant DNA amounts, transfection was performed as described in chapter 6.11. Approximately 6 hours after transfection, the transfection medium was replaced with 6 ml fresh 293T culture medium and the cells were incubated for an additional 3 days at 37°C and 5% CO_2 under S2-safty conditions. The cell supernatant was collected, centrifuged at 800 rpm for 3 min, and sterile filtered (pore size 0.45 µm). For transduction, 1x 10^6 HL60-CEACAM3-mKate-Cerulean cells were seeded in 1 ml HL60 culture medium in a 24-well plate and pre-treated with 8 µg/ml hexadimethrine bromide. 500 µl of the pLentiCRISPRv2-sgCerulean-(sgCer)-w/o-Cas9-containing virus supernatant and 500 µl of the pLentiCRISPRv2-sgPTPRJ-containing virus supernatant were added to the HL60 cells. Samples were centrifuged at 800 g (RT) for 1 hour and cells were sunsequently incubated at 37°C and 5% CO_2 for three days. After the three-day transduction period, cells were passaged several times with trypsin/EDTA and subjected to treatment with puromycin (final concentration 1µg/ml puromycin) to kill non-transduced cells. To obtain clonal cell populations, single Cerulean-

negative cells were FACS-sorted by the Flowkon facility (Flowkon, University of Konstanz, Germany), and the expaned populations were analyzed for the lack of PTPRJ.

6.16 Binding studies with soluble CEACAMs

Soluble GFP-labelled CEACAM domains were produced according to the procedure described in chapter 6.12. For binding analyses, CEACAM-containing supernatants were first adjusted to comparable protein levels using Opti-MEM (Gibco), distributed at 500 µl each into 1.5 ml Eppendorf tubes, and clustered overnight at 4 °C with polyclonal GFP-binding antibodies (tag-tools GmbH, Konstanz, Germany; 1:1000). The next day, the CEACAM-containing supernatant was mixed with $2x10^7$ bacteria and rotated at RT for 1 hour. To wash out unbound CEACAM domains, samples were centrifuged at 3000 rpm for 5 min, the supernatant was aspirated, and the pelleted bacteria were resuspended in 1 ml PBS. After another repetition of this washing step (5 min, 3000 rpm), the bacterial pellet was taken up in 35 µl of 2xSDS buffer, heated at 95 °C for 10 min, and the lysates were either loaded directly onto SDS-PA gels or were frozen at -20 °C.

6.17 Enrichment of CEACAM receptors from HL60 cell lysates

To enrich CEACAMs from HL60 cell lysates with Opa_{52}-expressing *N. gonorrhoeae*, bacteria were fixed in 4%-PFA-containing PBS for 20 min and then washed 3 times with PBS. $5x10^6$ HL60 cells were lysed in 300 µl protease inhibitor-enriched-RIPA buffer and incubated with $7x10^7$ fixed bacteria for 3 hours at 4°C during constant rotation. To pulldown the bacteria-bound CEACAMs, samples were centrifuged at 5000 rpm and 4°C for 5min, the supernatant was discarded, and the bacterial pellet was washed again with ice-cold PBS and centrifuged as before. The bacterial pellet was taken up in 15 µl 2xSDS buffer, boiled at 95°C and the enriched CEACAMs were analysed by immunoblotting.

6.18 Analysis of bacterial invasion by flow cytometry

For analysis of bacterial invasion by flow cytometry, bacteria were suspended in 1 ml PBS and stained with 2 µg carboxyfluorescein succinimidyl ester (CFSE) for 25 minutes in the dark at 37°C with constant shaking (750 rpm). To remove the unbound CFSE, bacteria were washed three times with PBS and centrifuged at 4000 rpm for 3 minutes between each wash. Invasion

assays with HL60 cells were performed as previously described (Goob et al., 2022). 1x10^6 cells in 1 ml phagocytosis buffer were infected for 10 minutes at an MOI of 10 under gentle rotation. To stop the bacterial uptake, samples were transferred to ice and cells were washed once with ice-cold PBS. Cells were taken up in cold phagocytosis buffer and trypan blue was added to a final concentration of 0.2 mg/ml to quench the fluorescence of extracellular bacteria (Pils et al., 2006). The CFSE fluorescence of intracellular bacteria was measured using a FACS Fortessa (BD Biosciences) flow cytometer, and the data obtained were analyzed using the FlowJo software.

To study bacterial uptake in 293T cells, cells were transfected with CEACAM3-mkate2- or CEACAM3-RQAP-mkate2-encoding plasmids 2 days before infection and seeded into 6-well plates at a cell count of 1.5×10^6 cells/well the day after transfection. Infection was performed with CFSE-stained bacteria for 1 hour and an MOI of 60 at 37°C. Subsequently, samples were placed on ice. Cells were washed with ice-cold PBS, detached from the bottom of the wells with trypsin/EDTA, suspended in cold cell culture medium, and pelleted at 800 rpm for 3 minutes. The supernatant was removed, and the cells were taken up in phagocytosis buffer, mixed with trypan blue, and analyzed as previously described.

6.19 CEACAM3 phosphorylation and immunoprecipitation

293T cells were transfected with CEACAM3-GFP-encoding plasmids according to the procedure described in chapter 6.11. Tyrosine phosphorylation of the CEACAM3-ITAM motif was either achieved by co-transfection of the cells with constructs encoding the constitutively active kinase vSrc or was induced two days after transfection by infection of the cells with Opa_{52}-expressing *N. gonorrhoeae* as previously described (Goob et al., 2022). Briefly, cells were infected for 15 minutes at an MOI of 30 with Opa_{52}-expressing *N. gonorrhoeae* or *N. gonorrhoeae* lacking Opa expression (Opa-). Cells were lysed in NP40 lysis buffer containing 10 mM p-nitrophenyl phosphate and 1 mM Na_3VO_4 and the lysate was cleared of cell debris by centrifugation at 13.000 rpm and 4°C. The supernatant was incubated with GFP-binding nanobodies coupled to sepharose beads for 3 h at 4°C. Subsequently, the CEACAM3-GFP fusion proteins were precipitated by centrifugation (2700 g, 5 min, 4°C). The immunoprecipitated CEACAM3 proteins were washed three times with NP40 lysis buffer, taken up in 2xSDS buffer, heated at 95°C for 5 min, and analyzed by immunoblotting.

6.20 Gentamycin protection assays

293T cells were transfected with the desired plasmids by calcium phosphate precipitation (see chapter 6.11) and seeded the following day in triplicates of $5x10^5$ cells/well in poly-L-lysine-coated 24-well plates in 1 ml culture medium. The next day, the transfected cells were infected with a MOI of 30 for 45 min at 37°C and 5% CO_2. To kill the extracellular bacteria, the cells were incubated for 30 min in culture medium containing 100 µg/ml gentamicin. Cells were lysed with 0.5% (w/v) saponin in PBS for 15 min at RT and the released bacteria were plated on GC plates at appropriate dilutions. CFU were counted the following day. Statistical analysis was performed using the Student's two-tailed t-test and was based on at least three independent experiments (if more experiments were performed, the number of independent experiments is indicated in the figure legend).

6.21 Immunofluorescence staining and confocal microscopy

To examine the bacterial uptake in CEACAM3-GFP- or CEACAM3-RQAP-GFP-transfected 293T cells, cells were seeded on poly-L-lysine-coated 12-mm glass coverslips in 24-well plates ($8x10^4$ cells/well in 1 ml culture medium) the day after transfection. The following day, *N. gonorrhoeae* expressing either no Opa protein (Opa-), the adhesin Opa_{52}, or the meningococcal serogroup C (C1938) adhesin Opa41 or Opa40 were suspended in 1 ml PBS and labeled with 2 µg Pacific blue and 100 µg sulfo-NHS-SS-biotin for 25 min in the dark (750 rpm). Bacteria were washed three times with PBS and centrifuged at 4000 rpm for 3 minutes between each wash step. Bacteria were taken up in cell culture medium, added to the cells at an MOI of 40, and incubated for 1 hour at 37°C and 5% CO_2. The infection medium was removed, the cells were carefully washed with PBS and fixed with 4% PFA in PBS for 20 min at RT in the dark. After carefully washing the coverslips with PBS three times, the samples were blocked with 10% heat-inactivated FCS in PBS for 10 minutes. To label the extracellular bacteria with an additional dye, the samples were incubated with Cy5-coupled streptavidin for 45 minutes. The coverslips were washed three times with PBS and mounted on glass slides using Dako Mounting Medium (Dako). Finally, the samples were imaged using a Leica SP5 confocal microscope and the images were digitally processed using ImageJ.

To analyze the co-localization of myristoylated PTPRJ- or PTPRJ-D/A-phosphatase domains with CEACAM3, 293T cells were co-transfected with expression plasmids encoding GFP-tagged CEACAM3 and mScarlet-tagged myr-PTPRJ or myr-PTPRJ-D/A. As a control, 293T cells were co-transfected with plasmids encoding either GFP and myr-PTPRJ or mScarlet and CEACAM3-GFP. The co-localization experiments were performed as described before (Goob et al., 2022). Two days after transfection, $2x10^5$ cells were seeded on coverslips coated with poly-L-lysine and allowed to adhere for 2 hours. Opa_{52}-expressing *N. gonorrhoeae* were suspended in PBS and stained with 4 µg/ml PacificBlue-NHS (Molecular Probes, Karlsruhe, Germany). Bacteria were washed, and cells were infected with an MOI 30 for 1 h. Samples were washed once with PBS, fixed, and transferred to glass slides after an additional three washes with PBS.

To determine the PTPRJ expression in PTPRJ-deficient (HL60-CEACAM3-mKate-sgPTPRJ (sgPTPRJ)) and PTPRJ-expressing (HL60-CEACAM3-mKate-sgCer (sgCer)) cells, $5x10^5$ cells in PBS were seeded on poly-L-lysine-coated coverslips in 24-well plates and centrifuged at 800 rpm for 4 minutes. After removing the PBS, cells were fixed and gently washed with PBS. Samples were processed as described previously (Goob et al., 2022). Briefly, samples were blocked for 5 minutes in blocking solution (10% heat-inactivated FCS in PBS), stained with an α-PTPRJ antibody (clone 143-41, Santa Cruz; 1:100) or an IgG isotype control antibody in blocking solution for 1 hour, and then washed three times with PBS. Samples were again blocked in blocking solution for 5 minutes and then stained with an Dylight 488-conjugated secondary goat anti-mouse antibody (1:200) in the dark for 45 minutes. Hoechst33342 was added 15 minutes before the end of the 45-minute incubation period. Samples were washed three times with PBS and mounted on coverslips.

6.22 Immunofluorescence staining for flow cytometry

For immunofluorescence stainings, $1x10^6$ cells were transferred to FACS buffer and pelleted at 800 rpm for 3 min. Cells were incubated with appropriate amounts of the primary antibody or an IgG isotype control antibody in 300 µl FACS buffer at 4°C for 1.5 h. To wash out unbound antibodies, samples were centrifuged at 2500 rpm for 2 min at 4°C, and the cell pellet was washed three times with FACS buffer. Cells were stained with the secondary antibody (Dylight 488-conjugated AffiniPure goat anti-mouse antibody, Jackson ImmunoResearch; 1:200) in 300 µl FACS buffer at 4°C in the dark for 30 min. Cells were washed three times with FACS buffer

as before and were subsequently analyzed by flow cytometry using the LSRFortessa™ Cell Analyzer (BD Biosciences); raw data were analyzed using the FlowJo software.

6.23 Scanning electron microscopy

Samples werer prepared as previously described (Goob et al., 2022). Briefly, $4x10^4$ cells were seeded in phagocytosis buffer onto poly-L-lysine-coated glass coverslips (12 mm) in 24-well plates and allowed to sink to the coverslips by centrifugation at 800 rpm (10 min, at RT). For infection, Opa_{52}-expressing *N. gonorrhoeae* were suspended in PBS and added to the cells at an MOI of 30 ($1.2x10^6$ bacteria/well). Samples were centrifuged at 800 rpm for 3 min to allow the bacteria to sink onto the coverslips and then incubated at 37°C and 5% CO_2 for 30 min. Further processing of the samples was performed by the Electron Microscopy Center of the University of Konstanz. Samples were fixed in EM-fixative for a total of 1 h at 4 °C, which was renewed three times during fixation. After three washes with EM-wash buffer, samples were dehydrated in an ethanol gradient series. Samples were critical point dried with liquid CO_2 (BAL-TEC SCD 030 Critical Point Dryer), sputter-coated with 8 mm gold-palladium, and images were acquired at 5 kV in a field emission scanning electron microscope (Auriga; Carl Zeiss AG, Jena, Germany) with the support of the Electron Microscopy Center at the University of Konstanz.

6.24 Phosphatase assay with 4-Methylumbelliferyl phosphate (4-MUP)

4-MUP phosphatase assays were performed as previously described (Goob et al., 2022). The recombinant PTPRJ and PTPRJ-D/A phosphatase domains were diluted in phosphatase buffer to the desired concentration and added in quadruplicates (40 µl/well) to black flat-bottom 384-well plates (Greiner Bio-One, Germany). The 4-MUP phosphatase substrate was diluted to a concentration of 1 mM in phosphatase buffer and 40 µl of the 1mM 4-MUP was added to the recombinant phosphatase domains to give a final concentration of 500 µM 4-MUP. The turnover of the 4-MUP substrate into the fluorescent product 4-MU was measured at an excitation of 360 nm and an emission of 448 nm at 30°C using a microplate reader (Varioscan,

Thermo Fisher Scientific). Fluorescence intensities were recorded every 2 minutes over a 60-minute period.

6.25 *In vitro* phosphatase assay with malachite green

Malachite green assays were performed with CEACAM3 phospho-peptides as previously described (Goob et al., 2022). The peptide sequences can be found in the material section (5.10). First, the recombinant 6xHis-Sumo-labeled phosphatase domains of PTPRJ and PTPRJ-D/A (Goob et al., 2022) were diluted to the desired concentrations in phosphatase buffer and distributed in quadruplicates (20 µl/well) in white 384-well plates with transparent bottoms (Greiner Bio-One, Germany). As a control, four wells were filled with phosphatase buffer only (without phosphatases). The *in vitro* phosphatase assays were started by adding 20 µl of CEACAM3 phospho-peptides diluted to 100 µM in phosphatase buffer, and samples were incubated for 60 min (or the indicated time) at 30 °C in a microplate reader (Varioscan, Thermo Fisher Scientific). To stop the reaction, 40 µl malachite green solution was added and samples were incubated for 20 min at RT in the dark. Subsequently, the absorbance was measured at OD_{615} nm in a microplate reader (Varioscan, Thermo Fisher Scientific).

6.26 Analysis of the human CEACAM3 polymorphism CEACAM3-RQAP

The human CEACAM3-RQAP polymorphism has been described previously (Adrian et al., 2019). We used the 1000 Genomes Project Phase 3 Ensemble Browser to determine the frequency of the CEACAM3-RQAP polymorphism for populations in sub-Saharan Africa and other regions of the world. Using the Population Genetics module, we were able to examine the four polymorphisms by continent and continent-derived populations. For each genome, we examined whether these 4 polymorphisms co-occur in CEACAM3 to determine the occurrence of the CEACAM3-RQAP allele in populations of African ancestry and in genomes of European and Asian ancestry (**Supplementary Table 1**).

Table 1: Deposited Data

SNP	Source	Link
SNP: S43R	1000 Genomes Project Phase 3	rs61738270 https://www.ensembl.org/Homo_sapiens/Variation/Explore?db=core;g=ENSG00000170956;r=19:41796587-41811554;v=rs61738270;vdb=variation;vf=205419517
SNP: L44Q	1000 Genomes Project Phase 3	rs61738269 https://www.ensembl.org/Homo_sapiens/Variation/Explore?db=core;g=ENSG00000170956;r=19:41796587-41811554;v=rs61738269;vdb=variation;vf=205419508
SNP: V49A	1000 Genomes Project Phase 3	rs61737019 https://www.ensembl.org/Homo_sapiens/Variation/Explore?db=core;g=ENSG00000170956;r=19:41796587-41811554;v=rs61737019;vdb=variation;vf=205418057
SNP: T69P	1000 Genomes Project Phase 3	rs61737014 https://www.ensembl.org/Homo_sapiens/Variation/Explore?db=core;g=ENSG00000170956;r=19:41796587-41811554;v=rs61737014;vdb=variation;vf=205418024

6.27 Mice and mice maintenance

C57BL/6J mice carrying the human CEA gene (CEAtg mice) were established by Eades-Perner et al. (Eades-Perner et al., 1994). Later, this gene was also introduced into mice of the Balb/c inbred line by crossbreeding. To maintain the CEAtg mouse lines, heterozygous male CEA transgenic mice were crossed with wild-type female mice of the corresponding line. Genotyping of the offspring was performed by PCR (forward primer: 5'-CATTTGCAACAGCTACAGTC-3'; reverse primer 5'-AGTGCAGTGGTATCAGAAAC-3'). Mice were kept in fully air-conditioned rooms (21°C and 55% humidity) under a 12-hour light-dark cycle in groups of 3-6 animals and had *ad libitum* access to food and water. Female mice aged 6 to 8 weeks were used for the infection experiments.

6.28 Vaginal infection of mice with Opa_{52}-expressing *N. gonorrhoeae*

Female CEAtg mice aged 6 to 8 weeks were used for the infection experiments. Four days before infection, mice were treated with 50 µg of 17β-estradiol in 100 µl corn oil by subcutaneous injection. To reduce the growth of the commensal flora, trimethoprim (40 mg/100 ml) was added to the animals' drinking water until the end of the experiment. In the optimized protocol, mice were additionally injected intraperitoneally with streptomycin sulfate (2.4 mg/mouse) and vancomycin HCl (0.6 mg/mouse) in 100 µl PBS on day -4 (four days

before infection) as well as on day -2 (two days before infection) and the day of infection. Two days before infection, (mouse-passaged or non-mouse-passaged) Opa_{52}-expressing *N. gonorrhoeae* were streaked out on GC-Erm/Cam plates and single colonies were further passaged the following day on GC-plates. Bacteria were collected from the GC plates and suspended in vitamin-supplements-containing PPM medium. For infection, mice were sedated with ketamine and xylazine, and the vagina was cleaned three times with 30 µl of PBS. Mice were inoculated intravaginally with 10^8 bacteria in a volume of 15 µl vitamin-enriched PPM medium. Mice treated according to the optimized protocol additionally received a subcutaneous injection of 50 µg 17β-estradiol in 100 µl corn oil on the day of infection. To prevent the lack of nutrients important for gonococcal survival, 10 µl of vitamin-containing PPM medium was applied to the vagina of the mice 24 h after infection. At 48 h post-infection (or 24 h after infection), mice were killed by cervical dislocation, and mucosa-associated gonococci were re-isolated using very fine cotton swabs. The vagina was additionaly rinsed with 20 µl of PPM medium to re-isolate residual bacteria. Serial dilutions of the re-isolates were plated on both Erm/Cam-containing GC plates and GC agar plates without antibiotics. Colonies were counted the following day.

7. Declaration of contributions

All experiments presented in this study were conducted by Griseldis Goob with the exception of:

Figure 7, panel A, D, F: Experiments designed by Griseldis Goob and Alena Kress; conducted by Alena Kress; **Figure 7**, panel G: The binding profiles of CEACAM family members to *E. coli* expressing the *N. meningitidis* serogroup A (00170/F6124) Opa proteins (*) were analysed in a study by Muenzner et al. (Muenzner et al., 2000).

Figure 8, panel D-F and H: Experiments designed by Griseldis Goob and Alena Kress; conducted by Alena Kress.

Figure 9, panel A-D: Experiments designed by Griseldis Goob; conducted by Griseldis Goob, Alisia Gärtner and Katharina v. Werthern.

Figure 14, panel A-B: Experiment designed by Griseldis Goob; conducted by Griseldis Goob; recorded at the SEM by Michael Laumann (Electron Microscopy Service of the Department of Biology, University of Konstanz) and Griseldis Goob.

Suppl. Figure S1: Experiment designed by Griseldis Goob; conducted by Griseldis Goob, Alisia Gärtner and Katharina v. Werthern.

8. List of publications

Publications part of this thesis:

Goob G., Adrian J., Cossu C., Hauck C. R. “Phagocytosis mediated by the human granulocyte receptor CEACAM3 is limited by the receptor-type protein tyrosine phosphatase PTPRJ.” (2022) Journal of Biological Chemistry, 298(9), 102269. https://doi.org/10.1016/j.jbc.2022.102269

Goob G.*, **Kress A.***, Roth A., Seiffert C., von Werthern K., Hauck C. R. “A CEACAM3 polymorphism prevalent in subsaharan Africa directs opsonin-independent recognition of *Neisseria meningitidis* by human phagocytes.” (***** both authors contributed equally). Manuscript in preparation.

Publications not part of this thesis:

Bonsignore P., Kuiper J. W. P., Adrian J., **Goob G.,** Hauck C.R. “CEACAM3 - A Prim(at)e Invention for Opsonin-Independent Phagocytosis of Bacteria.” (2020) Frontiers in Immunology; https://doi.org/10.3389/fimmu.2019.03160

Mix A-K., **Goob G.,** Sontowski E., Hauck C. R. “Microscale communication between bacterial pathogens and the host epithelium.” (2021) Gene and Immunity; https://doi.org/10.1038/s41435-021-00149-1

9. Appendix

9.1 Supplementary Figures

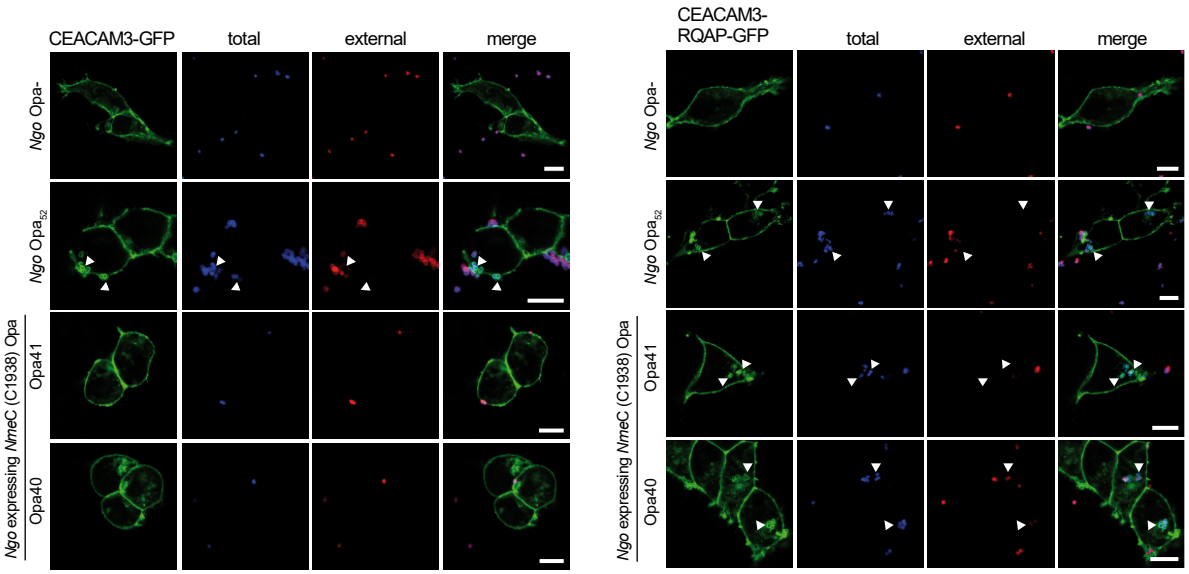

Suppl. Figure S1. CEACAM3-RQAP, but not the major CEACAM3 variant, mediates phagocytosis of bacteria expressing *Neisseria meningitidis* serogroup C Opa proteins. 293T cells were transfected to express CEACAM3-GFP or CEACAM3-RQAP-GFP fusion proteins. Transfected cells were infected for 1 hour at an MOI of 40 with pacific blue and biotin-labelled *N. gonorrhoeae* expressing the indicated Opa protein or lacking Opa protein expression (Opa-). After fixation of the samples, extracellular bacteria were additionally stained with Cy5-streptavidin (red). Internalized bacteria are indicated by white arrows. Scale bars indicate 10 µm. The experiment was designed by Griseldis Goob and was conducted by Alisia Gärtner, Katharina v. Werthern and Griseldis Goob.

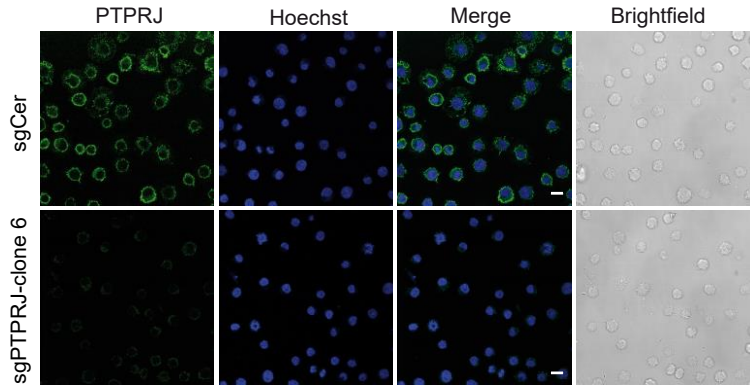

Suppl. Figure S2. CRISPR/Cas9-mediated disruption of PTPRJ expression in HL60 CEACAM3-mKate cells. HL60 CEACAM3-mKate Cerulean cells were treated with sgRNAs against cerulean (HL60 CEACAM3-mKate control; sgCer) or a combination of sgRNAs against cerulean and PTPRJ (HL60 CEACAM3-mKate sgPTPRJ-clone6). PTPRJ expression was examined by staining the cells with α-PTPRJ antibodies and an Alexa Fluor-488-conjugated secondary antibody (green). Nuclear staining by Hoechst33342 is depicted in blue. Scale bars represent 10 µm. This figure is published in (Goob et al., 2022).

9.2 Supplementary Tables

Supplementary Table 1

ESN - Esan in Nigeria (African sub-population)

Genomes: **total: 99; with at least one of the four selected SNPs in CEACAM3: 29**

Variant ID		**rs61738270**	**rs61738269**	**rs61737019**	**rs61737014**	CEACAM3-RQAP
Allels		A=common, C=polymorphic	T=common, A=polymorphic	T=common, C=polymorphic	A=common, C=polymorphic	
Variant		S43R	L44Q	V83A	T103P	
Sample name and gender	HG02923 (M)	C|C	A|A	C|C	C|C	XX
	HG02938 (M)	C|A	A|T	C|T	C|A	X
	HG02968 (M)	C|A	A|T	C|T	C|A	X
	HG02976 (F)	A|C	T|A	T|C	A|C	X
	HG02977 (M)	A|C	T|A	T|C	A|C	X
	HG02981 (M)	C|A	A|T	C|T	C|A	X
	HG03115 (M)	C|A	A|T	C|T	C|A	X
	HG03118 (M)	A|C	T|A	T|C	A|C	X
	HG03126 (F)	A|C	T|A	T|C	A|C	X
	HG03127 (M)	C|A	A|T	C|T	C|A	X
	HG03135 (F)	A|C	T|A	T|C	A|A	
	HG03163 (M)	C|A	A|T	C|T	C|A	X
	HG03166 (M)	A|C	T|A	T|C	A|C	X
	HG03169 (M)	A|C	T|A	T|C	A|C	X
	HG03189 (F)	A|C	T|A	T|C	A|C	X
	HG03193 (M)	C|A	A|T	C|T	C|A	X
	HG03198 (F)	C|A	A|T	C|T	C|A	X
	HG03265 (M)	A|C	T|A	T|C	A|C	X
	HG03267 (F)	C|A	A|T	C|T	C|A	X
	HG03268 (M)	C|A	A|T	C|T	C|A	X
	HG03311 (M)	A|C	T|A	T|C	A|C	X
	HG03313 (M)	A|C	T|A	T|C	A|C	X
	HG03343 (M)	A|C	T|A	T|C	A|C	X
	HG03354 (F)	C|A	A|T	C|T	C|A	X
	HG03372 (F)	C|C	A|A	C|C	C|C	XX
	HG03499 (F)	A|C	T|A	T|C	A|C	X
	HG03511 (F)	C|A	A|T	C|T	C|A	X
	HG03514 (F)	C|A	A|T	C|T	C|A	X
	HG03517 (F)	A|A	T|T	C|T	C|A	

Genomes with CEACAM3-RQAP allele: 27 (27,272727%); CEACAM3-RQAP allele frequency: 0,146

GWD – Gambians in Gambia (African sub-population)

Genomes: **total: 113; with at least one of the four selected SNPs in CEACAM3: 49**

Variant ID		**rs61738270**	**rs61738269**	**rs61737019**	**rs61737014**	CEACAM3-RQAP
Allels		A=common, C=polymorphic	T=common, A=polymorphic	T=common, C=polymorphic	A=common, C=polymorphic	
Variant		S43R	L44Q	V83A	T103P	
	HG02464 (M)	C|A	A|T	C|T	C|A	X
	HG02465 (F)	C|A	A|T	C|T	C|A	X
	HG02561 (M)	C|A	A|T	C|T	C|A	X

Sample name and gender						
	HG02570 (M)	C|A	A|T	C|T	C|A	X
	HG02573 (M)	C|C	A|A	C|C	C|C	XX
	HG02583 (F)	A|C	T|A	T|C	A|C	X
	HG02589 (F)	C|A	A|T	C|T	A|A	
	HG02594 (M)	C|A	A|T	C|T	C|A	X
	HG02595 (F)	C|C	A|A	C|C	C|C	XX
	HG02611 (F)	C|A	A|T	C|T	C|A	X
	HG02623 (M)	A|C	T|A	T|C	A|C	X
	HG02624 (F)	C|A	A|T	C|T	C|A	X
	HG02629 (F)	C|A	A|T	C|T	C|A	X
	HG02666 (M)	A|C	T|A	T|C	A|C	X
	HG02667 (F)	A|A	T|T	C|T	C|A	
	HG02679 (F)	A|C	T|A	T|C	A|C	X
	HG02721 (M)	C|A	A|T	C|T	C|A	X
	HG02722 (F)	A|C	T|A	T|T	A|A	
	HG02756 (M)	C|A	A|T	C|T	C|A	X
	HG02759 (M)	C|A	A|T	C|T	C|A	X
	HG02763 (F)	A|C	T|A	T|C	A|C	X
	HG02771 (M)	C|A	A|T	C|T	C|A	X
	HG02799 (F)	A|A	T|T	T|C	A|C	
	HG02804 (M)	C|A	A|T	C|T	C|C	X
	HG02805 (F)	A|C	T|A	T|C	A|C	X
	HG02810 (M)	A|A	T|T	T|C	A|C	
	HG02811 (F)	C|A	A|T	T|T	C|A	
	HG02813 (M)	A|C	T|A	T|C	A|C	X
	HG02816 (M)	C|C	A|A	C|C	C|C	XX
	HG02817 (F)	C|A	A|T	C|T	C|A	X
	HG02819 (M)	C|A	A|T	C|T	C|A	X
	HG02836 (M)	A|C	T|A	T|C	A|C	X
	HG02840 (F)	A|A	T|T	T|T	A|C	
	HG02852 (F)	A|C	T|A	T|C	A|C	X
	HG02854 (M)	C|A	A|T	C|T	C|A	X
	HG02855 (F)	C|A	A|T	C|T	C|A	X
	HG02860 (M)	C|C	A|A	C|C	C|C	XX
	HG02882 (F)	A|C	T|A	T|C	A|C	X
	HG02884 (M)	C|A	A|T	C|T	C|A	X
	HG02887 (M)	C|A	A|T	C|T	C|A	X
	HG02896 (F)	C|C	A|A	C|C	C|C	XX
	HG03024 (M)	A|C	T|A	T|C	A|C	X
	HG03025 (F)	A|C	T|A	T|C	A|C	X
	HG03027 (M)	A|C	T|A	T|C	A|C	X
	HG03040 (F)	C|C	A|A	C|C	C|C	XX
	HG03045 (M)	A|C	T|A	T|C	A|C	X
	HG03240 (M)	C|A	A|T	C|T	C|A	X
	HG03247 (F)	A|C	T|A	T|C	A|C	X
	HG03258 (M)	C|A	A|T	C|T	C|A	X

Genomes with CEACAM3-RQAP allele: 42 (37,1681%); CEACAM3-RQAP allele frequency: 0,212

LWK – Luhya in Webuye (Kenya) (African sub-population)

Genomes: **total: 99; with at least one of the four selected SNPs in CEACAM3: 31**

Variant ID		**rs61738270**	**rs61738269**	**rs61737019**	**rs61737014**	CEACAM3-RQAP
Allels		A=common, C=polymorphic	T=common, A=polymorphic	T=common, C=polymorphic	A=common, C=polymorphic	
Variant		S43R	L44Q	V83A	T103P	
	NA19025 (M)	A|C	T|A	T|C	A|C	X
	NA19026 (M)	C|C	A|A	C|C	C|C	XX

Sample name and gender						
	NA19030 (F)	A|C	T|A	T|C	A|C	X
	NA19035 (M)	A|C	T|A	T|C	A|C	X
	NA19038 (F)	A|A	T|T	C|T	C|A	
	NA19041 (M)	A|A	T|T	T|C	A|C	
	NA19307 (M)	A|C	T|A	T|C	A|C	X
	NA19308 (M)	C|C	A|A	C|C	C|C	XX
	NA19309 (M)	A|A	T|T	T|C	A|C	
	NA19312 (M)	A|A	T|T	T|C	A|C	
	NA19314 (F)	A|C	T|A	T|C	A|C	X
	NA19315 (F)	C|A	A|T	C|T	C|A	X
	NA19323 (F)	C|A	A|T	C|T	C|A	X
	NA19332 (F)	A|C	T|A	T|C	A|C	X
	NA19338 (F)	A|C	T|A	T|C	A|C	X
	NA19347 (M)	A|C	T|A	T|T	A|C	
	NA19350 (M)	C|A	A|T	C|T	C|A	X
	NA19355 (F)	A|C	T|A	T|C	A|C	X
	NA19374 (M)	A|A	T|T	C|T	C|A	
	NA19385 (M)	A|C	T|A	T|C	A|C	X
	NA19393 (M)	C|A	A|T	C|T	C|A	X
	NA19399 (F)	A|A	T|T	T|C	A|C	
	NA19430 (M)	A|C	T|A	T|C	A|C	X
	NA19438 (F)	A|A	T|T	T|C	A|C	
	NA19443 (M)	A|A	T|T	C|T	C|A	
	NA19445 (F)	C|A	A|T	C|T	C|A	X
	NA19446 (F)	A|A	T|T	C|T	C|A	
	NA19454 (M)	C|A	A|T	C|T	C|A	X
	NA19457 (F)	A|C	T|A	T|C	A|C	X
	NA19473 (F)	C|C	A|A	C|C	C|C	XX
	NA19474 (F)	A|C	T|A	T|C	A|C	X

Genomes with CEACAM3-RQAP allele: 21 (21,2121%); CEACAM3-RQAP allele frequency: 0,121

MSL – Mende in Sierra Leone (African sub-population)

Genomes: **total: 85; with at least one of the four selected SNPs in CEACAM3: 57**

Sample name and gender	**Variant ID**	**rs61738270**	**rs61738269**	**rs61737019**	**rs61737014**	CEACAM3-RQAP
	Allels	A=common, C=polymorphic	T=common, A=polymorphic	T=common, C=polymorphic	A=common, C=polymorphic	
	Variant	S43R	L44Q	V83A	T103P	
	HG03052 (F)	A|C	T|A	T|T	A|A	
	HG03054 (M)	A|C	T|A	T|C	A|C	X
	HG03057 (M)	A|C	T|A	T|C	A|C	X
	HG03061 (F)	A|C	T|A	T|C	A|C	X
	HG03064 (F)	C|A	A|T	C|T	C|A	X
	HG03066 (M)	A|C	T|A	T|C	A|C	X
	HG03069 (M)	C|A	A|T	C|T	C|A	X
	HG03072 (M)	C|A	A|T	C|T	C|A	X
	HG03073 (F)	A|C	T|A	T|C	A|C	X
	HG03074 (M)	C|C	A|A	C|C	C|C	XX
	HG03078 (M)	A|C	T|A	T|C	A|A	
	HG03081 (M)	A|C	T|A	T|C	A|C	X
	HG03082 (F)	A|C	T|A	T|C	A|C	X
	HG03085 (F)	A|C	T|A	T|C	A|C	X
	HG03086 (F)	C|A	A|T	C|T	C|A	X
	HG03088 (F)	A|C	T|A	T|C	A|C	X
	HG03091 (F)	A|C	T|A	T|C	A|C	X
	HG03095 (F)	C|C	A|A	C|C	C|C	XX
	HG03096 (M)	A|C	T|A	T|C	A|C	X

Sample name and gender						
	HG03097 (F)	A|A	T|T	C|T	C|A	
	HG03209 (M)	A|C	T|A	T|C	A|C	X
	HG03225 (M)	A|C	T|A	T|C	A|C	X
	HG03376 (M)	A|C	T|A	T|C	A|C	X
	HG03378 (F)	C|A	A|T	C|T	C|A	X
	HG03380 (F)	A|C	T|A	T|C	A|C	X
	HG03382 (M)	C|C	A|A	C|C	C|C	XX
	HG03385 (M)	A|C	T|A	T|C	A|C	X
	HG03397 (M)	A|C	T|A	T|T	A|C	
	HG03401 (F)	A|C	T|A	T|C	A|C	X
	HG03419 (F)	C|C	A|A	C|C	C|C	
	HG03428 (F)	A|C	T|A	T|C	A|C	XX
	HG03436 (M)	C|A	A|T	C|T	C|A	X
	HG03437 (F)	C|C	A|A	C|C	C|C	X
	HG03439 (M)	A|A	T|T	T|C	A|C	XX
	HG03442 (M)	C|C	A|A	C|C	C|C	
	HG03445 (M)	C|A	A|T	C|T	C|A	XX
	HG03446 (F)	C|A	A|T	C|T	C|A	X
	HG03449 (F)	A|C	T|A	T|C	A|C	X
	HG03455 (F)	A|C	T|A	T|C	A|C	X
	HG03457 (M)	A|C	T|A	T|C	A|C	X
	HG03458 (F)	C|A	A|T	C|T	C|A	X
	HG03461 (F)	A|C	T|A	C|T	C|A	X
	HG03469 (M)	C|A	A|T	T|T	A|A	
	HG03470 (F)	C|A	A|T	C|T	C|A	X
	HG03472 (M)	C|A	A|T	C|T	C|A	X
	HG03476 (F)	A|C	T|A	T|C	A|C	X
	HG03479 (F)	A|C	T|A	T|C	A|C	X
	HG03484 (M)	A|C	T|A	T|C	A|C	X
	HG03559 (M)	A|C	T|A	T|C	A|C	X
	HG03563 (F)	C|A	A|T	C|T	C|A	X
	HG03565 (M)	C|A	A|T	C|T	C|A	X
	HG03567 (F)	C|C	A|A	C|C	C|C	XX
	HG03571 (M)	A|A	T|T	T|C	A|C	
	HG03572 (F)	C|A	A|T	C|T	C|A	X
	HG03575 (F)	C|A	A|T	C|T	C|A	X
	HG03578 (F)	A|C	T|A	C|C	C|C	X
	HG03583 (F)	C|A	A|T	C|T	C|A	X

Genomes with CEACAM3-RQAP allele: 49 (57,64%); CEACAM3-RQAP allele frequency: 0,329

YRI – Yoruba in Ibadan (Nigeria) (African sub-population)

Genomes: **total: 108; with at least one of the four selected SNPs in CEACAM3: 37**

Variant ID		**rs61738270**	**rs61738269**	**rs61737019**	**rs61737014**	CEACAM3-RQAP
Allels		A=common, C=polymorphic	T=common, A=polymorphic	T=common, C=polymorphic	A=common, C=polymorphic	
Variant		S43R	L44Q	V83A	T103P	
Sample name and gender	NA18486 (M)	A|C	T|A	T|C	A|C	X
	NA18498 (M)	A|C	T|A	T|C	A|C	X
	NA18502 (F)	A|A	T|T	T|T	A|C	
	NA18504 (M)	C|C	A|A	C|C	C|C	XX
	NA18505 (F)	A|A	T|T	T|T	A|C	
	NA18507 (M)	A|A	T|T	T|T	A|C	
	NA18510 (M)	A|C	T|A	T|C	A|C	X
	NA18516 (M)	C|A	A|T	C|T	C|A	X
	NA18519 (M)	C|A	A|T	C|T	C|A	X
	NA18520 (F)	C|A	A|T	C|T	C|A	X
	NA18861 (F)	A|C	T|A	T|C	A|C	X
	NA18878 (F)	C|A	A|T	C|T	C|A	X

Sample name and gender						
	NA18879 (M)	C|A	A|T	C|T	C|A	X
	NA18909 (F)	A|C	T|A	T|C	A|C	X
	NA18912 (F)	A|C	T|A	T|C	A|C	X
	NA18916 (F)	A|C	T|A	T|C	A|C	X
	NA18923 (M)	A|C	T|A	T|C	A|C	X
	NA18924 (F)	A|C	T|A	T|C	A|C	X
	NA18933 (F)	C|A	A|T	C|T	C|A	X
	NA19096 (M)	C|C	A|A	C|C	C|C	XX
	NA19099 (F)	A|A	T|T	T|C	A|C	
	NA19102 (F)	C|C	A|A	C|C	C|C	XX
	NA19113 (M)	C|A	A|T	C|T	C|A	X
	NA19114 (F)	C|A	A|T	C|T	C|A	X
	NA19121 (M)	A|C	T|A	T|C	A|C	X
	NA19144 (M)	A|C	T|A	T|C	A|C	X
	NA19147 (F)	C|A	A|T	C|T	C|A	X
	NA19153 (M)	C|A	A|T	C|T	C|A	X
	NA19159 (F)	C|A	A|T	C|T	C|A	X
	NA19171 (M)	A|C	T|A	T|C	A|C	X
	NA19190 (F)	C|A	A|T	C|T	C|A	X
	NA19198 (M)	C|A	A|T	C|T	C|A	X
	NA19206 (F)	C|A	A|T	C|T	C|A	X
	NA19213 (M)	A|C	T|A	T|C	A|C	X
	NA19222 (F)	A|A	T|T	T|C	A|C	
	NA19225 (F)	C|A	A|T	C|T	C|A	X
	NA19256 (M)	C|A	A|T	C|T	C|A	X

Genomes with CEACAM3-RQAP allele: 32 (29,6296%); CEACAM3-RQAP allele frequency: 0,162

EAS (East Asian)

Genomes: **total: 504; with at least one of the four selected SNPs in CEACAM3: 1**

Variant ID		**rs61738270**	**rs61738269**	**rs61737019**	**rs61737014**	CEACAM3-RQAP
Allels		A=common, C=polymorphic	T=common, A=polymorphic	T=common, C=polymorphic	A=common, C=polymorphic	
Variant		S43R	L44Q	V83A	T103P	
Sample name and gender	HG00692 (M)	A|A	T|T	T|T	C|A	

Genomes with CEACAM3-RQAP alelle: 0 (0%); CEACAM3-RQAP allele frequency: 0

EUR (European)

Genomes: **total: 503; with at least one of the four selected SNPs in CEACAM3: 2**

Variant ID		**rs61738270**	**rs61738269**	**rs61737019**	**rs61737014**	CEACAM3-RQAP
Allels		A=common, C=polymorphic	T=common, A=polymorphic	T=common, C=polymorphic	A=common, C=polymorphic	
Variant		S43R	L44Q	V83A	T103P	
Sample name and gender	HG01620 (F)	C|A	A|T	C|T	C|A	X
	NA20759 (M)	A|A	T|T	T|T	A|C	

Genomes with CEACAM3-RQAP allele: 1 (0,1988%); CEACAM3-RQAP allele frequency: 0,000994

SAS (South Asian)

Genomes: **total: 489 with at least one of the four selected SNPs in CEACAM3: 0**

Variant ID		**rs61738270**	**rs61738269**	**rs61737019**	**rs61737014**	CEACAM3-RQAP
Allels		A=common, C=polymorphic	T=common, A=polymorphic	T=common, C=polymorphic	A=common, C=polymorphic	
Variant		S43R	L44Q	V83A	T103P	
Sample name and gender						

Genomes with CEACAM3-RQAP allele: 0 (0%); CEACAM3-RQAP allele frequency: 0

Supplementary Table 1. Distribution of the CEACAM3-RQAP allele in populations of African ancestry and in Europeans, South Asians, and East Asians. The sample names and genotypes given in the table were taken from the 1000 Genomes Project data. In the Ensemble Browser, these data can be viewed under the Variant Table for each variant in the Population Genetics module. The table includes only those samples in which at least one of the four SNPs searched for was found in CEACAM3. (Ensemble Database; 1000 Genomes Project Phase 3; last accessed 7/2022).

9.3 List of Figures

9.4 Abbreviations

δ	Delta (Greek small letter)
γ	Gamma (Greek small letter)
ζ	Zeta (Greek small letter)
Amp	Ampicillin
App	adhesin and penetration protein
APS	ammonium persulfate
Arp2/3	actin-related protein 2/3
ATCC	American Type Culture Collection
bp	base pair
BSA	bovine serum albumin
Cam	Chloramphenicol
CARD9	Caspase recruitment domain-containing protein 9
Cas9	CRISPR-associated 9
cDNA	complementary DNA
CEA	carcinoembryonic antigen
CEAtg	CEA transgene
CEACAM	carcinoembryonic antigen-related cell adhesion molecule
CFSE	carboxyfluorescein succinimidyl ester
cfu	colony forming units
CLEC	C-type lectin receptors
CR	complement receptor
CRISPR	clustered regularly interspaced short palindromic repeats
CS	calf serum
C-terminal	carboxy-terminal
DAG	Diacylglycerol
DC	dendritic cell
dCTP	Deoxycytidine triphosphate
ddH_20	double distilled water
DMEM	Dulbecco's modified Eagle's medium
DMSO	Dimethyl sulfoxide
DNA	deoxyribonucleic acid
dNTP	Desoxynucleoside triphosphate
DSMZ	German collection of microorganisms and cell cultures

DTT	Dithiothreitol
ECL	Enhanced chemiluminescence
E. coli	*Escherichia coli*
EDTA	Ethylenediaminetetraacetic acid
EGFP	enhanced green fluorescent protein
EGTA	Ethylene glycol-bis(2-aminoethylether)-*N,N,N',N'*-tetraacetic acid
Erm	Erythromycin
EtOH	Ethanol
FACS	fluorescence-activated cell sorting
FCS	Fetal calf serum
FcγR	Fcγ receptor
GEF	guanine nucleotide exchange factor
GFP	green fluorescent protein
GPI	glycosylphosphatidylinositol
Grb14	Growth factor receptor-bound protein 14
GTP	guanosine triphosphate
HBS	hepes buffered saline
HemITAM	hemi-immunoreceptor tyrosine-based activation motif
HEPES	2-[4-(2-hydroxyethyl)piperazin-1-yl]ethanesulfonic acid
His-tag	Histidine-tag
HIV	human immunodeficiency virus
HSPG	heparansuphate proteoglycan
HRP	Horseradish peroxidase
IF	Immunofluorescence
Ig	immunglobulin
IgC	immunoglobulin constant
IgV	immunoglobulin variable
IP	immuno-precipitation
IP_3	inositol-(1,4,5)-trisphosphate
IPTG	isopropyl β-D-1-thiogalactopyranoside
ITAM	immunoreceptor tyrosine-based activation motif
ITIM	immunoreceptor tyrosine-based inhibition motif
Kan	Kanamycin
kb	Kilobase
LB	Lysogeny Broth

LOS	lipooligosaccharide
LPS	lipopolysaccharide
LSH	Lehrstuhl Hauck
M	Molar
mA	Milliampere
MeOH	Methanol
MFI	median fluorescent intensity
min	minute
mM	Millimolar
MOI	multiplicity of infection
Myr	myristoilated
n.s	not significant
NAD	nicotinamide adenine dinucleotide
NadA	Neisseria adhesin A
NADPH	nicotinamide adenine dinucleotide phosphate
NETs	neutrophil extracellular traps
NFκB	nuclear factor 'kappa-light-chain-enhancer' of activated B-cells
Ngo	*Neisseria gonorrhoeae*
NLR	nucleotide-binding oligomerization domain-like receptor
Nme	*Neisseria meningitidis*
N-terminal	amino-terminal
OD	Optical density
Omp P1	outer-membrane protein P1
Opa	opacity-associated
PAMP	Pathogen-associated molecular pattern
PBS	phosphate-buffered saline
PCR	polymerase chain reaction
PFA	paraformaldehyde
PI3K	phosphatidylinositol 3'-kinase
PID	pelvic inflammatory disease
PIP	phosphatidylinositide
PKC	Protein kinase C
PLCγ	Phospholipase C γ
PMN	polymorphonuclear granulocytes
PMSF	Phenylmethylsulfonylfluorid

pNPP	p-Nitrophenyl phosphate
PPM	Proteon peptone medium
PRR	pattern-recognition receptors
PSG	pregnancy-specific glycoproteins
PTPR	receptor-type protein tyrosine phosphatase
PTPRJ	receptor-type protein tyrosine phosphatase J
PVDF	Polyvinylidene fluoride
RNA	ribonucleic acid
ROS	reactive oxygen species
rpm	rounds per minute
RPMI	Roswell Park Memorial Institute
RT	Room temperature
SD	Standard deviation
SDS	sodium dodecyl sulfate
SDS-PAGE	sodium dodecyl sulfate polyacrylamide gel electrophoresis
sec	seconds
SEM	Scanning electron microscopy
SEM	standard error of means
sgRNA	single guide RNA
SH2	Src-homology 2
SNP	single nucleotide polymorphism
Strep	Streptomycin
Syk	spleen tyrosine kinase
TBS	Tris-buffered saline
TCR	T-cell receptor
TEMED	*N*,*N*,*N*',*N*'-Tetramethylethane-1,2-diamine
TLR	toll-like receptors
Tris	2-Amino-2-(hydroxymethyl)propane-1,3-diol
UV	Ultraviolet
V	Volt
Van	Vancomycin
WAVE	wiskott-aldrich syndrome verprolin homologous protein
WCL	whole cell lysate

10. Danksagung (Acknowledgment)

An dieser Stelle möchte ich mich herzlich bei all jenen bedanken, die mir diese Arbeit ermöglicht haben und mich während der Promotionszeit begleitet und unterstützt haben.

Mein besonderer Dank geht an Prof. Dr. Christof R. Hauck, der mir die Möglichkeit gegeben hat in seiner Gruppe an diesen spannenden Themen zu arbeiten. Lieber Christof, danke für deine hervorragende Betreuung während meiner gesamten Zeit in deiner Arbeitsgruppe. Danke für deine motivierende Art, deine vielen fachlichen Ideen und Ratschläge und dass deine Tür für Fragen jederzeit offenstand.

Des Weiteren möchte ich mich bei Prof. Dr. Thomas U. Mayer und Prof. Dr. Alexander Bürkle für die freundliche Übernahme des Zweitgutachtens und des Prüfungsvorsitzes bedanken.

Mein Dank gilt der Flow Cytometry Core Facility Konstanz (FlowKon) für die Einführung in das Gebiet der Durchflusszytometrie und die Hilfe beim Sorting verschiedener Zelllinien.

Bei Michael Laumann und Paavo Bergmann bedanke ich mich, dass sie mich in die Welt der Elektronenmikroskopie eingeführt haben und mich bei der Verarbeitung der Proben und der Aufnahme der Bilder am Elektronenmikroskop großartig unterstützt haben.

Weiterhin möchte ich mich bei den Mitarbeitern der Tierforschungsanlage der Universität Konstanz für die Zucht und Versorgung der Mäuse und ihre Unterstützung und Hilfsbereitschaft bei Fragen bedanken.

Ein großer Dank geht an alle ehemaligen und gegenwärtigen Kolleginnen und Kollegen, die meine Zeit im Hauck-Labor unvergesslich gemacht haben.

Besonders bedanke ich mich bei Petra, für die Organisation aller Angelegenheiten bürokratischer Natur, ihre stets offene Tür und ihre herzliche Art.

Petra, Claudia und Susanne danke ich von Herzen, dass sie unentwegt dafür gesorgt haben, dass zu jeder Zeit alle Medien, Puffer, Materialien und Chemikalien zur Verfügung standen, dass sie immer ein offenes Ohr für mich hatten und mir den Laboralltag nahezu täglich mit Mon Chéri versüßt haben. Ihr seid einfach großartig und ich werde euch sehr vermissen!!

Ein großes Dankeschön geht an Jonas, der mit seiner Arbeit den Grundstein für zwei der hier beschriebenen Projekte gelegt hat. Du hast mir mit deiner Hilfe und deinem fachlichen Rat nicht nur den Einstieg in die CEACAM-Welt erleichtert, sondern warst auch ein wertvoller Diskussionspartner bei nicht-wissenschaftlichen Themen. Ich habe unendlich viel von dir gelernt und bin froh, dass wir uns weiterhin sehen, auch wenn sich unsere beruflichen Wege getrennt haben.

Besonders danken möchte ich dir, liebe Patrizia. Ohne dich wäre meine Zeit im Labor nicht annähernd so schön gewesen. Ich konnte in allen Lebenslagen auf deinen fachlichen und freundschaftlichen Rat zählen. Danke für die gute gemeinsame Zeit, insbesondere für die vielen schönen Stunden, die wir außerhalb des Labors verbracht haben, und für deine Freundschaft.

Tamara, dir danke ich für deine grenzenlose Hilfsbereitschaft egal ob es um wissenschaftliche Fragen oder sonstige Probleme ging. Du warst die gute Seele des Labors. Danke für die schönen und lustigen Kürbisschnitz-, Cocktail-, und Irish-Pub-Abende.

Tanja danke ich für ihre fachliche Unterstützung, die netten kleinen Briefe und die vielen privaten Gespräche zwischendurch, die die Tage im Labor schöner gemacht haben. Außerdem danke ich dir, dass du es so viele Jahre tapfer mit meiner angeblich nervigen Tastatur ausgehalten hast (seither hat sich keiner mehr beschwert...), für die zahlreichen Haarflecht-Pausen und ganz einfach für die schöne Zeit mit dir als Büro- und Laborpartnerin.

Timo und Jan danke ich für die unvergesslichen schmozigen Donnerstage, die schönen Kaffeerunden und Feierabendbiere und die sportliche Herausforderung, beim Joggen mit euch mitzuhalten. Ihr habt mit eurer angenehmen Art wesentlich dazu beigetragen, dass ich (fast) immer sehr gerne zur Arbeit gekommen bin. Ich hoffe sehr, dass wir noch zahlreiche schmotzige Donnerstage zusammen feiern werden!

Ann-Kathrin danke ich für ihre großartige Unterstützung und ihren wertvollen Beistand in der TFA. Du hast mir mit deiner Hilfe die Maus-Arbeit um Welten erträglicher gemacht. Danke auch für die vielen leckeren Kuchen, die immer wieder Anlass für eine schöne Kaffee- und Kuchenpause mit der gesamten Arbeitsgruppe waren.

Meinem treuen Zellkultur-Nebensitzer Clovis danke ich für die schönen und meist erheiternden Gespräche an der Bench, zum Beispiel über das vergangene „klassische“ oder „nicht-klassische Wochenende“. Unser gemeinsames Guten-Morgen-Ritual hat mir den Start in viele Arbeitstage erheitert und wird mir immer in guter Erinnerung bleiben.

Liebe Marleen, lieber Erik, herzlichen Dank für eure Hilfsbereitschaft und den frischen Wind, den ihr ins Labor gebracht habt. Ich wünsche euch viel Erfolg bei euren zahlreichen Projekten und freue mich, dass ich dank euch noch ein paar Jahre auf bekannte Gesichter in der AG-Hauck hoffen kann.

Außerdem danke ich allen Studentinnen und Studenten, die ich in den letzten Jahren betreuen durfte. Danke für eure Unterstützung und Mithilfe bei verschiedenen Projekten meiner Doktorarbeit. Meiner ehemaligen Masterstudentin Alena gilt hier nochmal mein besonderer Dank. Ich habe viel von deiner Hilfe profitiert und hoffe, dass du auch das eine oder andere von mir lernen konntest.

Bedanken möchte ich mich auch bei einigen, die außerhalb des Labors wichtige Begleiter meiner Promotion waren: bei Franzi, die mich während meiner gesamten Zeit in Konstanz als treue Freundin begleitet hat, sowie bei Lena und Lars, für die schönen „Old-Fashioned-Abende“.

Von Herzen möchte ich mich bei meinen Eltern, meinen Geschwistern (Sarah, Janosch und Johanna) und bei Fritz bedanken. Danke für eure Unterstützung, euren Glauben an mich und euer Vertrauen. Ohne euch wäre das alles nicht möglich gewesen.

Nicht zuletzt gilt ein besonderer Dank dir, lieber Simon. Du hast mir immer wieder gezeigt, dass es auch noch ein Leben „da draußen“ gibt. Danke für deine Unterstützung und dass du mich immer wieder aufbaust. Ich bin unendlich dankbar, dich an meiner Seite zu haben.

11. References

Abad, R., López, E. L., Debbag, R., & Vázquez, J. A. (2014). Serogroup W meningococcal disease: global spread and current affect on the Southern Cone in Latin America. *Epidemiol. Infect.*, *142*, 2461–2470.

Adrian, J. (2019). The mechanisms behind CEACAM3-mediated recognition and uptake of pathogenic bacteria. *Dissertation, University of Konstanz*.

Adrian, J., Bonsignore, P., Hammer, S., Frickey, T., & Hauck, C. R. (2019). Adaptation to host-specific bacterial pathogens drives rapid evolution of a human innate immune receptor. *Current Biology*, *29*, 616–630.

Alexander, E. R. (1988). Gonorrhea in the newborn. *Ann. N. Y. Acad. Sci.*, *549*, 180–186.

Anderson, C. L., Shen, L., Eicher, D. M., Wewers, M. D., & Gill, J. K. (1990). Phagocytosis mediated by three distinct Fc gamma receptor classes on human leukocytes. *J Exp Med*, *171*, 1333–1345.

Apicella, M. A., Shero, M., Jarvis, G. A., Griffiss, J. M., Mandrell, R. E., & Schneider, H. (1987). Phenotypic variation in epitope expression of the Neisseria gonorrhoeae lipooligosaccharide. *Infection and Immunity*, *55*, 1755–1761.

Arora, D., Stopp, S., Bohmer, S. A., Schons, J., Godfrey, R., Masson, K., Razumovskaya, E., Ronnstrand, L., Tanzer, S., Bauer, R., Bohmer, F. D., & Muller, J. P. (2011). Protein-tyrosine phosphatase DEP-1 controls receptor tyrosine kinase FLT3 signaling. *J Biol Chem*, *286*, 10918–10929.

Baker, J. E., Majeti, R., Tangye, S. G., & Weiss, A. (2001). Protein tyrosine phosphatase CD148-mediated inhibition of T-cell receptor signal transduction is associated with reduced LAT and phospholipase Cgamma1 phosphorylation. *Mol Cell Biol*, *21*, 2393–2403.

Baroni, A., Buommino, E., De Gregorio, V., Ruocco, E., Ruocco, V., & Wolf, R. (2012). Structure and function of the epidermis related to barrier properties. *Clinics in Dermatology*, *30*, 257–262.

Bedard, K., & Krause, K.-H. (2007). The NOX family of ROS-generating NADPH oxidases: physiology and pathophysiology. *Physiological Reviews*, *87*, 245–313.

Belambri, S. A., Rolas, L., Raad, H., Hurtado-Nedelec, M., Dang, P. M., & El-Benna, J. (2018). NADPH oxidase activation in neutrophils: Role of the phosphorylation of its subunits. *Eur J Clin Invest*, *48 Suppl 2*, e12951.

Belley, A., Keller, K., Göettke, M., & Chadee, K. (1999). Intestinal mucins in colonization and host defense against pathogens. *American Journal of Tropical Medicine and Hygiene*, *60*, 10–15.

Belley, A., Keller, K., Grove, J., & Chadee, K. (1996). Interaction of LS174T human colon cancer cell mucins with Entamoeba histolytica: An in vitro model for colonic disease. *Gastroenterology*, *111*, 1484–1492.

Benchimol, S., Fuks, A., Jothy, S., Beauchemin, N., Shirota, K., & Stanners, C. P. (1989). Carcinoembryonic antigen, a human tumor marker, functions as an intercellular adhesion molecule. *Cell*, *57*, 327–334.

Berger, C. N., Billker, O., Meyer, T. F., Servin, A. L., & Kansau, I. (2004). Differential recognition of members of the carcinoembryonic antigen family by Afa/Dr adhesins of diffusely adhering Escherichia coli (Afa/Dr DAEC). *Mol Microbiol*, *52*, 963–983.

Beutler, B. (2004). Innate immunity: An overview. *Molecular Immunology*, *40*, 845–859.

Bhat, K. S., Gibbs, C. P., Barrera, O., Morrison, S. G., Jahnig, F., Stern, A., Kupsch, E. M., Meyer, T. F., & Swanson, J. (1992). The opacity proteins of Neisseria gonorrhoeae strain MS11 are encoded by a family of 11 complete genes. *Molecular Microbiology*, *6*, 1073–1076.

Bianco, C., Griffin, F. M., & Silverstein, S. C. (1975). Studies of the macrophage complement receptor. Alteration of receptor function upon macrophage activation. *Journal of Experimental Medicine*, *141*, 1278–1290.

Bibel, D. J., Aly, R., & Shinefield, H. R. (1992). Antimicrobilal Activity of Sphingosines. *Journal of Investigative Dermatology*, *98*, 269–273.

Bilek, N., Ison, C. A., & Spratt, B. G. (2009). Relative contributions of recombination and mutation to the diversification of the opa gene repertoire of Neisseria gonorrhoeae. *J Bacteriol*, *191*, 1878–1890.

Billker, O., Popp, A., Brinkmann, V., Wenig, G., Schneider, J., Caron, E., & Meyer, T. F. (2002). Distinct mechanisms of internalization of Neisseria gonorrhoeae by members of the CEACAM receptor family involving Rac1- and Cdc42- dependent and -independent pathways. *The EMBO Journal*, *21*, 560-571.

Blanton, K. J., Biswas, G. D., Tsai, J., Adams, J., Dyer, D. W., Davis, S. M., Koch, G. G., Sen, P. K., & Sparling, P. F. (1990). Genetic evidence that Neisseria gonorrhoeae produces specific receptors for transferrin and lactoferrin. *Journal of Bacteriology*, *172*, 5225–5235.

Boggon, T. J., & Eck, M. J. (2004). Structure and regulation of Src family kinases. *Oncogene*, *23*, 7918–7927.

Bonilla, F. A., & Oettgen, H. C. (2010). Adaptive immunity. *Journal of Allergy and Clinical Immunology*, *125*, 33–40.

Bonsignore, P., Kuiper, J. W. P., Adrian, J., Goob, G., & Hauck, C. R. (2020). CEACAM3-A Prim(at)e Invention for Opsonin-Independent Phagocytosis of Bacteria. *Front Immunol*, *10*, 3160.

Booth, J. W., Telio, D., Liao, E. H., McCaw, S. E., Matsuo, T., Grinstein, S., & Gray-Owen, S. D. (2003). Phosphatidylinositol 3-kinases in carcinoembryonic antigen-related cellular adhesion molecule-mediated internalization of Neisseria gonorrhoeae. *J Biol Chem*, *278*, 14037–14045.

Borregaard, N., & Cowland, J. B. (1997). Granules of the human neutrophilic polymorphonuclear leukocyte. *Blood*, *89*, 3503–3521.

Borregaard, N., Sehested, M., Nielsen, B. S., Sengelov, H., & Kjeldsen, L. (1995). Biosynthesis of granule proteins in normal human bone marrow cells. Gelatinase is a marker of terminal neutrophil differentiation. *Blood*, *85*, 812–817.

Bos, M. P., Kao, D., Hogan, D. M., Grant, C. C. R., & Belland, R. J. (2002). Carcinoembryonic antigen family receptor recognition by gonococcal Opa proteins requires distinct combinations of hypervariable Opa protein domains. *Infection and Immunity*, *70*, 1715–1723.

Boulton, I. C., & Gray-Owen, S. D. (2002). Neisserial binding to CEACAM1 arrests the activation and proliferation of CD4+ T lymphocytes. *Nature Immunology*, *3*, 229–236.

Bowmer, M. I., Leggat, I., & Borrowman, J. A. (1982). Disseminated gonococcal infection. *Can Med Assoc J*, *126*, 1188–1190.

Brinkmann, V., Reichard, U., Goosmann, C., Fauler, B., Uhlemann, Y., Weiss, D. S., Weinrauch, Y., & Zychlinsky, A. (2004). Neutrophil extracellular traps kill bacteria. *Science*, *303*, 1532–1535.

Broeker, M., Emonet, S., Fazio, C., Jacobsson, S., Koliou, M., Kuusi, M., Pace, D., Paragi, M., Pysik, A., Joao Simoes, M., Skoczynska, A., Stefanelli, P., Toropainen, M., Taha, M.-K., & Tzanakaki, G. (2015). Meningococcal serogroup Y disease in Europe: Continuation of high importance in some European regions in 2013. *Human Vaccines & Immunotherapeutics*, *11*, 2281–2286.

Buntru, A., Kopp, K., Voges, M., Frank, R., Bachmann, V., & Hauck, C. R. (2011). Phosphatidylinositol 3'-kinase activity is critical for initiating the oxidative burst and bacterial destruction during CEACAM3-mediated phagocytosis. *Journal of Biological Chemistry*, *286*, 9555–9566.

Buntru, A., Roth, A., Nyffenegger-Jann, N. J., & Hauck, C. R. (2012). HemITAM signaling by CEACAM3, a human granulocyte receptor recognizing bacterial pathogens. *Arch Biochem Biophys*, *524*, 77–83.

Burn, G. L., Foti, A., Marsman, G., Patel, D. F., & Zychlinsky, A. (2021). The Neutrophil. *Immunity*, *54*, 1377–1391.

Capecchi, B., Adu-Bobie, J., Di Marcello, F., Ciucchi, L., Masignani, V., Taddei, A., Rappuoli, R., Pizza, M., & Aricò, B. (2005). Neisseria meningitidis NadA is a new invasin which promotes bacterial adhesion to and penetration into human epithelial cells. *Molecular Microbiology*, *55*, 687 – 698.

Caugant, D. A., & Brynildsrud, O. B. (2020). Neisseria meningitidis: using genomics to understand diversity, evolution and pathogenesis. *Nature Reviews Microbiology*, *18*, 84–96.

Caugant, D. A., & Maiden, M. C. J. (2009). Meningococcal carriage and disease — Population biology and evolution. *Vaccine*, *27*, B64–B70.

Chambers, E. S., & Vukmanovic-Stejic, M. (2020). Skin barrier immunity and ageing. *Immunology*, *160*, 116–125.

Chan, P. A., Robinette, A., Montgomery, M., Almonte, A., Cu-Uvin, S., Lonks, J. R., Chapin, K. C., Kojic, E. M., & Hardy, E. J. (2016). Extragenital Infections Caused by Chlamydia trachomatis and Neisseria gonorrhoeae: A Review of the Literature. *Infectious Diseases in Obstetrics and Gynecology*, *2016*, 1–17.

Chen, T., Belland, R. J., Wilson, J., & Swanson, J. (1995). Adherence of pilus- Opa+ gonococci to epithelial cells in vitro involves heparan sulfate. *Journal of Experimental Medicine*, *182*, 511–517.

Chen, T., Bolland, S., Chen, I., Parker, J., Pantelic, M., Grunert, F., & Zimmermann, W. (2001). The CGM1a (CEACAM3/CD66d)-mediated phagocytic pathway of Neisseria gonorrhoeae expressing Opacity proteins is also the pathway to cell death. *Journal of Biological Chemistry*, *276*, 17413–17419.

Chen, T., & Gotschlich, E. C. (1996). CGM1a antigen of neutrophils, a receptor of gonococcal opacity proteins. *Proceedings of the National Academy of Sciences of the United States of America*, *93*, 14851–14856.

Chen, T., Grunert, F., Medina-Marino, A., & Gotschlich, E. C. (1997). Several carcinoembryonic antigens (CD66) serve as receptors for gonococcal opacity proteins. *The Journal of Experimental Medicine*, *185*, 1557–1564.

Chen, T., Zimmermann, W., Parker, J., Chen, I., Maeda, A., & Bolland, S. (2001). Biliary glycoprotein (BGPa, CD66a, CEACAM1) mediates inhibitory signals. *Journal of Leukocyte Biology*, *70*, 335-40.

Cohen, M. S. (1998). Sexually transmitted diseases enhance HIV transmission: no longer a hypothesis. *Lancet*, *351 Suppl*, 5–7.

Connell, T. D., Black, W. J., Kawula, T. H., Barritt, D. S., Dempsey, J. A., Kverneland Jr., K., Stephenson, A., Schepart, B. S., Murphy, G. L., & Cannon, J. G. (1988). Recombination among Protein II genes of Neisseria gonorrhoeae generates new coding sequences and increases structural variability in the Protein II family. *Molecular Microbiology*, *2*, 227–236.

Cooper, M. D., & Alder, M. N. (2006). The evolution of adaptive immune systems. *Cell*, *124*, 815–822.

Cordoba, S. P., Choudhuri, K., Zhang, H., Bridge, M., Basat, A. B., Dustin, M. L., & van der Merwe, P. A. (2013). The large ectodomains of CD45 and CD148 regulate their segregation from and inhibition of ligated T-cell receptor. *Blood*, *121*, 4295–4302.

Cornelissen, C. N., Biswas, G. D., & Sparling, P. F. (1993). Expression of gonococcal transferrin-binding protein 1 causes Escherichia coli to bind human transferrin. *Journal of Bacteriology*, *175*, 2448–2450.

Coureuil, M., Join-Lambert, O., Lécuyer, H., Bourdoulous, S., Marullo, S., & Nassif, X. (2012). Mechanism of meningeal invasion by Neisseria meningitidis. *Virulence*, *3*, 164–172.

Cox, D., & Greenberg, S. (2001). Phagocytic signaling strategies: Fc(gamma)receptor-mediated phagocytosis as a model system. *Semin Immunol*, *13*, 339–345.

Crum-Cianflone, N., & Sullivan, E. (2016). Meningococcal Vaccinations. *Infectious Diseases and Therapy*, *5*, 89–112.

da Costa-Lourenco, A. P. R., dos Santos, K. T. B., Moreira, B. M., Fracalanzza, S. E. L., & Bonelli, R. R. (2017). Antimicrobial resistance in Neisseria gonorrhoeae: history, molecular mechanisms and epidemiological aspects of an emerging global threat. *Brazilian Journal of Microbiology*, *48*, 617–628.

De Jonge, M. I., Hamstra, H. J., Van Alphen, L., Dankert, J., & Van der Ley, P. (2003). Mapping the binding domains on meningococcal Opa proteins for CEACAM1 and CEA receptors. *Molecular Microbiology*, *50*, 1005–1015.

de Oliveira, S., Rosowski, E. E., & Huttenlocher, A. (2016). Neutrophil migration in infection and wound repair: going forward in reverse. *Nat Rev Immunol*, *16*, 378–391.

de Vries, F. P., Cole, R., Dankert, J., Frosch, M., & van Putten, J. P. (1998). Neisseria meningitidis producing the Opc adhesin binds epithelial cell proteoglycan receptors. *Molecular Microbiology*, *27*, 1203-12.

Degn, S. E., & Thiel, S. (2013). Humoral pattern recognition and the complement system. *Scand J Immunol*, *78*, 181–193.

den Hertog, J., Ostman, A., & Bohmer, F. D. (2008). Protein tyrosine phosphatases: regulatory mechanisms. *Febs J*, *275*, 831–847.

Doron, S., & Gorbach, S. L. (2008). Bacterial Infections: Overview. *International Encyclopedia of Public Health*, 273–282.

Dustin, M. L. (2016). Complement receptors in myeloid cell adhesion and phagocytosis. *Microbiol Spectr*, *4*, 1–26.

Eades-Perner, A. M., van der Putten, H., Hirth, A., Thompson, J., Neumaier, M., von Kleist, S., & Zimmermann, W. (1994). Mice transgenic for the human carcinoembryonic antigen gene maintain its spatiotemporal expression pattern. *Cancer Res*, *54*, 4169–4176.

Edwards, J. L., & Apicella, M. A. (2004). The molecular mechanisms used by Neisseria gonorrhoeae to initiate infection differ between men and women. *Clin Microbiol Rev*, *17*, 965–981.

Elsner, J., Oppermann, M., Czech, W., & Kapp, A. (1994). C3a activates the respiratory burst in human polymorphonuclear neutrophilic leukocytes via pertussis toxin-sensitive G-proteins. *Blood*, *83*, 3324–3331.

Fällman, M., Andersson, R., & Andersson, T. (1993). Signaling properties of CR3 (CD11b/CD18) and CR1 (CD35) in relation to phagocytosis of complement-opsonized particles. *Journal of Immunology*, *151*, 330–338.

Fitzgerald, K. A., & Kagan, J. C. (2020). Toll-like Receptors and the Control of Immunity. *Cell*, *180*, 1044–1066.

Flanagan, J. L., & Willcox, M. D. P. (2009). Role of lactoferrin in the tear film. *Biochimie*, *91*, 35–43.

Flannagan, R. S., Jaumouillé, V., & Grinstein, S. (2012). The cell biology of phagocytosis. *Annual Review of Pathology*, *7*, 61–98.

Fleming, D. T., & Wasserheit, J. N. (1999). From epidemiological synergy to public health policy and practice: the contribution of other sexually transmitted diseases to sexual transmission of HIV infection. *Sex Transm Infect*, *75*, 3–17.

Flemming, A. L. (1922). On a remarkable bacteriolitic element found in tissues and secretions. *Proc R Soc London B.*

Furr, P. M., & Taylor-Robinson, D. (1991). The influence of hormones on the bacterial flora of the murine vagina and implications for human disease. *Microbial Ecology in Health and Disease*, *4*, 141–148.

Furukawa, T., Itoh, M., Krueger, N. X., Streuli, M., & Saito, H. (1994). Specific interaction of the CD45 protein-tyrosine phosphatase with tyrosine-phosphorylated CD3 zeta chain. *Proc Natl Acad Sci U S A*, *91*, 10928–10932.

Ganz, T. (2003). Defensins: Antimicrobial peptides of innate immunity. *Nature Reviews Immunology*, *3*, 710–720.

Ghys, P. D., Fransen, K., Diallo, M. O., Ettiègne-Traoré, V., Coulibaly, I.-M., Yeboué, K. M., Kalish, M. L., Maurice, C., Whitaker, J. P., Greenberg, A. E., & Laga, M. (1997). The associations between cervicovaginal HIV shedding, sexually transmitted diseases and immunosuppression in female sex workers in Abidjan, Cote d'Ivoire. *Aids*, *11*, 85–93.

Godfrey, R., Arora, D., Bauer, R., Stopp, S., Muller, J. P., Heinrich, T., Bohmer, S. A., Dagnell, M., Schnetzke, U., Scholl, S., Ostman, A., & Bohmer, F. D. (2012). Cell transformation by FLT3 ITD in acute myeloid leukemia involves oxidative inactivation of the tumor suppressor protein-tyrosine phosphatase DEP-1/ PTPRJ. *Blood*, *119*, 4499–4511.

Goldstein, I. M., Roos, D., Kaplan, H. B., & Weissmann, G. (1975). Complement and immunoglobulins stimulate superoxide production by human leukocytes independently of phagocytosis. *Journal of Clinical Investigation*, *56*, 1155–1163.

Goob, G., Adrian, J., Cossu, C., & Hauck, C. R. (2022). Phagocytosis mediated by the human granulocyte receptor CEACAM3 is limited by the receptor-type protein tyrosine phosphatase PTPRJ. *Journal of Biological Chemistry*, *298*, 102269.

Goodridge, H. S., Reyes, C. N., Becker, C. A., Katsumoto, T. R., Ma, J., Wolf, A. J., Bose, N., Chan, A. S. H., Magee, A. S., Danielson, M. E., Weiss, A., Vasilakos, J. P., & Underhill, D. M. (2011). Activation of the innate immune receptor Dectin-I upon formation of a 'phagocytic synapse.' *Nature*, *472*, 471–475.

Gray-Owen, S. D. (2003). Neisserial Opa proteins: impact on colonization, dissemination and immunity. *Scandinavian Journal of Infectious Diseases*, *35*, 614–618.

Gray-Owen, S. D., & Blumberg, R. S. (2006). CEACAM1: contact-dependent control of immunity. *Nat Rev Immunol*, *6*, 433–446.

Gray-Owen, S. D., Dehio, C., Haude, A., Grunert, F., & Meyer, T. F. (1997). CD66 carcinoembryonic antigens mediate interactions between Opa-expressing Neisseria gonorrhoeae and human polymorphonuclear phagocytes. *The EMBO Journal*, *16*, 3435–3445.

Gray-Owen, S. D., Lorenzen, D. R., Haude, A., Meyer, T. F., & Dehio, C. (1997). Differential Opa specificities for CD66 receptors influence tissue interactions and cellular response to Neisseria gonorrhoeae. *Molecular Microbiology*, *26*, 971–980.

Greenwood, B. (1999). Manson Lecture. Meningococcal meningitis in Africa. *Royal Society of Tropical Medicine and Hygiene*, *93*, 341–353.

Grimm, T. M., Dierdorf, N. I., Betz, K., Paone, C., & Hauck, C. R. (2020). PPM1F controls integrin activity via a conserved phospho-switch. *J Cell Biol*, *219*, e202001057.

Hadi, H. A., Wooldridge, K. G., Robinson, K., & Ala'Aldeen, D. A. A. (2001). Identification and characterization of App: an immunogenic autotransporter protein of Neisseria meningitidis. *Molecular Microbiology*, *41*, 611–623.

Hammarström, S. (1999). The carcinoembryonic antigen (CEA) family: structures, suggested functions and expression in normal and malignant tissues. *Seminars in Cancer Biology*, *9*, 67–81.

Hauck, C. R., Meyer, T. F., Lang, F., & Gulbins, E. (1998). CD66-mediated phagocytosis of Opa52 Neisseria gonorrhoeae requires a Src-like tyrosine kinase- and Rac1-dependent signalling pathway. *The EMBO Journal*, *17*, 443–454.

Heinrich, A., Heyl, K. A., Klaile, E., Muller, M. M., Klassert, T. E., Wiessner, A., Fischer, K., Schumann, R. R., Seifert, U., Riesbeck, K., Moter, A., Singer, B. B., Bachmann, S., & Slevogt, H. (2016). Moraxella catarrhalis induces CEACAM3-Syk-CARD9-dependent activation of human granulocytes. *Cell Microbiol*, *18*, 1570–1582.

Hermiston, M. L., Xu, Z., & Weiss, A. (2003). CD45: a critical regulator of signaling thresholds in immune cells. *Annu Rev Immunol*, *21*, 107–137.

Hermiston, M. L., Zikherman, J., & Zhu, J. W. (2009). CD45, CD148, and Lyp/Pep: critical phosphatases regulating Src family kinase signaling networks in immune cells. *Immunol Rev*, *228*, 288–311.

Hill, D. J., & Virji, M. (2003). A novel cell-binding mechanism of Moraxella catarrhalis ubiquitous surface protein UspA: Specific targeting of the N-domain of carcinoembryonic antigen-related cell adhesion molecules by UspA1. *Molecular Microbiology*, *48*, 117–129.

Hill, S. A., & Davies, J. K. (2009). Pilin gene variation in Neisseria gonorrhoeae: reassessing the old paradigms. *FEMS Microbiology Reviews*, *33*, 521–530.

Hunte, T., Alcaide, M., & Castro, J. (2010). Rectal infections with chlamydia and gonorrhoea in women attending a multiethnic sexually transmitted diseases urban clinic. *International Journal of STD and AIDS*, *21*, 819–822.

Islam, E. A., Anipindi, V. C., Francis, I., Shaik-Dasthagirisaheb, Y., Xu, S., Leung, N., Sintsova, A., Amin, M., Kaushic, C., Wetzler, L. M., & Gray-Owen, S. D. (2018). Specific binding to differentially expressed human carcinoembryonic antigen-related cell adhesion molecules determines the outcome of Neisseria gonorrhoeae infections along the female reproductive tract. *Infect Immun*, *86*, e00092-18.

Jarvis, G. A., & Chang, T. L. (2012). Modulation of HIV transmission by Neisseria gonorrhoeae: molecular and immunological aspects. *Curr HIV Res*, *10*, 211–217.

Jerse, A. E. (1999). Experimental Gonococcal Genital Tract Infection and Opacity Protein Expression in Estradiol-Treated Mice. *Infection and Immunity*, *67*, 5699–5708.

Jerse, A. E., & Deal, C. D. (2013). Vaccine research for gonococcal infections: Where are we? *Sexually Transmitted Infections*, *89*, 63–68.

Jerse, A. E., Wu, H., Packiam, M., Vonck, R. A., Begum, A. A., Garvin, L. E., & Cornelissen, C. N. (2011). Estradiol-treated female mice as surrogate hosts for Neisseria gonorrhoeae genital tract infections. *Frontiers in Microbiology*, *2*, 1–13.

Johswich, K. O., McCaw, S. E., Islam, E., Sintsova, A., Gu, A., Shively, J. E., & Gray-Owen, S. D. (2013). In vivo adaptation and persistence of Neisseria meningitidis within the nasopharyngeal mucosa. *PLoS Pathog*, *9*, e1003509.

Kaiser, E., Chiba, P., & Zaky, K. (1990). Phospholipases in biology and medicine. *Clinical Biochemistry*, *23*, 349–370.

Kammerer, R., Hahn, S., Singer, B. B., Luo, J. S., & Von Kleist, S. (1998). Biliary glycoprotein (CD66a), a cell adhesion molecule of the immunoglobulin superfamily, on human lymphocytes: Structure, expression and involvement in T cell activation. *European Journal of Immunology*, *28*, 3664–3674.

Kanai, F., Liu, H., Field, S. J., Akbary, H., Matsuo, T., Brown, G. E., Cantley, L. C., & Yaffe, M. B. (2001). The PX domains of p47phox and p40phox bind to lipid products of PI(3)K. *Nature Cell Biology*, *3*, 675–678.

Kennedy, A. D., Willment, J. A., Dorward, D. W., Williams, D. L., Brown, G. D., & DeLeo, F. R. (2007). Dectin-1 promotes fungicidal activity of human neutrophils. *Eur J Immunol*, *37*, 467–478.

Kim, Y. K., Shin, J. S., & Nahm, M. H. (2016). NOD-Like Receptors in Infection, Immunity, and Diseases. *Yonsei Med J*, *57*, 5–14.

Knapp, J. S., & Clark, V. L. (1984). Anaerobic growth of Neisseria gonorrhoeae coupled to nitrite reduction. *Infect Immun*, *46*, 176–181.

Kobayashi, K., Kuroda, S., Fukata, M., Nakamura, T., Nagase, T., Nomura, N., Matsuura, Y., Yoshida-Kubomura, N., Iwamatsu, A., & Kaibuchi, K. (1998). p140Sra-1 (specifically Rac1-associated protein) is a novel specific target for Rac1 small GTPase. *Journal of Biological Chemistry*, *273*, 291–295.

Königer, V., Holsten, L., Harrison, U., Busch, B., Loell, E., Zhao, Q., Bonsor, D. A., Roth, A., Tchoupa, A. K., Smith, S. I., Mueller, S., Sundberg, E. J., Zimmermann, W., Fischer, W., Hauck, C. R., & Haas, R. (2016). Helicobacter pylori exploits human CEACAMs via HopQ for adherence and translocation of CagA. *Nature Microbiology*, *2*, 16188.

Kopp, K., Buntru, A., Pils, S., Zimmermann, T., Frank, R., Zumbusch, A., & Hauck, C. R. (2012). GRB14 is a negative regulator of CEACAM3-mediated phagocytosis of pathogenic bacteria. *J Biol Chem*, *287*, 39158–39170.

Krone, M., Gray, S., Abad, R., Skoczyńska, A., Stefanelli, P., van der Ende, A., Tzanakaki, G., Mölling, P., Joao Simoes, M., Křížová, P., Emonet, S., Caugant, D. A., Toropainen, M., Vazquez, J., Waśko, I., Knol, M. J., Jacobsson, S., Bettencourt, C. R., Musilek, M., … Borrow, R. (2019). Increase of invasive meningococcal serogroup W disease in Europe, 2013 to 2017. *Eurosurveillance*, *24*, e2807.

Kuespert, K., Pils, S., & Hauck, C. R. (2006). CEACAMs: their role in physiology and pathophysiology. *Current Opinion in Cell Biology*, *18*, 565–571.

Kuespert, K., Roth, A., & Hauck, C. R. (2011). Neisseria meningitidis has two independent modes of recognizing its human receptor CEACAM1. *PLoS One*, *6*, e14609.

Kupsch, E.-M., Aubel, D., Gibbs, C. P., Kahrs, A. F., Rudel, T., & Meyer, T. F. (1996). Construction of Hermes shuttle vectors: a versatile system useful for genetic complementation of transformable and non-transformable Neisseria mutants. *Molecular & General Genetics*, *250*, 558–569.

Kupsch, E.-M., Knepper, B., Kuroki, T., Heuer, I., & Meyer, T. F. (1993). Variable opacity (Opa) outer membrane proteins account for the cell tropisms displayed by Neisseria gonorrhoeae for human leukocytes and epithelial cells. *The EMBO Journal*, *12*, 641–650.

Kuroki, M., Arakawa, F., Matsuo, Y., Oikawa, S., Misumi, Y., Nakazato, H., & Matsuoka, Y. (1991). Molecular cloning of nonspecific cross-reacting antigens in human granulocytes. *Journal of Biological Chemistry*, *266*, 11810–11817.

Lebensohn, A. M., & Kirschner, M. W. (2009). Activation of the WAVE complex by coincident signals

controls actin assembly. *Mol Cell*, *36*, 512–524.
Lee, B. C., & Schryvers, A. B. (1988). Specificity of the lactoferrin and transferrin receptors in Neisseria gonorrhoeae. *Mol Microbiol*, *2*, 827–829.
Lehman, H. K., & Segal, B. H. (2020). The role of neutrophils in host defense and disease. *Journal of Allergy and Clinical Immunology*, *145*, 1535–1544.
Li, G., Jiao, H., Yan, H., Wang, J., Wang, X., & Ji, M. (2011). Establishment of a human CEACAM1 transgenic mouse model for the study of gonococcal infections. *Journal of Microbiological Methods*, *87*, 350–354.
Lin, T. M., Halbert, S. P., & Spellacy, W. N. (1974). Measurement of pregnancy-associated plasma proteins during human gestation. *The Journal of Clinical Investigation*, *54*, 576–582.
Maclean, C. A., Chue Hong, N. P., & Prendergast, J. G. (2015). hapbin: An Efficient Program for Performing Haplotype-Based Scans for Positive Selection in Large Genomic Datasets. *Mol Biol Evol*, *32*, 3027–3029.
Malorny, B., Morelli, G., Kusecek, B., Kolberg, J., & Achtman, M. (1998). Sequence diversity, predicted two-dimensional protein structure, and epitope mapping of neisserial Opa proteins. *J Bacteriol*, *180*, 1323-1330.
Mayadas, T. N., Cullere, X., & Lowell, C. A. (2014). The multifaceted functions of neutrophils. *Annu. Rev. Pathol. Mech. Dis.*, *9*, 181–218.
Mayer, L. W. (1982). Rates in vitro changes of gonococcal colony opacity phenotypes. *Infect Immun*, *37*, 481–485.
Mazamay, S., Guégan, J. F., Diallo, N., Bompangue, D., Bokabo, E., Muyembe, J. J., Taty, N., Vita, T. P., & Broutin, H. (2021). An overview of bacterial meningitis epidemics in Africa from 1928 to 2018 with a focus on epidemics "outside-the-belt." *BMC Infectious Diseases*, *21*, https://doi.org/10.1186/s12879-021-06724-1.
McCaw, S. E., Schneider, J., Liao, E. H., Zimmermann, W., & Gray-Owen, S. D. (2003). Immunoreceptor tyrosine-based activation motif phosphorylation during engulfment of Neisseria gonorrhoeae by the neutrophil-restricted CEACAM3 (CD66d) receptor. *Molecular Microbiology*, *49*, 623–637.
McDaniel, M. M., Meibers, H. E., & Pasare, C. (2021). Innate control of adaptive immunity and adaptive instruction of innate immunity: bi-directional flow of information. *Current Opinion in Immunology*, *73*, 25–33.
McDermott, A. M. (2013). Antimicrobial compounds in tears. *Experimental Eye Research*, *117*, 1–20.
Medzhitov, R. (2007). Recognition of microorganisms and activation of the immune response. *Nature*, *449*, 819–826.
Medzhitov, R., & Janeway Jr., C. A. (2002). Decoding the patterns of self and nonself by the innate immune system. *Science*, *296*, 298-300.
Medzhitov, R., & Janeway Jr., C. (2000). Innate immunity. *N Engl J Med*, *343*, 338-44.
Mellies, J., Jose, J., & Meyer, T. F. (1997). The Neisseria gonorrhoeae gene aniA encodes an inducible nitrite reductase. *Molecular and General Genetics*, *256*, 525–532.
Merle, N. S., Church, S. E., Fremeaux-Bacchi, V., & Roumenina, L. T. (2015). Complement system part I - molecular mechanisms of activation and regulation. *Frontiers in Immunology*, *6*, doi: 10.3389/fimmu.2015.00262.
Mickelsen, P. A., Blackman, E., & Sparling, P. F. (1982). Ability of Neisseria gonorrhoeae, Neisseria meningitidis, and commensal Neisseria species to obtain iron from lactoferrin. *Infection and Immunity*, *35*, 915–920.
Mistry, D., & Stockley, R. A. (2006). IgA1 protease. *International Journal of Biochemistry and Cell Biology*, *38*, 1244–1248.
Moore, T., & Dveksler, G. S. (2014). Pregnancy-specific glycoproteins: complex gene families regulating maternal-fetal interactions. *International Journal of Developmental Biology*, *58*, 273–280.
Muenzner, P., Bachmann, V., Hentschel, J., Zimmermann, W., & Hauck, C. R. (2010). Human-restricted bacterial pathogens block shedding of epithelial cells by stimulating integrin activation. *Science*, *329*, 1197–1201.

Muenzner, P., Dehio, C., Fujiwara, T., Achtman, M., Meyer, T. F., & Gray-owen, S. D. (2000). Carcinoembryonic Antigen Family Receptor Specificity of Neisseria meningitidis Opa Variants Influences Adherence to and Invasion of Proinflammatory Cytokine-Activated Endothelial Cells. *Infection & Immunity*, *68*, 3601–3607.

Muenzner, P., & Hauck, C. R. (2020). Neisseria gonorrhoeae Blocks Epithelial Exfoliation by Nitric-Oxide-Mediated Metabolic Cross Talk to Promote Colonization in Mice. *Cell Host and Microbe*, *27*, 793-808.e5.

Muenzner, P., Rohde, M., Kneitz, S., & Hauck, C. R. (2005). CEACAM engagement by human pathogens enhances cell adhesion and counteracts bacteria-induced detachment of epithelial cells. *Journal of Cell Biology*, *170*, 825–836.

Murphy, G. L., Connell, T. D., Barritt, D. S., Koomey, M., & Cannon, J. G. (1989). Phase variation of gonococcal protein II: regulation of gene expression by slipped-strand mispairing of a repetitive DNA sequence. *Cell*, *56*, 539–547.

Nagel, G., Grunert, F., Kuijpers, T. W., Watt, S. M., Thompson, J., & Zimmermann, W. (1993). Genomic organization, splice variants and expression of CGM1, a CD66-related member of the carcinoembryonic antigen gene family. *Eur. J. Biochem.*, *214*, 27–35.

Nassif, X., Marceau, M., Pujol, C., Pron, B., Beretti, J.-L., & Taha, M.-K. (1997). Type-4 pili and meningococcal adhesiveness. *Gene*, *192*, 149–153.

Noble, R. C., Cooper, R. M., & Miller, B. R. (1979). Pharyngeal colonisation by Neisseria gonorrhoeae and Neisseria meningitidis in black and white patients attending a venereal disease clinic. *Br J Vener Dis*, *55*, 14–19.

Oikawa, S., Inuzuka, C., Kuroki, M., Arakawa, F., Matsuoka, Y., Kosaki, G., & Nakazato, H. (1991). A specific heterotypic cell adhesion activity between members of carcinoembryonic antigen family, W272 and NCA, is mediated by N-domains. *Journal of Biological Chemistry*, *266*, 7995-8001.

Oram, J. D., & Reiter, B. (1968). Inhibition of bacteria by lactoferrin and other iron-chelating agents. *Biochimica et Biophysica Acta*, *170*, 351–365.

Othman, A., Sekheri, M., & Filep, J. G. (2022). Roles of neutrophil granule proteins in orchestrating inflammation and immunity. *FEBS J*, *289*, 3932–3953.

Parkin, J., & Cohen, B. (2001). An overview of the immune system. *Immunology*, *357*, 1777–1789.

Pillay, J., den Braber, I., Vrisekoop, N., Kwast, L. M., de Boer, R. J., Borghans, J. A. M., Tesselaar, K., & Koenderman, L. (2010). In vivo labeling with 2H2O reveals a human neutrophil lifespan of 5.4 days. *Blood*, *116*, 625–627.

Pils, S., Gerrard, D., Meyer, A., & Hauck.C.R. (2008). CEACAM3: an innate immune receptor directed against human-resticted bacterial pathogens. *International Journal of Medical Microbiology*, *298*, 553–560.

Pils, S., Kopp, K., Peterson, L., Delgado-Tascon, J., Nyffenegger-Jann, N. J., & Hauck, C. R. (2012). The adaptor molecule Nck localizes the WAVE complex to promote actin polymerization during CEACAM3-mediated phagocytosis of bacteria. *PLoS One*, *7*, e32808.

Pils, S., Schmitter, T., Neske, F., & Hauck, C. R. (2006). *Quantification of bacterial invasion into adherent cells by flow cytometry*. *65*, 301–310.

Pizza, M., & Rappuoli, R. (2015). Neisseria meningitidis: pathogenesis and immunity. *Current Opinion in Microbiology*, *23*, 68–72.

Plaut, A. G., Gilbert, J., Artenstein, M. S., & Carpa, J. D. (1975). Neisseria gonorrhoeae and Neisseria meningitidis: Extracellular enzyme cleaves human immunoglobulin A. *Science*, *190*, 1103–1105.

Prall, F., Nollau, P., Neumaier, M., Haubeck, H. D., Drzeniek, Z., Helmchen, U., Löning, T., & Wagener, C. (1996). CD66a (BGP), an adhesion molecule of the carcinoembryonic antigen family, is expressed in epithelium, endothelium, and myeloid cells in a wide range of normal human tissues. *The Journal of Histochemistry and Cytochemistry*, *44*, 35–41.

Prüfer, K., de Filippo, C., Grote, S., Mafessoni, F., Korlević, P., Hajdinjak, M., Vernot, B., Skov, L., Hsieh, P., Peyrégne, S., Reher, D., Hopfe, C., Nagel, S., Maricic, T., Fu, Q., Theunert, C., Rogers, R., Skoglund, P., Chintalapati, M., … Pääbo, S. (2017). A high-coverage Neandertal genome from

Vindija Cave in Croatia. *Science*, *358*, 655–658.

Quillin, S. J., & Seifert, H. S. (2018). Neisseria gonorrhoeae host-adaptation and pathogenesis. *Nat Rev Microbiol.*, *16*, 226–240.

Rehwinkel, J., & Gack, M. U. (2020). RIG-I-like receptors: their regulation and roles in RNA sensing. *Nat Rev Immunol*, *20*, 537–551.

Rincon, E., Rocha-Gregg, B. L., & Collins, S. R. (2018). A map of gene expression in neutrophil-like cell lines. *BMC Genomics*, *19*, https://doi.org/10.1186/s12864-018-4957-6.

Roth, A., Mattheis, C., Münzner, P., Unemo, M., & Hauck, C. R. (2013). Innate recognition by neutrophil granulocytes differs between Neisseria gonorrhoeae strains causing local or disseminating infections. *Infect Immun*, *81*, 2358–2370.

Rougerie, P., Miskolci, V., & Cox, D. (2013). Generation of membrane structures during phagocytosis and chemotaxis of macrophages: role and regulation of the actin cytoskeleton. *Immunol Rev*, *256*, 222–239.

Rouphael, N. G., & Stephens, D. S. (2012). Neisseria meningitidis: biology, microbiology, and epidemiology. *Methods Mol Biol.*, *799*, 1–20.

Rowley, J., Hoorn, S. Vander, Korenromp, E., Low, N., Unemo, M., Abu-Raddad, L. J., Chico, R. M., Smolak, A., Newman, L., Gottlieb, S., Thwin, S. S., Broutet, N., & Taylor, M. M. (2019). Chlamydia, gonorrhoea, trichomoniasis and syphilis: Global prevalence and incidence estimates, 2016. *Bull World Health Organ*, *97*, 548–562.

Sa, E. C. C., Griffiths, N. J., & Virji, M. (2010). Neisseria meningitidis Opc invasin binds to the sulphated tyrosines of activated vitronectin to attach to and invade human brain endothelial cells. *PLoS Pathog*, *6*, e1000911.

Sadarangani, M., Pollard, A. J., & Gray-Owen, S. D. (2011). Opa proteins and CEACAMs: Pathways of immune engagement for pathogenic Neisseria. *FEMS Microbiology Reviews*, *35*, 498–514.

Sandstrom, I. (1987). Etiology and diagnosis of neonatal conjunctivitis. *Acta Paediatr Scand*, *76*, 221–227.

Sarantis, H., & Gray-Owen, S. D. (2007). The specific innate immune receptor CEACAM3 triggers neutrophil bactericidal activities via a Syk kinase-dependent pathway. *Cell Microbiol*, *9*, 2167–2180.

Sarantis, H., & Gray-Owen, S. D. (2012). Defining the roles of human carcinoembryonic antigen-related cellular adhesion molecules during neutrophil responses to Neisseria gonorrhoeae. *Infect Immun*, *80*, 345–358.

Sarma, J. V, & Ward, P. A. (2011). The complement system. *Cell Tissue Res*, *343*, 227–235.

Schmitter, T., Agerer, F., Peterson, L., Munzner, P., & Hauck, C. R. (2004). Granulocyte CEACAM3 is a phagocytic receptor of the innate immune system that mediates recognition and elimination of human-specific pathogens. *The Journal of Experimental Medicine*, *199*, 35–46.

Schmitter, T., Pils, S., Sakk, V., Frank, R., Fischer, K. D., & Hauck, C. R. (2007). The granulocyte receptor CEACAM3 directly associates with Vav to promote phagocytosis of human pathogens. *Journal of Immunology*, *178*, 3797–3805.

Schmitter, T., Pils, S., Weibel, S., Agerer, F., Buntru, A., Kopp, K., & Hauck, C. R. (2007). Opa proteins of pathogenic Neisseriae initiate Src-kinase-dependent or lipid raft-mediated uptake via distinct human CEACAM isoforms. *Infection & Immunity*, *75*, 4116–4126.

Serruto, D., Adu-Bobie, J., Scarselli, M., Veggi, D., Pizza, M., Rappuoli, R., & Aricò, B. (2003). Neisseria meningitidis App, a new adhesin with autocatalytic serine protease activity. *Molecular Microbiology*, *48*, 323 – 334.

Shiokawa, M., Yamasaki, S., & Saijo, S. (2017). C-type lectin receptors in anti-fungal immunity. *Curr Opin Microbiol*, *40*, 123–130.

Sintsova, A., Sarantis, H., Islam, E. A., Sun, C. X., Amin, M., Chan, C. H., Stanners, C. P., Glogauer, M., & Gray-Owen, S. D. (2014). Global analysis of neutrophil responses to Neisseria gonorrhoeae reveals a self-propagating inflammatory program. *PLoS Pathog*, *10*, e1004341.

Song, W., Ma, L., Chen, R., & Stein, D. C. (2000). Role of lipooligosaccharide in Opa-independent

invasion of Neisseria gonorrhoeae into human epithelial cells. *J Exp Med*, *191*, 949–960.

Stepanek, O., Kalina, T., Draber, P., Skopcova, T., Svojgr, K., Angelisova, P., Horejsi, V., Weiss, A., & Brdicka, T. (2011). Regulation of Src family kinases involved in T cell receptor signaling by protein-tyrosine phosphatase CD148. *Journal of Biological Chemistry*, *286*, 22101–22112.

Stephens, D. S., Greenwood, B., & Brandtzaeg, P. (2007). Epidemic meningitis, meningococcaemia, and Neisseria meningitidis. *Lancet*, *369*, 2196–2210.

Stern, A., Brown, M., Nickel, P., & Meyer, T. F. (1986). Opacity genes in Neisseria gonorrhoeae: Control of phase and antigenic variation. *Cell*, *47*, 61–71.

Stern, A., & Meyer, T. F. (1987). Common mechanism controlling phase and antigenic variation in pathogenic Neisseriae. *Molecular Microbiology*, *1*, 5–12.

Stevens, J. S., & Criss, A. K. (2018). Pathogenesis of Neisseria gonorrhoeae in the female reproductive tract: neutrophilic host response, sustained infection, and clinical sequelae. *Curr Opin Hematol*, *25*, 13–21.

Suzaki, A., Hayashi, K., Kosuge, K., Soma, M., & Hayakawa, S. (2011). Disseminated gonococcal infection in Japan: a case report and literature review. *Intern Med*, *50*, 2039–2043.

Swanson, J. (1973). Studies on gonococcus infection. IV. Pili: their role in attachment of gonococci to tissue culture cells. *Journal of Experimental Medicine*, *137*, 571–589.

Swanson, J. (1982). Colony opacity and protein II compositions of gonococci. *Infection and Immunity*, *37*, 359–368.

Takeuchi, O., & Akira, S. (2010). Pattern Recognition Receptors and Inflammation. *Cell*, *140*, 805–820.

Taylor-Robinson, D., Furr, P. M., & Hetherington, C. M. (1990). Neisseria gonorrhoeae colonises the genital tract of oestradiol-treated germ-free female mice. *Microb Pathog*, *9*, 369–373.

Tchoupa, A. K., Lichtenegger, S., Reidl, J., & Hauck, C. R. (2015). Outer membrane protein P1 is the CEACAM-binding adhesin of Haemophilus influenzae. *Mol Microbiol*, *98*, 440–455.

Tchoupa, A. K., Schuhmacher, T., & Hauck, C. R. (2014). Signaling by epithelial members of the CEACAM family - mucosal docking sites for pathogenic bacteria. *Cell Communication and Signaling*, *12*, doi: 10.1186/1478-811X-12-27.

Teixeira, A. M., Fawcett, J., Simmons, D. L., & Watt, S. M. (1994). The N-domain of the biliary glycoprotein (BGP) adhesion molecule mediates homotypic binding: domain interactions and epitope analysis of BGPc. *Blood*, *84*, 211–219.

Tennant, S. M., Hartland, E. L., Phumoonna, T., Lyras, D., Rood, J. I., Robins-Browne, R. M., & van Driel, I. R. (2008). Influence of gastric acid on susceptibility to infection with ingested bacterial pathogens. *Infection and Immunity*, *76*, 639–645.

Thompson, J. A. (1995). Molecular cloning and expression of carcinoembryonic antigen gene family members. *Tumour Biol*, *16*, 10–16.

Thompson, J. A., Grunert, F., & Zimmermann, W. (1991). Carcinoembryonic Antigen Gene Family: Molecular Biology and Clinical Perspectives. *Journal of Clinical Laboratory Analysis*, *5*, 344–366.

Turvey, S. E., & Broide, D. H. (2010). Innate Immunity. *J Allergy Clin Immunol*, *125*, S24–S32.

Tzeng, Y.-L., Thomas, J., & Stephens, D. S. (2016). Regulation of capsule in Neisseria meningitidis. *Critical Reviews in Microbiology*, *42*, 759–772.

Underhill, D. M., & Goodridge, H. S. (2007). The many faces of ITAMs. *Trends in Immunology*, *28*, 66–73.

Unemo, M., Del Rio, C., & Shafer, W. M. (2016). Antimicrobial resistance expressed by Neisseria gonorrhoeae: A major global public health problem in the 21st century. *Microbiology Spectrum*, *4*, doi:10.1128/microbiolspec.EI10-0009-2015.

Unemo, M., Seifert, H. S., Hook, E. W., Hawkes, S., Ndowa, F., & Dillon, J.-A. R. (2019). Gonorrhoea. *Nature Reviews Disease Primers*, *5*, https://doi.org/10.1038/s41572-019-0128-6.

Unkmeir, A., Latsch, K., Dietrich, G., Wintermeyer, E., Schinke, B., Schwender, S., Kim, K. S., Eigenthaler, M., & Frosch, M. (2002). Fibronectin mediates Opc dependent internalisation of Neisseria meningitidis in human brain microvascular endothelial cells. *Molecular Microbiology*, *42*, 933–946.

Uria, M. J., Zhang, Q., Li, Y., Chan, A., Exley, R. M., Gollan, B., Chan, H., Feavers, I., Yarwood, A., Abad, R., Borrow, R., Fleck, R. A., Mulloy, B., Vazquez, J. A., & Tang, C. M. (2008). A generic mechanism in Neisseria meningitidis for enhanced resistance against bactericidal antibodies. *Journal of Experimental Medicine*, *205*, 1423–1434.

Uribe-Querol, E., & Rosales, C. (2020). Phagocytosis: our current understanding of a universal biological process. *Frontiers in Immunology*, *11*, doi: 10.3389/fimmu.2020.0106.

van Putten, J. P., & Paul, S. M. (1995). Binding of syndecan-like cell surface proteoglycan receptors is required for Neisseria gonorrhoeae entry into human mucosal cells. *The EMBO Journal*, *14*, 2144–2154.

Virji, M. (2009). Pathogenic Neisseriae: surface modulation, pathogenesis and infection control. *Nat Rev Microbiol*, *7*, 274–286.

Virji, M., Alexandrescu, C., Ferguson, D. J. P., Saunders, J. R., & Moxon, E. R. (1992). Variations in the expression of pili: the effect on adherence of Neisseria meningitidis to human epithelial and endotheliai cells. *Molecular Microbiology*, *6*, 1271–1279.

Virji, M., Evans, D., Griffith, J., Hill, D., Serino, L., Hadfield, A., & Watt, S. M. (2000). Carcinoembryonic antigens are targeted by diverse strains of typable and non-typable Haemophilus influenzae. *Molecular Microbiology*, *36*, 784-95.

Virji, M., Makepeace, K., Ferguson, D. J., Achtman, M., Sarkari, J., & Moxon, E. R. (1992). Expression of the Opc protein correlates with invasion of epithelial and endothelial cells by Neisseria meningitidis. *Molecular Microbiology*, *6*, 2785-95.

Virji, M., Makepeace, K., Ferguson, D. J. P., & Watt, S. M. (1996). Carcinoembryonic antigens (CD66) on epithelial cells and neutrophils are receptors for Opa proteins of pathogenic neisseriae. *Molecular Microbiology*, *22*, 941–950.

Virji, M., Watt, S. M., Barker, S., Makepeace, K., & Doyonnas, R. (1996). The N-domain of the human CD66a adhesion molecule is a target for Opa proteins of Neisseria meningitidis and Neisseria gonorrhoeae. *Molecular Microbiology*, *22*, 929–939.

Vogel, U., & Frosch, M. (1999). Mechanisms of neisserial serum resistance. *Molecular Microbiology*, *32*, 1133-9.

Vyse, A., Anonychuk, A., Jäkel, A., Wieffer, H., & Nadel, S. (2013). The burden and impact of severe and long-term sequelae of meningococcal disease. *Expert Rev. Anti Infect. Ther.*, *11*, 597–604.

Wan, W., Farkas, G. C., May, W. N., & Robin, J. B. (1986). The clinical characteristics and course of adult gonococcal conjunctivitis. *American Journal of Ophthalmology*, *102*, 575–583.

Wang, J., Gray-Owen, S. D., Knorre, A., Meyer, T. F., & Dehio, C. (1998). Opa binding to cellular CD66 receptors mediates the transcellular traversal of Neisseria gonorrhoeae across polarized T84 epithelial cell monolayers. *Molecular Microbiology*, *30*, 657–671.

Wertz, P. W. (2018). Lipids and the permeability and antimicrobial barriers of the skin. *Journal of Lipids*, *2018*, 1–7.

WHO. (2016). *WHO guidelines for the treatment of Neisseria gonorrhoeae*. World Health Organization.

Xu, S. X., Leontyev, D., Kaul, R., & Gray-Owen, S. D. (2018). Neisseria gonorrhoeae co-infection exacerbates vaginal HIV shedding without affecting systemic viral loads in human CD34+ engrafted mice. *PLoS One*, *13*, e0191672.

Yu, Q., Chow, E. M., McCaw, S. E., Hu, N., Byrd, D., Amet, T., Hu, S., Ostrowski, M. A., & Gray-Owen, S. D. (2013). Association of Neisseria gonorrhoeae Opa(CEA) with dendritic cells suppresses their ability to elicit an HIV-1-specific T cell memory response. *PLoS One*, *8*, e56705.

Zarantonelli, M. L., Szatanik, M., Giorgini, D., Hong, E., Huerre, M., Guillou, F., Alonso, J. M., & Taha, M. K. (2007). Transgenic mice expressing human transferrin as a model for meningococcal infection. *Infect Immun*, *75*, 5609–5614.

Zhan, Y., Virbasius, J. V, Song, X., Pomerleau, D. P., & Zhou, G. W. (2002). The p40phox and p47phox PX domains of NADPH oxidase target cell membranes via direct and indirect recruitment by phosphoinositides. *J Biol Chem*, *277*, 4512–4518.

Zimmermann, W. (2019). Evolution: Decoy receptors as unique weapons to fight pathogens. *Current*

Biology, *29*, R128–R130.